FIRE PERFORMANCE OF TIMBER-CONCRETE COMPOSITE FLOOR SYSTEMS UTILIZING CROSS-LAMINATED TIMBER PANELS WITH SELF-TAPPING SCREWS AS SHEAR CONNECTORS

By

Sarah Barclay

A thesis submitted to the Faculty of
Graduate Studies in partial fulfilment of
the requirements for the Degree of Master
of Science in

Civil Engineering

Supervisor

Prof. Osama (Sam) Salem, Ph.D., P. Eng.
Associate Professor and Chair – Dept. of Civil Engineering

Lakehead University
Thunder Bay, Ontario
January 2023

AUTHOR'S DECLARATION PAGE

I hereby declare that I am the sole author of this thesis. This is a true copy of the thesis, including any required final revisions, as accepted by my examiners. I understand that my thesis may be made electronically available to the public.

ABSTRACT

One of the main reasons that hinder more utilization of combustible material, such as wood, as the primary construction material in tall buildings is the required duration a structure must withstand applied loads under fire exposure without losing its structural integrity, which is refereed to the fire resistance rating required by applicable building codes. However, the increased availability of cross-laminated timber (CLT) sections in Canada and its successful use in mass timber construction have generated interest in its properties and performance when subjected to fire.

Floor systems in mass timber buildings can be more robust and span longer distances by adding a top layer of concrete to form timber-concrete composite (TCC) floor systems when adequate shear connections are utilized. The primary technique for shear connections in TCC systems is a wide variety of metal connectors, with the self-tapping screws (STS) being one of the most used shear connectors. Therefore, proper design guidelines and methodologies are needed to determine the accurate fire resistance of TCC floor systems. Currently, there is no design procedure for the TCC floor systems included in the Canadian *Engineering design in wood* standard (CSA O86-19) but is implemented in other international design codes, such as the European codes.

The experimental program of this research study involves fire testing of full-size, one-way TCC floor slabs that utilize STS as shear connectors. The main objective of this study is to investigate the influence of the insertion angle of the STS on the fire performance of TCC sections comprised of 143-mm thick, 5-ply CLT panels and 90-mm thick normal strength concrete layer. A total of four full-size TCC floor assemblies have been tested under standard fire exposure, two of which have their STS orientated at 45° from the horizontal, while the other two assemblies have their STS orientated at 30°. Each TCC assembly has a clear span of 5000 mm and a width of 900 mm.

The 5-ply CLT panel composition was chosen to investigate how its listed one-hour fire resistance rating can be increased to two hours by developing a composite action between the added concrete top layer and the supporting CLT panel. While applying a four-point flexure bending on the TCC floor slabs, test assemblies were exposed to elevated temperatures that followed the CAN/ULC S101 standard fire time-temperature curve throughout the fire tests.

The experimental results show that all test assemblies achieved the two-hour fire resistance with an average residual wood thickness of at least 50 mm. This remaining uncharred thickness of the CLT panels allowed the TCC floor slabs to safely sustain the applied load for the required two-hour fire resistance time. The results of this new experimental study on full-size TCC floor slabs exposed to standard fire allow better understanding of how such composite floor systems can behave under applied loads when exposed to fire within the framework of mass timber buildings in Canada. Most importantly, the unique experimental data of this new study will fill some of the knowledge gap regarding the missing experimental data on TCC floor systems needed to develop fire resistance design guidelines for mass timber buildings in Canada.

ACKNOWLEDGEMENTS

This research project was mainly funded using the Discovery Grant awarded to Prof. Salem by Natural Sciences and Engineering Council of Canada (NSERC). Thanks are due for the generous in-kind contributions provided by Nordic Structures Inc., Miller Precast, and Pioneer Construction. Any opinions, findings, conclusions, or recommendations are those of the author and do not necessarily reflect the views of the funding/sponsoring parties.

I express sincere gratitude to my thesis supervisor, Dr. Salem for his motivation, knowledge, guidance, and continued support. For giving this great opportunity of pursuing graduate studies and for always believing in me and that I could do more even when I began to question the possibility. You kept me moving forward and always focused on the next task.

This project wouldn't have been possible without our research group members, Adam Petrycki and Javad Tashakori. I have learned so much from each of you in terms of engineering, learning new skills, and growing as a person. There have been countless hours spent in the lab and discussions over the last couple of years that would have made this unbearable without you. You have made such a difference that I never know how to thank you enough.

I would also like to thank Cory Hubbard for his great help throughout my experimental program in the Civil Engineering's Structures Laboratory and Lakehead University Fire Testing and Research Laboratory (LUFTRL). You have provided your assistance, guidance, time, and expertise in all aspects of the project, from preparation to testing. Fire testing would have been insurmountable without you; you were vital to the success of completing the fire testing program and spent numerous hours of your time making this achievable.

I want to extend my gratitude to my fellow graduate students in Civil Engineering at Lakehead University. You have provided your support and insight throughout my studies and believed in my success. I am thankful; you are all fantastic and will do great things.

Thank you to Miro Gawinski and Tom Outhwaite. Without you, I wouldn't be where I am today and studying engineering at the graduate level. You were the first ones to introduce me to drafting and design at CPRSS and always provided counsel and advice. I genuinely appreciate your support and insight into architecture and engineering, and I am forever thankful.

Thank you to the continued support of my family and especially my mom, who has inspired, pushed, and believed in me since day one. Without you, I wouldn't have the drive, motivation, and courage to pursue my dreams and goals. My success is a result of you, it's the character and values that you raised me with, for me to be able to reach this point.

I want to extend my gratitude to my friends and roommates that I have meet throughout out my studies at Lakehead University. Both from engineering and other departments, this journey is a result from your support along the way and became my family away from home. Especially, like to dedicate to Jennifer Smith, who unfortunately passed away earlier last year. You were an amazing person and made everyone's life better for those that had the privilege to know you.

My final acknowledgment is to my two cats, Ryder and Rex. Who I adopted during the first summer of my program and while they will never understand this, if it wasn't for them, I wouldn't be at this point. They are the best emotional support that one could have asked for.

Table of Contents

LIST OF TABLES

LIST OF EQUATIONS

LIST OF FIGURES

LIST OF ABBREVIATIONS

CLT	Cross-Laminated Timber
DF	Douglas Fir
ECSM	Effective Cross-Section Method
EPM	Elasto-Plastic Method
EWP	Engineered Wood Products
FLD	Fire Load Density
Glulam	Glued Laminated Timber
HSC	High Strength Concrete
ICI buildings	Industrial, Commercial, and Institutional buildings
LUFTRL	Lakehead University Fire Testing and Research Laboratory
LVDTs	Linear Variable Differential Transformers
LVL	Laminated Veneer Lumber
MF	Melamine Formaldehyde
MSR	Machine Stress Rated
SPF	Spruce Pine Fir
NBCC	National Building Code of Canada
EMTC	Encapsulated Mass Timber Construction
NLGA	National Lumber Grades Authority
NLT	Nail-Laminated Timber
NSC	Normal Strength Concrete
PRF	Phenol Resorcinol Formaldehyde
PUR	Polyurethane
RPM	Reduced Properties Method
SLS	Serviceability Limit States
STS	Self-Tapping Screws
SYP	Southern Yellow Pine
TCC	Timber-Concrete Composites
UDL	Uniformly Distributed Load
ULS	Ultimate Limit States

CHAPTER 1: INTRODUCTION

1.1 Background

A key aspect of structural engineering research and design is looking at the optimization of sections and finding more efficient solutions to fundamental behaviours. That is the primary motivation and reasoning behind the design of composite structural members. They are maximizing the strengths of materials and compensating for the weaknesses. While many composite members can be designed, Timber-Concrete Composites (TCC) sections are of great interest, with the timber material in the tension side and concrete in the compression.

They were initially studied extensively from 1900-1930 during post-world war times, with the inflated price of steel looking at alternative solutions. TCCs were commonly used in bridge construction as the concrete slab acted as a barrier and protected the timber components from weather effects. In recent years there has been a new surge of interest and study with the introduction of Engineered Wood Products (EWP) and building tall mass timber structures. TCC sections are an excellent solution for both new structures in the design and restoring existing timber construction since a fundamental improvement is in service for vibration and drastic change possible for fire resistance rating requirements in current building codes and design standards. Thereby increasing the possibility of not only building tall with timber but also leaving the material exposed, impacting the architectural concept of the structure, and increasing the use of EWP as a design solution.

It is typical in mass timber construction to pour a concrete layer on top of timber floor slabs to improve the vibration and acoustic characteristics as well as to provide a space for conduits to run electrical and plumbing utilities. However, this practice is a missed opportunity to improve the

section's fire resistance and structural performance. There is the behaviour of three different materials in TCC sections (i.e., timber, concrete, and shear connectors), and it becomes more complicated at the interface between materials. Therefore, with the original design, adding concrete without shear connectors is not improving the strength properties and ultimate capacity but rather adding concrete as a dead weight to the supporting timber material. In contrast, TCC sections have the materials working together in each respective strength and altering the location of the neutral axis to the interface.

There are two ways that these sections can be used, beam-type assembly and slab-type assembly. In the beam-type assembly, the timber section is in the form of beams connected to the above concrete slab, giving a more T-section design. While in the slab-type assembly, the timber is an entire slab component, providing a rectangular section design. According to the available literature, the beam-type assembly is much more extensively researched than the slab-type assembly. TCC sections are also more studied in ambient condition than elevated fire temperatures.

When designing such sections, there are two methods to follow, the γ-method and the Elasto-Plastic Method (EPM). The former is the more common and original design concept. At the same time, the latter is relatively new and explicitly implemented for ductile connectors as the γ-method assumes elastic behaviour before the point of yielding. When EPM is within the plastic range and after, the shear connectors begin to yield. Both design methodologies need to be checked, but EPM is critical to the design of TCC sections for shear connectors with less stiffness.

One of the three fundamental aspects of the design of TCC sections is the shear connectors used to connect the two materials, giving the location to transfer stresses between the different materials. This results in many possible connectors that can be used, with their pros and cons in quantity

required, level of skilled labour for insulation, cost per unit, availability, and research studied with validated results and behaviour in ambient and fire conditions. Therefore, to advance the understanding of TCC sections need more testing of the various shear connectors in full-scale testing setup to capture in-situ conditions and the overall performance of the sections.

1.2 Problem Statement

The design of all structural elements includes a considerable factor of safety when accounting for ambient and elevated temperatures. A key difference in design approaches is that fire follows ultimate limit states and is concerned about the maximum duration of structural integrity, giving time for evacuation and safety for firefighters. At the same time, ambient temperature design is restricted to serviceability limits and considers comfortability to occupants. The difference in approach lends to a typical pattern that the structural utilization doubles comparing ambient design to fire resistance design. An ambient design with a higher percentage of section utilization leaves no allowance for safety in fire scenarios with additional fireproofing or insulation. Therefore, from a structural design for fire resistance point of view; design should always consider fire exposure before element sizes are finalized.

Contrary to popular belief and hesitation when considering mass timber materials for construction, they have excellent fire resistance and perform well under high-temperature conditions. Although without verified test results, it causes a limitation of the industry's progression and possibilities when considering building tall in timber and options to have elements left exposed. Research and analysis in developing knowledge of TCC sections are vital, as they can create new opportunities for growing the industry and opening new possibilities when using EWP from a structural and architectural point of views.

There are many advantages to studying the behaviour of TCC sections, although the problem is the need for more experimental results, especially when considering fire conditions. While those TCC sections have been studied both in Canada and Internationally, there remains a research gap before being able to be implemented into our building codes and design standards. Therefore, this thesis aims to begin closing this gap and develop a deeper understanding of the fire performance of TCC sections to provide design recommendations for such composite sections using CLT slabs.

1.3 Scope and Objectives

In the study presented in this thesis, the fire performance of TCC sections utilizing CLT panels and STS as the shear connectors were studied to better understand the influence of the inclination angle of screws and how it affects the overall behaviour of TCC floor assemblies. Additionally, the possibility of providing more experimental results and analysis can enhance the understanding of the behaviour of TCC sections. This can allow more expansion of the use of EWP because of improving their structural fire resistance compared to standalone timber elements. This provides valuable knowledge required to develop the framework of TCC section design in Canada with more focus on the performance-based design approach. A total of four full-size, one-way floor assemblies were tested with duplication of each study parameter, giving validation and confirmation of results and findings. All specimens were exposed to elevated temperatures following the CAN/ULC-S101 standard fire time-temperature curve. During fire exposure, both thermal and mechanical behaviours were monitored and analyzed. Afterwards, the exposure charring time, rate, and depth were evaluated to determine the actual residual section post-fire exposure.

The main objectives of this unique experimental study are listed below.

1. Achieving a 2-hour Fire Resistance Rating (FRR) for the TCC floor assemblies studied, thereby increasing the fire performance of the CLT panels utilized instead of being used as a flooring system separately.
2. Studying the influence of different angles of inclination of the self-tapping screws utilized in the studied TCC floor systems as shear connectors.
3. Enhancing the understanding of TCC floor systems behaviour and framework in Canada.
4. Verifying the actual charring rates and behaviour of CLT panels under one-dimensional heat transfer.

1.4 Research Methodology

The research project presented in this thesis began with a quantitative literature review on the topic of TCC sections, aimed to examine the design of composite sections when tested in ambient and fire conditions, with a focus on sections that utilized CLT panels as the timber component. Information was reviewed using secondary data to evaluate other trends in research, experimental results, and areas of limited focus. Such sources were found in scientific articles published and become accessible in the available literature. Little research has been conducted in Canada, so TCC sections are only considered on a performance-based design; however, more extensive design procedures and recommendations can be found in European and Australian publications.

By conducting a content analysis, thereby identifying patterns and conclusions across each study was completed to learn of research gaps in knowledge and to validate continued work that is required to better understand the goal of improving the framework of TCC section design in Canada. The experimental programs that were shown varied in terms of their assembly types,

materials, testing scale completed, and the number of specimens studied. Although many of the same conclusions were drawn, the results were consistent to so extent. This suggests certain degree of the validity of the experimental outcomes since lab-based experiments cannot consistently be replicated especially considering the changes in the different types of material used and the assembly type.

After conducting a comprehensive literature review, it was clearly shown that while there is sufficient coverage on the topic and TCC section behaviours in ambient condition, there is lack of research studies on their fire resistance design and behaviour. Therefore, the research project of this thesis was designed to reduce this gap in understanding with a focus on full-size experimental fire testing including both thermal and mechanical performance of TCC floor assemblies utilizing CLT slabs and STS as shear connectors. This is a one project of a more extensive research program aimed at investigating the fire performance of these TCC floor systems being conducted at Lakehead University Fire Testing and Research Laboratory (LUFTRL). The larger research program being conducted at LUFTRL involves comprehensive experimental and numerical studies with varying parameters and types of shear connectors to enhance the fire performance of those TCC floor systems.

The experimental project presented in this thesis involved the complete design, fabrication, and testing of four full-size, one-way TCC floor slabs using STS as shear connectors. The study examined the thermal and mechanical behaviours, focusing on charring performance and deflection values, of the experimentally examined floor assemblies. The experimental study includes a qualitative analysis of the obtained results and comparison between all test assemblies,

thereby allowed new observations and conclusions that resulted in providing recommendations on the current study and future work.

1.5 Thesis Structure

The structure of this thesis includes five distinct chapters. First, an introduction gives an extended summary of background information on the topic of TCC sections and structural fire design, the problem statement and current research gap, an overview of the objectives and scope of the research program, and a brief overview of research and experimental methodology. Following in Chapter two is a comprehensive literature review including a summary of CLT panels, a discussion of the purpose and motivation for mass timber construction, a study of how each material behaves under fire exposure, and an extensive examination of TCC sections and resulting behaviour during ambient and elevated temperature conditions. The third chapter covers the research methodology and details of the experimental program, including shear connection design procedure, instrumentation and data collection details, and specimen fabrication and testing set-up. Chapter four includes the experimental results for thermal and mechanical performance as well as detailed discussions on resulting behaviours of interest, with particular focus on the development of temperatures throughout the section and ensuing deflections. While the most part of Chapter four represents the direct results and outcomes of the experimental program, the last section of this chapter present detailed discussion of the behaviours and observations on STS, CLT and insulation layers. The final chapter, Chapter 5, concludes the current study with a summary of the most important obtained results and provides a few recommendations regarding research impact and future work.

CHAPTER 2: LITERATURE REVIEW AND BACKGROUND RESEARCH

Engineered-wood products (EWP) such as Cross-Laminated Timber (CLT) have been gaining popularity since they were first introduced in the early 1990s in Europe. Not initially examined in Canada until 2007, and not until 2017 when it was fully implemented into CSA-O86 *Engineering design in wood* standard (CSA 2019). CLT panels are mass timber sections made by gluing and pressing wood lamellas with alternating fibre directions (±90°) (Mindeguia et al., 2021). The panels shall have an odd number of lamellae (Typ. 3, 5, 7, or 9) arranged symmetrically around the centre layer, with the thickness of each layer ranging from 20 to 45 mm. A typical cross-section of Nordic X-Lam CLT panel is shown in Figure 2.1.

Figure 2.1: Nordic X-Lam CLT panel.

Recent changes in provincial and national building codes and wood design standards have amplified the desire to further understand mass timber products. Research, experimentally, and analytical studies have resulted in this shift in needing to build greener and use renewable resources. It increased demand for the construction of mid-rise residential and Industrial,

Commercial, and Institutional (ICI) buildings utilizing engineered wood products. While CLT has been used in many countries, there are still limits to use and to better understand its behaviour. Further research is still needed with a focus on the fire performance of CLT panels, as fire resistance is one of the control variables limiting the designs of structures. This leads to increased research around Timber-Concrete Composite (TCC) sections utilizing CLT panels, which are comprised of three aspects: the timber material located in the tensile zone, concrete in the compressive zone; and a type of shear connector joining and transferring forces between the two materials. The addition of concrete top layer and shear connectors carries a key benefit of improving the fire performance of the timber section. By better understanding the behavior of TCC sections, we can further develop the use and possible application for CLT panels while simultaneously expanding the framework for TCC sections. Utilizing such innovative structural systems has many key advantages, such as using sustainable and renewable construction materials like wood and CLT panels with excellent acoustic, thermal, and seismic performance. Also, CLT specifically offers dimension stability since the crosswise laminations control the changes due to swelling and shrinkage (Schmid et al., 2018).

2.1 CLT Manufacturing and Grading

From a manufacturing perspective, engineered-wood products are very advantageous to the growth and expansion of designing structural systems with timber materials compared to their steel or concrete counterparts. In the 1990s, when CLT was initially introduced in Europe, it was motivated by the desire for the sawmill industry to create a more profitable use for the small sideboards (Brandner et al., 2016). The development of Glued-Laminated Timber (Glulam) and CLT resulted

from utilizing smaller sections of timber that would be ejected due to size or poor mechanical properties.

2.1.1 Grading

CLT panels are manufactured and certified by ANSI/APA PRG 320, Standard for Performance-Rated Cross-Laminated Timber (CSA O86, 2019, p. 96). Utilizing two methods, machine stress-rated (MSR or E-rated) lumber and visually graded lumber (V-rated). While graded visually has been the practice for many decades, MSR has been used for many years in highly demanding engineering applications such as truss manufacturing.

The panels are graded in two distinctive ways, grades for each lamella and grades for the overall panel. The lamellae are further separated between longitudinal and transverse directions. The minimum grades of lumber in the longitudinal direction of the CLT panel (the major strength direction) permitted are visually graded lumber No.1/No.2 (stress grade V1 and V2) or machine-stress graded lumber 1200f-1 .2E MSR (stress grade E1, E2, and E3). The minimum grade in the transverse direction (minor strength direction) is the visually graded lumber No.3. Thereby yielding five primary CLT stress grades for the overall panels (E1, E2, E3, V1 and V2). Stress grades E1, E2 and E3 consist of MSR lumber in all longitudinal layers and visually graded lumber in the transverse layers. In contrast, stress grades V1 and V2 consist of visually graded lumber in longitudinal and transverse layers.

In addition to grading the panels in terms of mechanical properties and grading process, there is an appearance grade given to the panels (Industrial Appearance and Architectural Appearance). These requirements are based on the appearance at the time of the manufacturing (Nordic Structures, 2020).

2.1.2 Wood Species

Different wood species and grades can be used in manufacturing depending on design requirements and regional availability. CLT is manufactured from any softwood lumber species or species combinations recognized by the Canadian Lumber Standards Accreditation Board under CSA O141 standard (CWC, 2020, p. V2-1035) and has a minimum density of 0.35 g/cm^3. Species include Larch, Fir, Douglas Fir, Pine, or species combinations such as Spruce-Pine-Fir (S-P-F). From an economic and availability point of view, S-P-F is most used as it can be found across the entire Canadian geographic region and encompass a wide variety of Spruce, Pine, and Fir species. Different species can be used for alternate layers within the panel, but the same lumber species or species combinations are used in every single layer of CLT (CSA O86, 2019, p.96). Using lower mechanical properties of timber is due to the solid composition and homogenization of the board properties within CLT (Brandner et al., 2016). Therefore, it simulates growth in the industry and makes use of otherwise disregarded lumber.

2.1.3 Finger Joints

Finger joints are formed by adhesive bonding of machined complementary interlocking profiles at the ends of consecutive pieces of lumber, Figure 2.2. They are a crucial part of manufacturing engineered wood products as including them allows for lengthening pieces of lumber and not being limited by the length of the tree size. This is required as Nordic Structures CLT panels can be manufactured at a maximum of 2.70 m in the major strength direction and up to 19.5 m in the minor strength direction. In addition, they allow the removal of strength-reducing characteristics, resulting in better use and conservation of wood fibres. Canadian finger-joined lumber is manufactured in conformance with the National Lumber Grades Authority (NLGA) Special Products Standards SPS 1, Finger joined Structural Lumber, SPS 3, Finger joined “Vertical Stud

Use Only" Lumber, or SPS 4, Finger joined Machine Graded Lumber (CWC, 2020 p. V2-912). The final step in forming these joints must be bonded with adhesives outlined in NLGA Special Product Standards. Which states what types of adhesives can be used in SPS 1, SPS 3 and SPS 4 finger-joined lumber, as well as the test standards that those adhesives must meet.

Figure 2.2: Typical CLT finger joint.

2.1.4 Adhesives

Structural adhesives used in bonding laminations are required to meet the requirements of CSA O112.10 standard, Evaluation of Adhesives for Structural Wood Products (Limited Moisture Exposure), and ASTM D7247 standard for heat durability (CWC, 2020, p. V2-1036). In addition, adhesives are evaluated for heat performance by Section 6.1.3.4 of Voluntary Product Standard PS 1, Structural Plywood. Heat durability requirements aim to assess the likelihood of delamination characteristics. Delamination is described as the sudden failure and falling of plys before the point of being charred. Either on a local or global scale, with local being minimal locations of the ply prematurely falling or global where the majority of ply across the panel falling at the same time. Delamination is a characteristic of the adhesive types used and have profound

impacts on the charring rate and behaviour, discussed further in section 2.4. Another critical parameter when designing CLT members is for them to only be in dry service conditions due to the type of adhesives and behaviour of the panel.

PRG 320 standard (ANSI/APA PRG 320, 2019) requires that end joints or edge and face joints in laminations meet requirements specified for strength, wood failure and durability per Section 9 of CSA O177 standard (CWC, 2020, p. V2-1036). Face-glued lumber is formed by using adhesive to bond the pieces of lumber along their longitudinal faces, so the grain of the laminations remains parallel. CLT panels from Nordic Structures use a one-component polyurethane (PUR) adhesive with a primer for surfaces or face gluing, specifically Henkel Loctite/Purbond HB-X (PUR) with PR 3105 Primer. While for the finger joints, a polyurethane emulsion polymer (PEP) adhesive, specifically Ashland Isoset UX-160/WD3-A322 (PEP), is used.

While it is possible also to edge glue the pieces that make up the lamellae, it is not a common practice due to the extra manufacturing cost and time to produce the panels. Panels used in this study from Nordic Structures have not edged glued panels. While not edge gluing has an economic advantage, it influences structural performance, especially during fire conditions. Without an edge gluing CLT panels are more susceptible to delamination when subjected to fire. If higher performance is required, then edge gluing the pieces within the outer layers is a more cost-effective method (CWC, 2020, p. V2-999).

2.1.5 Manufacturing Process

The typical manufacturing process of CLT panels can be divided into two essential steps: preparation and treatment of the primary material and arranging and gluing the basic material. The first includes the first three steps, which involves drying the raw timber materials; CLT moisture

tolerances of the primary material are 12 ± 2 %. Then is the grading of raw material as discussed in Section 2.1.1 with how which panel is graded for all CLT from Nordic Structures, including ones examined in this study of Grade E1. The last stage in the preparation process is the longitudinal joining of the lamellae, achieved by utilizing finger joints, as discussed in Section 2.1.3. After completion of finger joints, lamellae are finally cut to the dimensions needed for the fabrication of CLT elements.

First is arranging the panel in terms of panel dimensions and the number of ply and applying adhesive on all faces of the boards. As mentioned previously, it is uncommon to glue the edges of the boards during manufacturing due to the extra expense and time required. After adhesive application, the assembly pressing follows. If hydraulic jacks are used, the values range from 0.10 to 1.0 N/mm^2. While the corresponding values vary from 0.05 to 0.10 N/mm^2 for vacuum jacks, and the values range from 0.01 to 0.20 N/mm^2 for pressure exerted by bolts, clamps and nails (Jeleč et al., 2018). Regardless of the method used for applying pressure, the most important is uniform and even distribution, allowing all the small boards to act as one overall panel. The final step is cutting and final machining of the panels to be made to order specifications in terms of dimensions and geometrical corrections.

2.1.6 Mechanical Properties

Now that CLT is included in CSA O86-19: *Engineering design in wood* standard (CSA 2019), the Wood Design Manual (CWC, 2020) includes tables of specified strengths and moduli of elasticity of laminations for primary CLT stress grades (E1, E2, E3, V1, and V2). In addition, a design checklist must be met to pull values directly from the tables listed in WDM. The load duration factor (K_D), service condition (K_S), and treatment factor (K_T) must all be equal to one, as well the

thickness of all plys must be 35 mm. If these conditions are not met, then the following equations are required to determine the custom panel's moment and shear capacity. Except for, load duration can be modified from the table values corrodingly for the short or long duration instead of standard.

The flatwise factored bending moment resistance, $M_{r,f}$, of CLT panels.

Equation 2.1: CLT - Bending Moment Resistance in the Major Strength Direction

$$\boldsymbol{M_{r,f,0} = \phi F_b S_{eff,f,0} K_{rb,0}}$$

where:

$\phi = 0.9$

$F_b = f_b(K_D K_H K_{Sb} K_T)$

where:

f_b = specified bending strength of laminations in the longitudinal layers (MPa)

$S_{eff,f,0} = \frac{EI_{eff,f,0}}{E}\frac{2}{h}$

where:

$EI_{eff,f,0}$ = effective flatwise bending stiffness of the panel in the major strength direction (N•mm2)

E = specified modulus of elasticity of laminations in the longitudinal layers (MPa)

h = thickness of the panel (mm)

$K_{rb,0} = 0.85$

Equation 2.2: CLT - Bending Moment Resistance in the Minor Strength Direction

$$\boldsymbol{M_{r,f,90} = \phi F_b S_{eff,f,90} K_{rb,90}}$$

where:

$\phi = 0.9$

$F_b = f_b(K_D K_H K_{Sb} K_T)$

where:

f_b = specified bending strength of laminations in the transverse layers (MPa)

$S_{eff,f,90} = \frac{EI_{eff,f,90}}{E}\frac{2}{h_{90}}$

where:

$EI_{eff,f,90}$ = effective flatwise bending stiffness of the panel in the minor strength direction (N.mm2)

E = specified modulus of elasticity of laminations in the transverse layers (MPa)

h_{90} = thickness of the panel without the outer longitudinal layers (mm)

$K_{rb,90} = 1.0$

The factored flatwise shear resistance, $V_{r,f}$, of CLT panels

Equation 2.3: CLT - Shear Resistance in the Major Strength Direction

$$\boldsymbol{V_{r,f,0} = \phi F_s \frac{2A_{g,0}}{3}}$$

Equation 2.4: CLT - Shear Resistance in the Minor Strength Direction

$$\boldsymbol{V_{r,f,90} = \phi F_s \frac{2A_{g,90}}{3}}$$

where:

$\phi = 0.9$

$F_s = f_s(K_D K_H K_{Sv} K_T)$

where:

f_s = specified strength in rolling shear of laminations in the longitudinal layers (MPa)

$A_{g,0}$ = gross cross-sectional area of the panel measured perpendicular to the major strength direction (including all layers) (mm^2)

$A_{g,90}$ = gross cross-sectional area of the panel measured perpendicular to the minor strength direction (not including the outer layers) (mm^2)

These equations can determine moment and shear resistances for any panels with the difference in layup thickness and distribution of plys. Provided the CLT layup is balanced and manufactured with sawn lumber, the panels are of constant width. Also following, other provisions, such as PRG 320, stipulate that the laminations' actual dry thickness in both major and minor strength directions at the time of gluing should not be less than 16 mm or more than 51 mm. See Tables 2.1 and 2.2 for the technical specifics of the CLT panels manufactured from Nordic Structures. Table 2.1 shows the material design properties inputted into the above equations and Table 2.2 with resulting design properties for CLT when under flexure bending.

Table 2.1: Material Design Properties (adapted from Nordic Structures, 2020)

CLT Stress Grade	E1	
	Layers	
Orientation	Longitudinal	Transversal
Species Combination	S-P-F	S-P-F
Stress Class	1950 F_b – 1.7E MSR	No. 3 / Stud
Bending at Extreme Fibre, f_b (MPa)	28.2	7.0
Longitudinal Shear, f_v (MPa)	1.5	1.5
Rolling Shear, f_s (MPa)	0.5	0.5
Compression Parallel to Grain, f_c (MPa)	19.3	9.0
Compression Perpendicular to Grain, f_{cp} (MPa)	5.3	5.3
Tension Parallel to Grain, f_t (MPa)	15.4	3.2
Modulus of Elasticity, E (MPa)	11 700	9 000
Shear Modulus, G (MPa)	731	563
Rolling Shear Modulus, G_s (MPa)	73.1	56.3

Table 2.2: Floor Slabs – Design Properties (adapted from Nordic Structures, 2020)

CLT Stress Grade	E1(L = 1950 F_b – 1.7E S-P-F MSR and T= No.3 / Stud S-P-F)		
Layer Combination	105-3s	143-5s	175-5s
Bending about the Major Strength Axis (y-y)			
Bending Moment Resistance $M_{r,y}$ (10^6 N-mm/m)	38	65	87
Shear Resistance, $V_{r\text{-}zy}$ (10^3 N/m)	31	43	52
Bending Stiffness, $(EI)_{eff,y}$ (10^9 N-mm^2/m)	1 081	2 514	4 140
Shear Rigidity, $(GA)_{eff,zy}$ (10^6 N/m)	7.3	15	15
Bending about the Minor Strength Axis (x-x)			
Bending Moment Resistance $M_{r,x}$ (10^6 N-mm/m)	1.3	5.0	11
Shear Resistance, $V_{r\text{-}zx}$ (10^3 N/m)	10	22	31
Bending Stiffness, $(EI)_{eff,x}$ (10^9 N-mm^2/m)	32	261	832
Shear Rigidity, $(GA)_{eff,zx}$ (10^6 N/m)	9.0	11	18

2.2 Motivation for Expansion in Mass Timber Construction

2.2.1 Building Tall Mass Timber Building

The vast portfolio of available sections with varying thicknesses and numbers of ply increases the difficulty of understanding how CLT panels will behave in a structure since the layers that make up a CLT panel significantly affect the performance and structural capacity of the sections. This is

particularly true considering fire exposure and the change in measured temperature profiles, charred depth, and mid-span deflections observed during experimental testing.

Knowing how these changes influence the panel in structural performance can assist in meeting the appropriate standards. Therefore, extensive experimental testing is crucial as the need and desire to build tall mass timber buildings grows in North America and worldwide. The objective of the National Building Code of Canada (NBCC 2020) is to limit the probability that combustible construction materials within a story of a building will be involved in a fire, which could lead to the growth of the fire, which could lead to the spread of a fire within the story during the time required to achieve occupant safety and for emergency responders to perform their duties, which could lead to harm to persons and damage to the building (NRC, 2015).

Advanced understanding is required to develop further and increase the practice of constructing mass timber buildings and the evolution of design standards. The critical limitation when designing such structures satisfies the fire safety requirements by ensuring a minimum of two hours fire resistance rating is achieved. Over the last decade, there have been extensive changes with increasing the overall height allowed for buildings primarily made of wood and the development of performance-based design standards. Although building taller mass timber structures was possible before the recent release of the NBCC 2020, following a performance-based design provided evidence that the method is safe concerning structural and fire designs. Before 2015 this limited wood structures to no more than four stories; then, with NBCC 2015, it increased to six stories, then with the recent release of NBCC 2020, this was doubled to twelve stories. However, this significant change in height became possible by integrating a design protocol known as Encapsulated Mass Timber Construction (EMTC). The overall objective is to limit the probability

that the mass timber elements significantly contribute to the fire spread and duration of a fire incident (Su, 2018). Or, when following the ASTM E119 standard for fire resistance testing, there are qualification criteria related to their structural resistance, integrity, and insulation for the assigned fire resistance time.

2.2.2 Encapsulated Mass Timber Construction (EMTC)

The release of NBCC in 2020 incorporated a type of construction known as Encapsulated Mass Timber Construction (EMTC), which is an alternative solution for tall wood buildings to meet the code objectives and functional statements pertinent to the requirements of the non-combustible construction (Su, 2018). EMTC is defined as a type of construction in which a degree of fire safety is attained using encapsulated mass timber elements with an encapsulation rating and minimum dimensions for the structural timber members and other building assemblies (CWC, 2020, p. V1-773). The mass timber elements are not directly exposed but instead protected (typically Type X gypsum boards), thereby delaying the effect of fire on the timber element and increasing the fire resistance. An example is seen in the UBC Brock's Commons building in Vancouver, BC. At the time of completion in 2017 was the tallest hybrid wood-based building, having 18 stories with an overall height of 53.0 m (Connolly et al., 2018). This shows not only that building tall wood buildings is possible but also how to ensure fire resistance requirements are met.

The plan of the said building included CLT slabs directly supported on glulam columns without any beams. This means the whole structural skeleton was made from mass timber products. Apart from two exceptions: the foundation/first story and the staircase and elevator shafts were concrete to provide lateral stability from wind and earthquake loading. Additionally, to ensure a safe fire design, all but the top floor incorporated EMTC. Leaving the top floor exposed was to showcase

the novel construction methods used and inspiration for future tall mass timber buildings. What is essential to understand is that fire can only spread upward. Thereby leaving only the top floor left exposed means it does not interfere with fire safety and the protocols for leaving exposed combustible structural elements.

2.2.3 Exposing Mass Timber Elements

An advantage when designing Mass Timber buildings is the architectural concept of the structure. However, the development and use of EMTC in the latest release of the NBCC come at the cost of losing the appearance and natural beauty of the product. Therefore, there needs to be further knowledge and framework developed on exposing mass timber elements. As wood is a combustible product and having it make up a large percentage of a compartment fire surface area, it can increase the fire load and significantly affect the room's fire dynamics and overall structural system. Such effects include raising heat release rates, increasing compartment gas temperatures, higher incident heat fluxes to structural elements, prolonged fire duration (longer fully developed fire stage), more serve external flaming, etc.

Another concern that needs to be considered is whether the fire resistance of a building element obtained from the standard test might not represent its fire performance in natural/compartment fires (Li et al., 2015). As with natural fires, the time-temperature curves are hotter and shorter compared to a standard fire with distinct stages of growth, fully developed burning, and eventual decay stages. In comparison, standard fires have no decay but ever-increasing furnace temperatures with temperature up to 1260°C at an 8-hour duration. This means the period of higher temperatures experienced in natural fire testing could have sizeable effects on the panels' structural performance as it directly correlates to how quickly the timber burns and the loss of structural

resistance. The fire performance of CLT slabs under natural fire was studied by Mindeguia et al. (2021), Wiesner et al. (2020), and Li et al. (2015), thereby, realistic conditions with consistent results having higher charring rate values than those given in Eurocode 5. Additionally, Lineham et al. (2016) concluded the need for developing and validating a more detailed and rational procedure to model and predict the structural fire response of CLT elements exposed to non-standard fires. The current guidance in Eurocode 5 is used to determine the standard fire resistance of timber elements and may not be directly applicable to non-standard testing.

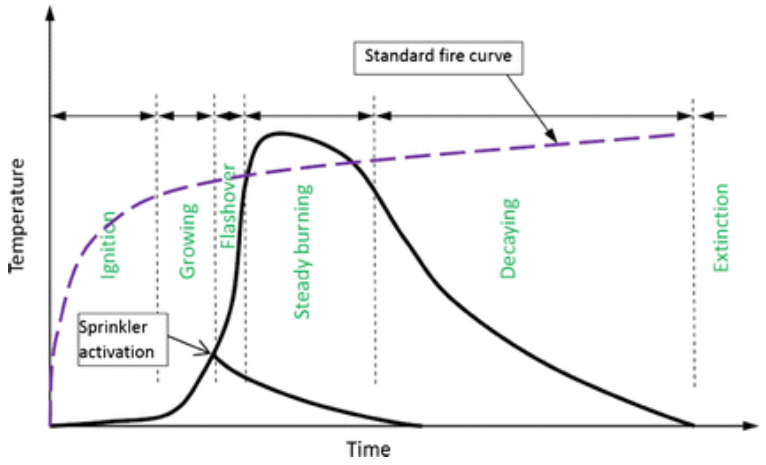

Figure 2.3: Illustration of a general compartment fire, a sprinkler-controlled fire and the standard fire (adapted from Zhang et al., 2012)

Limits on having exposed combustible materials in NBCC under section 3.1.6.4, shown in Table 2.3. To permit some exposed mass timber in EMTC with the understanding that it would unlikely increase the fire risks significantly to the life and property (Su et al., 2021). Therefore, having exposed mass timber elements is possible. Still, to increase these values, the implication and change in fire dynamics must be well understood as structures must expect surviving burn-out while considering the impact on fire development, the ability to undergo self-extinction, and the

ability of the system to support the applied loading during and beyond the fire event (Hopkin et al., 2020).

Table 2.3: Proposed Limits for Exposed Surfaces in EMTC from NBCC

Permitted Code-Prescribed Scenarios for Exposed Surface(s)		Limit of Proposed NBCC (2020) Section 3.1.6.4
1	Wall(s) only (facing one direction)	35% of total suite perimeter wall area
2	Wall(s) (facing one direction) + Ceiling (FSR ≤ 150)	Wall(s) at 35% total suite perimeter wall area + ceiling at 10% total suite ceiling area
3	Ceiling only	10% of total suite ceiling area if FSR ≤ 150 or 25% of total suite ceiling area if FSR ≤ 75
4	Beams/Columns/Arches only	10% of total suite or fire compartment perimeter wall area
5	Beams/Columns/Arches + Ceiling (FSR ≤ 150)	B/C/A at 10% of total suite or fire compartment perimeter wall area + ceiling at 10% of total suite ceiling area
6	Beams/Columns/Arches + Ceiling (FSR ≤ 75)	B/C/A at 10% of total suite or fire compartment perimeter wall area + ceiling at 25% of total suite ceiling area

Flame Spread Rating (FSR): is an index or classification indicating the extent of spread-of-flame on the surface of a material or an assembly of materials as determined in a standard fire test as prescribed in this Code.

Recent studies have attempted to expand the knowledge base on the possibility of exposing mass timber elements in the structure. One such was conducted by the National Research Council Canada, which included a series of compartment fires of five different scenarios to expand the understanding and technical basis for exposed mass timber elements in EMTC buildings without a significant increase in fire severity. Testing included five different scenarios, the first was fully encapsulated to provide a baseline and four different scenarios with unique combinations of amount and type of exposed elements. The amount of exposure and test results shown in Table 2.4.

When examining the influence of exposed CLT ceiling behaviour need to compare scenarios two, four and five. Test Two has a 10% of ceiling area and all of Wall A. Test Four has the entire ceiling exposed and a glulam beam running from Wall A to Wall C with one intermediate glulam column. Test Five has the ceiling fully exposed along with both Wall B and Wall C. The opening in Wall C was kept consistent for all tests, giving a ventilation factor of 0.03 $m^{1/2}$. This value was chosen to compare with a previous project where two ventilation factors were used, 0.03 $m^{1/2}$ and 0.06 $m^{1/2}$. The lower ventilation was picked for this project as in previous observations, the two values resulted in similar peak temperatures; however, the duration of the fully developed fire stage increased with a lower ventilation factor. Thereby creating a more severe fire exposure to the mass timber elements inside the compartment. Three wood cribs, made of 38 mm x 89 mm x 900 mm spruce pieces with a total weight of 360 kg, were used as the fuel load for each test, providing a fire load density (FLD) of 550 MJ/m^2 in the room. (Su et al., 2021) Tests were carried out until one of the criteria was met, either total burnout to self-extinguishment or an elapsed duration of 4 hours (240 min).

Table 2.4: Mass timber room compartment and fire test results (adapted from Su et al., 2021)

Component	Test 1	Test 2	Test 3	Test 4	Test 5
CLT Wall A	3 GB	Exposed	2 GB	2 GB	2 GB
CLT Walls B and D	3 GB	2 GB	2 GB	2 GB	exposed
CLT Wall C	3 GB	2 GB	2 GB	2 GB	2 GB
CLT Ceiling	3 GB	10% exposed 90% 2 GB	2 GB	exposed	exposed
Glulam Beam (327 mm x 457mm)	-	-	Exposed (4.54 m^2)	Exposed (2.46 m^2)	-
Glulam Column (457 mm x 457 mm)	-	-	Exposed (9.62 m^2)	Exposed (4.81 m^2)	-

Results	Test 1		Test 2		Test 3		Test 4		Test 5	
Flashover (min)	6.4		4.7		7.0		4.9		4.8	
GB back reaching 300°C	ceiling	walls	ceiling	walls	ceiling	walls	ceiling	walls	ceiling	walls
face layer (min)	16-19	15-20	20	16-21	20-22	19-23	-	15-25	-	18-23
mid layer (min)	30-35	51-54	-	-	-	-	-	-	-	-
base layer (min)	Nr	Nr	48-56	50-53	51-60	43-68	-	44-66	-	44-48
GB fall off time	ceiling	walls	ceiling	walls	ceiling	walls	ceiling	walls	ceiling	walls
face layer (min)	16-36	Nfo	95-135	70-90	86-125	Nfo	-	Nfo	-	230
mid layer (min)	Nfo	Nfo	-	-	-	-	-	-	-	-
base layer (min)	Nfo	Nfo	Nfo	Nfo	Nfo	Nfo	-	Nfo	-	250

Table 2.4: Mass timber room compartment and fire test results (adapted from Su et al., 2021), Continued

Results	Test 1	Test 2	Test 3	Test 4	Test 5
Test duration (min)	167	247	245	240	250
Wall A CLT char (mm)	0	50-95	38-56	17-45	38-87
Wall B CLT char (mm)	0	25-43	48-55	25-35	81-109
Wall C CLT char (mm)	0	3-42	30-79	34-40	50-90
Wall D CLT char (mm)	0	35	30-50	24-38	83-88
Ceiling CLT char (mm)	0	8-50 (45-63)*	0-66	47-66	70-90
Glulam char from each exposed side of beam (mm)	-	-	89-161	63-82	-
Glulam char from each exposed side of column (mm)	-	-	92-162	62-94	-

3GB: 1 layer of 15.9 mm thick Type X gypsum board + 2 layers of 12.7 mm thick Type X gypsum board

2GB: 2 layers of 12.7 mm thick Type X gypsum board

Nr: Not Reached 300°C

Nfo: No Fall Off

- Not used in Test Set-up

()* Exposed Ceiling Area

The study's main objective was to determine the fire performance of CLT panels manufactured with a thermal-resistant adhesive and how this altered behaviour and ability to resist the char layer fall-off. Whether this char layer falls off or remains intact, it has a significant effect on the fire performance of a CLT panel. Although it is important to note that no loading was applied to the compartment during testing, meaning loading was limited to the self-weight of the materials. After

this test series, there was no delamination of the CLT, even when the char proceeded past the bond line. Ultimately leading to a reduced charring rate as the char acted as a layer of protection to the inner layers. Tests 1, 2, and 4 had full self-extinguishment of the fire, with all fires having similar peak temperatures to the baseline with complete encapsulation. However, the fully developed fire stage was more prolonged for Tests 2-5, as the exposed timber added more fuel load to the rooms.

The main outcomes of this study are first that the type of adhesive used has significant effects on the panel's behaviour and that it is possible to avoid adverse effects that come with the delamination of CLT. Second, the results indicate that the current limits prescribed in the NBCC could be expanded. For example, Test 4 had much more exposed mass timber elements than the current proposed limit, yet it still achieved fire burnout and self-extinguished. As Test 2 verified the limits of exposed wall and/or ceiling surface(s) from Scenarios 1, 2 and 3 (Refer to Table 2.4) in NBCC. While Scenarios 3, 4, 5 and 6 for limits of exposed beam-column-arch and/or ceiling surface(s) are demonstrated by Test 4. (Su et al., 2021) Thusly, the amount of exposed combustible structural elements used in the study was unlikely to cause a significant increase in fire risk as results were highly comparable to Test 1. Therefore, further testing is required to expand our knowledge and develop the framework for exposing combustible materials. Currently, the building code has incomplete information in this regard and doesn't provide a meaningful way to evaluate or demonstrate safety. Showing that while these materials add to the fire load within a compartment, this doesn't necessarily correlate to an equal increase in fire risk. It is possible to expose mass timber products and maintain the required level of safety during fire events.

2.3 TCC Sections Background Research

Timber Concrete Composite (TCC) sections have been less extensively researched when subjected to fire as compared to normal temperatures. The idea of the composite sections is not new, as it stems from using each material in a way that exploits the strength of each material (Hozjan et al., 2019). Many different composite sections have been engineered using combinations of various building materials. The most common system is the combination of steel and concrete, but other composites include steel and timber, and timber and concrete (TCC). As the name suggests, TCC sections are composed of both wood and concrete aspects. Concrete is used to resist bending and compressive forces, and timber resists bending and tensile forces. Meaning TCC sections are designed to have the section's neutral axis located near the interface of the materials.

From a historical perspective, the concept of TCC first came during post-war reconstruction when the cost of steel was inflated. In the United States of America (USA), when hundreds of bridges were constructed using a combination of concrete and timber. The concrete slab protects the wood from water leaking, and the structural durability can be strongly enhanced (Nguyen et al., 2020). Nowadays, the motivation for using TCC sections is building tall timber buildings as they are an economically efficient solution for optimizing the floor performance, horizontal diaphragms, and the vertical bracing system (Auclair et al., 2016). The main incentive to understanding these sections is being able to build taller timber structures than what is currently allowed under the code. However, further testing is still required to verify and make design recommendations for such sections. The main factor prohibiting taller timber buildings is the required duration a structure must withstand fire without losing structural integrity. Therefore, understanding and developing proper design regulations must associate a correct and reliable fire resistance rating of

TCC floor assemblies. Currently, TCC floors are only being used in Canada's performance-based design. However, TCC sections have been used in other countries and are included in the European Code.

2.3.1 Types of Sections

The first important factor in understanding the fundamentals of the behaviour of TCC sections is understanding how the materials are used and the available different assembly types. Each type carries additional attributes that dictate the behaviour and response of the floor. The key reason for implicating such a flooring system is using multiple materials to exploit the strengths and minimize the weakness. As each construction material has benefits, TCC floors are always designed with concrete in compressive zones and timber tensile zones to use these strengths.

For TCC sections, two key assembly types of sections can be used: beam-type assembly and slab-type assembly. First, the beam-type group as shown in Figure 2.4 (a). It consists of a concrete slab supported by timber beams made of either mass timber or engineered wood products, typically Glulam. A thin wood layer can also be placed between the concrete and beams to act as permanent formwork. The second type is the slab-type assembly, as shown in Figure 2.4 (b). It consists of a concrete slab connected to a solid mass timber panel. While there are different options for the timber section, nail laminated timber (NLT), laminated stranded lumber (LVL), and cross-laminated-timber (CLT) panels, the most common is using CLT panels.

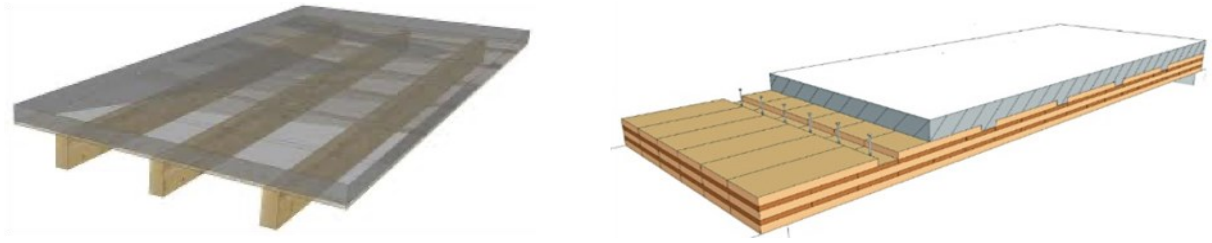

Figure 2.4: Schematic of assembly types of timber-concrete composite sections.

An important distinction between the two assembly types, besides the timber components being in either the shape of beams or slabs, is the exposure of the concrete to the fire. When considering the beam type assembly, both the timber sections and the concrete slab are directly exposed to the fire. While in the slab-type assembly, the CLT panels act as a protective layer for the concrete, thereby changing the temperature exposure to the concrete and resulting in different fire responses of the floor system depending on which type of assembly you are designing. This research will be focused on the slab-type assembly sections and utilizing CLT panels for the timber component.

2.3.2 Purpose and Advantages of Sections

Such sections can be used to retrofit or strengthen existing floor systems and in new construction of either residential or public building floors, bridges and prefabricated floors and walls (Auclair et al., 2016). Compared to traditional timber floors, the advantages of TCC floors include increased load-carrying capacity, reduced floor depth, reduction in floor weight, improved acoustic behaviour, and enhanced fire performance. Benefits over traditional concrete floors include a decrease in floor weight, increased renewable and sustainable materials, faster construction processes, and reduced formwork required.

2.3.3 Design of Connections

The key to benefitting from composite sections is understanding how to achieve composite action. The behaviour of TCC structures under bending is complex and further complicated by the phenomena of the non-linear behaviour of the material and connections (Auclair et al., 2016). Therefore, for TCC floors to be successful comes down to the understanding of the connection used. It is the crucial component of the hybrid system, and it must be strong and stiff enough to ensure an effective composite action (Hozjan et al., 2019). When it is not adequately designed, the two different materials would be working independently of each other, and both materials would experience tensile and compressive forces while not being designed in such a way to have the capabilities to absorb and resist such stresses. Therefore, the connection must be rigid to minimize the slip and strong enough to transfer the shear stresses through the interface between the materials. If this is achieved, then the section is forced to act as one, and there will be minimal tensile forces in the concrete and minimal compression in the timber sections.

The stiffness of the connection is how this behaviour is controlled, thereby influencing total stress distribution across the overall section. Theoretically, there are three possibilities: without connection, semi-rigid connection, and perfectly rigid connection. First, without connection, the section is not acting as a composite section, but rather the concrete is a dead load placed directly on the CLT slab. While having concrete slabs poured over CLT are being done to improve serviceability concerns with vibration and deflection. By having no connection, it is a missed opportunity to take advantage of the possibilities of TCC sections and increase the floor system's efficiency. This option results in the lowest bearing capacity of the cross-section with the most significant possible total normal stresses and deflections (Ogrin and Hozjan, 2021). The exact opposite would be a perfectly rigid connection with no horizontal slip between the two materials,

which means that the shear load is fully transferred and achieves full composite action. At the same time, this is the most desired type of connection as it results in the most significant bearing capacity and most efficient use of the materials cross-sections having minimal total normal stresses and lowest possible deflection. However, achieving this is practically impossible. Of the different connection types, the only possibility would be a glued connection, though these are not typically used due to the sudden and brittle failure mode. Therefore, the resulting connections that are used lie between the two extremes and are semi-ridged. Each connection type has different degrees between no connection and perfectly ridged and differences in failure mechanisms between more ductile or brittle failure.

2.3.3.1 Types of Connections

As previously mentioned, designing the connection is an essential aspect of designing TCC sections suitably and the variance in the different types. The ideal connection should be:

i) Strong enough to transmit the shear forces developed at the interface,
ii) Stiff enough to transmit the load with limited slip at the interface,
iii) Ductile enough to allow full load distribution and avoid failure on the fasteners,
iv) Other variables include connection cost, feasibility in practice or complexity.

Currently available and studied connections can only partially satisfy the requirements of an ideal connection. As slip cannot be neglected for most TCC assemblies, simple models are inefficient in the calculation procedure. Therefore, depending on the amount of slip at the interface affects the design of the connection and the system in its entirety. The choice of the connection will significantly influence the system's overall performance in both ambient temperatures and especially considering fire conditions. Literature on the design of TCC sections from the European

code groups the various connection types into four principal categories: dowel type fasteners, notches, notches combined with steel fasteners and other systems (e.g., nail plates, direct gluing, glued steel meshes). From Figure 2.5, it can be seen the research distribution of the different connection types. Assessment of the studies was mainly quantitative, with work that examined the mechanical properties of the connection and provided data suitable for analysis. Figure 2.5 (a) shows the main principal groups, and the (b) through (d) is the further division within the main groups. It is clearly shown that dowel-type fasteners occupy the largest percentage next to notch-type connections with/without steel fasteners. However, it is essential to note that this distribution is when examining completed research in the field and is not necessarily reflective of use in construction practice. It gives the picture of which connection types have the most scientific knowledge available when studying behaviour and designing for TCC slabs.

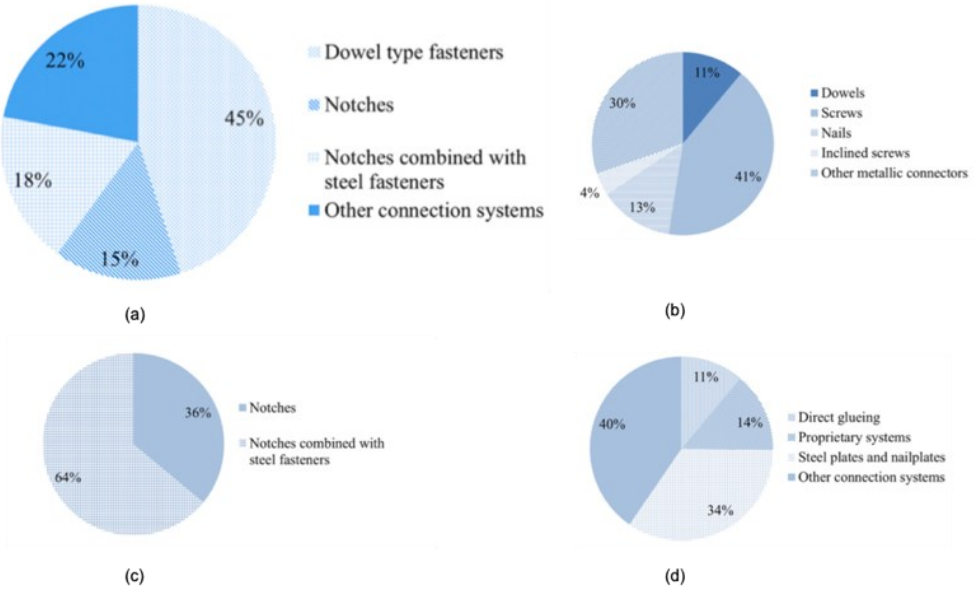

Figure 2.5: Distribution of research studied (adapted from COST Action FP1402, 2018)**.**

Values from Figure 2.5 (b) show that the use of screws dominates the use of different dowel-type fasteners, including screws and inclined screws. The screw is the most used fastener type out of

the group due to its high axial load-bearing capacity (COST Action FP1402, 2018). This is important for two key reasons. First, the axial load-bearing capacity could be necessary to improve the shear load transfer. Second to avoid the chance of separation between the materials. Therefore, this encourages using screws as the method of connection for TCC assemblies. This research will focus on the use of inclined screws for the connection type, specifically, how the degree of inclination affects the behaviour of the slab while exposed to fire conditions. As this relationship is well understood and researched in ambient temperature, there is little information considering elevated temperatures. As with steeper screw embedment angles, the screw is exposed to the temperature increase earlier, thereby reducing the shear capacity more rapidly.

2.3.3.2 Self-Tapping Screws (STS)

Self-Tapping Screws (STS) are a commonly used type of connection in timber structures, whether as a type of connection or to strengthen a connection. They can either be full-threaded or partial thread, while in this application, the fully threaded is the preference as this results in a more uniform load transfer between the screw and the timber materials and provides a better withdrawal resistance, thereby influencing the strength and stiffness of the connection. STSs that are fully threaded is hardened to produce a high yield moment, tensile, and torsional strength, while the large threads provide reliable embedment in the timber elements (Gerber, 2016). A benefit of their inherit design is that typically no pre-drilling is required, meaning they are faster to install than their counterparts. It is making them cost-efficient connectors requiring significantly less quality control measures and skilled labour during installation.

2.3.4 Method of Calculation

When designing TCC sections, two fundamental approaches must be checked: the traditional γ-method and, more recently, the Elasto Plastic Method (EPM) refer to Figure 2.7. The first for when the applied load to the connection remains in the linear elastic region until the wood component fails. However, if the connectors reach their load-carrying capacity, the outer connectors will begin to deform plastically; thus, the EPM needs to be considered. In this case, a non-linear behaviour must be considered, as the section is subjected to failure from combined bending and tension. Furthermore, each method is more accurate depending on the connection type and behaviour. The γ-method is for when the shear connectors are more brittle or not allowed to yield. More accurately for stiff notched timber, mechanical and glued connections but inappropriate in the case of flexible connectors. In contrast, EPM was developed for dowel-type fasteners as it is more appropriate for shear connectors that are ductile and allowed to yield.

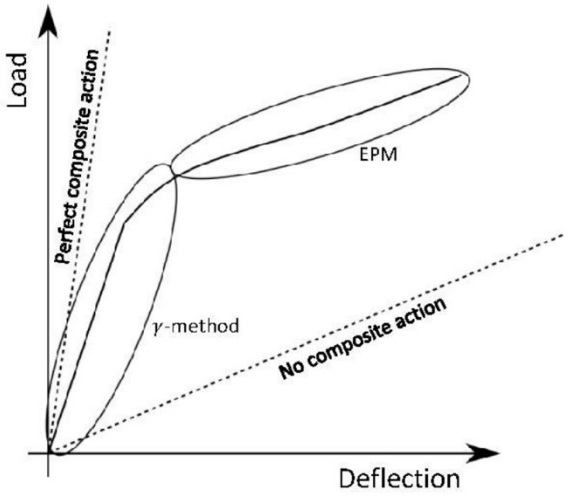

Figure 2.6: Calculation methods (adapted from Auclair, 2020).

Additionally, the initial assumptions of the EPM are the following:

i) The timber is subjected to combined tension and bending, resulting in brittle behaviour; therefore, linear elastic material behaviour is assumed,
ii) The timber portion of the TCC floor fails before the concrete exhibits' plastic behaviour; therefore, a linear-elastic model for concrete is used,
iii) The concrete in tension is neglected,
iv) In a fully composite section, the connection between the timber and the concrete is rigid,
v) The load-slip behaviour of the shear connectors is rigid-perfectly plastic.

2.4 CLT Behaviour under Fire

2.4.1 Research Methods

According to the reviewed articles, the research methods used while studying the fire performance of CLT panels can be seen in Table 2.5. The table provides a summarized breakdown of each study's experimental and numerical work. The critical difference is the type of testing, fire scenarios investigated, objectives, and modelling techniques. Full-size fire experiments are more desirable, as using larger specimens for fire resistance tests is more realistic and allows capturing the actual performance of structural components and assemblies under fire exposure. However, it is not always possible to perform such tests due to cost and laboratory capabilities and constraints. Therefore, some researchers performed smaller-scale tests. One such benefit is having samples with the same test parameters, thereby providing consistency in results; as for investigating the effects of different fire scenarios, comparing the influence of standard fire and natural compartment fires is very beneficial.

Figure 2.7 illustrates the different testing schematics for the natural fire conditions adopted in the experimental study conducted by Mindeguia et al. (2021). Figure 2.8 shows a general fire resistance test setup adopted in the experimental research conducted by Wang et al. (2020), which is also a typical schematic for standard fire tests of CLT floor assemblies. Most of the fire testing completed when studying the behaviour of CLT floor slabs followed standard fire testing conditions. It is the most straightforward approach for comparing results with different parameters or materials for equivalent fire severity. However, studying test specimens under natural fire conditions allows a more accurate representation of fire in a realistic setting. The key benefit of natural fire exposure is adjusting for different ventilation conditions. This mainly affects the fire growth rate, as when a fire reaches the point of flashover, this influences the duration of the steady state burning stage of the fire. The studies conducted by Mindequia et al. (2021) and Wiesner et al. (2020) were both part of the Epernon Fire Test Programme, a multi-partner collaborative research project launched in 2017 and focussed in its studies on the comparison between natural and standard fires in their effects on buildings.

Table 2.5: Summary of experiments conducted in the reviewed articles

	(Frangi et al., 2009)	(Mindeguia et al., 2021)	(Schmid et al., 2018)	(Wang et al., 2020)	(Wiesner et al., 2020)
No. of Test	11	5	25	10	5
Type/Size of Test	Small scale	Full scale	Small scale, (comparison to large scale tests performed IVALSA)	Small scale	Full scale
Dimension	1.15 x 0.95 m	5.90 x 3.90 m	Spans of 0.9 m and 1.5 m	1.8 x 1.2 m	5.90 x 3.90 m

	(Frangi et al., 2009)	(Mindeguia et al., 2021)	(Schmid et al., 2018)	(Wang et al., 2020)	(Wiesner et al., 2020)
Total Thickness	All 60 mm	All 165 mm	95 mm and 150 mm	All 105 mm	All 165 mm
Number of Ply's	Varying from 3 to 5 (Changing thickness of ply.)	5 ply of 33 mm	5 ply of 19 mm and series with (42+19+28+19+42) thicknesses	3 ply of 35 mm 5 ply of 21 mm	5 ply of 33 mm
Fire Scenario	Standard fire	Standard fire and natural Fire	Standard fire (some ambient temperature tests conducted)	Standard fire (some ambient temperature tests conducted)	Standard fire and natural Fire
Material Type	Spruce boards C24	Spruce boards C24	C24 strength boards	Canadian Hemlock grade E1	Spruce boards C24
Relationships that are studied during experiments	Measured temperatures, charring behavior,	Temperature fields, charring rates, mid-span deflections	Residual cross-sections, temperature measurements, (IVALSA test compared charring rates, temperature profile)	Temperature distribution, charring rate, fire resistance, mid-span deflection	In depth temperatures, deflection response, load bearing capacity

	(Frangi et al., 2009)	(Mindeguia et al., 2021)	(Schmid et al., 2018)	(Wang et al., 2020)	(Wiesner et al., 2020)
Type of Modeling	Only compared results existing Simplified Bilinear model adopted by EN 1995-1-2	Model based on 'Zero Stiffness Layer' which is complementary to conventional 'zero strength layer'	2 Step Process (i) residual cross-section, (ii) load bearing capacity of partly heated residual cross-section	3D Finite Element Method: looking at relationship of wood, cohesive elements, heat transfer and thermomechanical	Semi-Probabilistic Structural Model to predict reductions in flexural capacity

To demonstrate the importance of ventilation conditions and how a good understanding of the fire dynamics is necessary to predict the behaviour of the material being tested, the researchers followed the three different scenarios shown in Figure 2.7. All scenarios have different in-depth temperatures and structural behaviour recorded. Another important distinction between the fire experiments presented in the cited articles was the design and setup of the experiments and how the change of study parameters was altered. For the studies conducted by Frangi et al. (2009) and Wang et al. (2020), the primary study parameter was changing the thickness and number of plys used in the composition of the CLT panels, as well as the corresponding changes in the temperature profile and charring rate of their test specimens. In the study conducted by Mindeguia et al. (2021), the structural capacity of the CLT panels was investigated, while Wiesner et al. (2020) examined the thermo-mechanical behaviour of the CLT panels. All four studies mentioned above compared how the respective structural behaviour of the CLT panels in question changed during different

fire scenarios. In the study of Schmid et al. (2018), the focus was on the simulation through computer modelling of the CLT behaviour to develop simplified design equations.

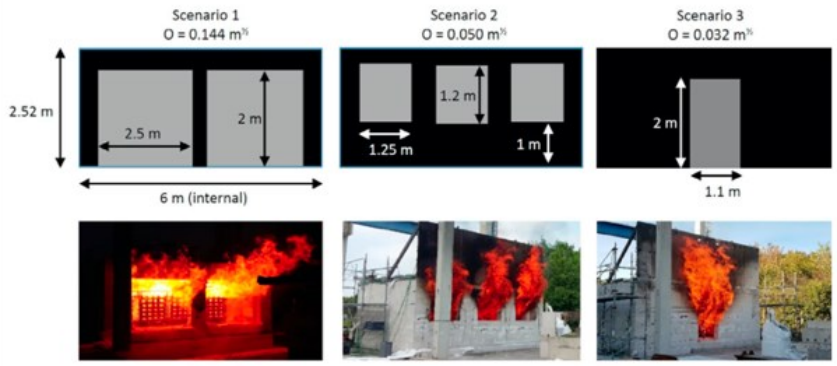

Figure 2.7: Illustration of compartment configurations and corresponding opening factors for three different natural fire tests (adapted from Mindeguia et al., 2021).

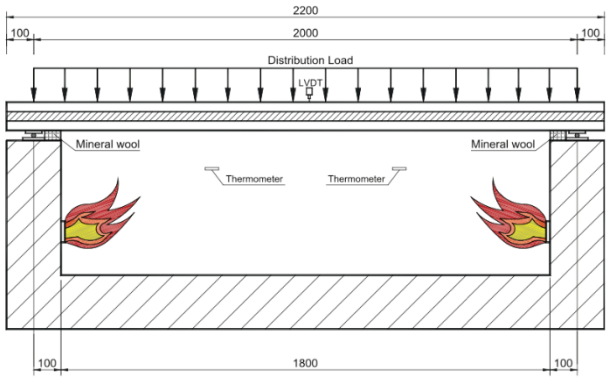

Figure 2.8: General fire test setup for CLT floor slabs (adapted from Wang et al., 2020).

2.4.2 Measured Temperatures

As with studying the fire performance of any construction material, it is crucial to understand the development and progression of heat transfer within the material. It is even more critical with CLT panels and other engineered wood products, such as glulam, LVL, etc. Such products are not homogenous, and their composition involves adhesives, even in relatively small amounts. Having

accurate temperature readings throughout the sections is critical, as this information is essential to determine the actual charring rates and depths. Thermocouples' installation procedure and orientation may considerably influence the in-depth temperature measurements (Wang et al., 2020). This means that poorly placed or improperly used thermocouples could affect thermal measurements and the resulting design calculations.

It should be noted that the thermocouple locations include different depths into each ply, thereby allowing temperature change tracking throughout the lamellas. This is important as the char line between charred and heated wood is determined when the 300°C isotherms are reached in the cross-section (Frangi et al., 2009). Thus, knowing when specific depths of the cross-section reached this temperature, it is predictable how much of the panel is still uncharred and able to sustain the applied loading for a particular fire duration. The measured temperatures are also necessary to compare different test parameters. It is a very effective way to determine equivalent fire severity, especially when similar specimens are experimentally tested under both standard and natural fire scenarios. It is worth mentioning that all-natural fire scenarios (refer to Figure 2.7) had much higher heating rates than those of the standard fires. This is justifiable as heating rates are directly correlated to opening factors since smaller opening factors cause less oxygen availability.

2.4.3 Charred Depth

An important characteristic when determining the fire performance of timber materials is evaluating the loss of cross section due to charring. When wood is exposed to increasing temperatures, a process of thermal degradation (pyrolysis) occurs, producing combustible gases and a mass loss (Frangi et al., 2009). When fire contacts wood, a charred layer on the side of contact is formed, and as the heat continues to grow, the thickness of the char layer increases.

Advantageously, this char layer protects the remaining uncharred core of the cross-section that is not yet exposed to fire. However, there is still a reduction in the cross-section area sustaining the applied loads. When studying the fire performance of CLT panels, a significant difference in the cross-section overall fire resistance is whether the charred layer falls off or remains intact. If the charred layer falls off, the protective function it gives is lost; thus, a new char layer starts forming. When these layers fall off, there is an increase in the charring rate as the temperature to the inner layers is exposed to greater than the initial temperature at the beginning of the fire test. A similar relationship is seen when a structural element has a fire protection layer applied, and when such a layer is removed, pyrolysis increases. This behaviour in CLT panels is mainly dictated by the type of adhesive used during the manufacturing of the CLT panels, as there are adhesives that are less sensitive to temperatures.

Accordingly, it is necessary for CLT panels to study the difference between local and global layers falling when subjected to fire. This results in a different strength capacity and charring rates; however, when locally charred pieces fall off, it is difficult to identify since the thermocouples can only measure temperatures at the locations they were installed. In general, the nominal charring rate of solid and glued-laminated timber sections under one-dimensional standard fire exposure is 0.65 mm/min, given by Eurocode 5.

As expected, the results from Wiesner et al. (2021) for the estimated char depths of the fires with higher heating rates initially had more rapid charring rates, as seen in the three natural fire scenarios (Scenarios 1, 2 and 3). However, the first natural fire scenario (Scenario 1) experienced the earliest and most rapid decay, halting the char progression in the second ply of the panel at a depth of 45 mm. While in the second natural fire scenario (Scenario 2), the char layer progressed

through the second ply and continued slightly into the third ply with a final char layer depth of 74 mm. Whereas in the third natural fire scenario (Scenario 3), the char layer advanced further through the third lamella during the decay phase of the fire until reaching a depth of 85 mm. While due to the specific profile of the standard fire time-temperature curve with ever-increasing temperature, the char layer depth in the tested CLT panels under standard fire exposure was 99 mm and 93 mm, for standard fire scenarios (Standard 1 and Standard 2), respectively. This suggests that the charring rate alone is insufficient for predicting the residual loading capability of CLT panels.

The different burning durations primarily cause the char layer depth at failure; however, it can also be attributed to the varying charring rates throughout the burning durations (Wiesner et al., 2020). While for the study conducted by Wang et al. (2020), the charring rate was found to be higher than the nominal charring rate (0.65 mm/min). This is believed because the CLT panels used in the said experiments were not edged glued. The gap between the lamellas gradually increased as the fire progressed, leading to local two-dimensional (2D) fire exposure and increased charring rate. Based on the developed time-temperature curves of those experiments, it was also concluded that the locally falling off might be the dominant condition for the five-ply CLT panels. Frangi et al. (2009) focused in their study on how the thickness of the lamellas altered the behaviour of the CLT panels. According to their research, the conclusion is that thicker layers are more favourable regarding fire performance than sections with thin layers. CLT panels with thinner layers lead to reduced time at which the fire exposed layer falls off, causing the next inner layer to become exposed to increased temperature once the external layer falls off. Therefore, the char layer depth recorded by each group of researchers is an important parameter as it influences the residual strength of the CLT section that remains after fire exposure to sustain the applied loads without collapse. While, in general, the values agree reasonably well with the standard value from Eurocode 5, there is still

some differences (Mindeguia et al., 2021). The charring rate was calculated at 0.71 and 0.75 mm/min for the CLT slabs exposed to the two standard fires. At the same time, the slabs exposed to the three natural fire scenarios were less well predicted. Other variances in experimental results included a change in the manufacturing process, as in the results of the study conducted by Wang et al. (2020), or a change in the adhesive type used, as in the results from the study conducted by Frangi et al. (2009). In summary, the char layer depth is an essential parameter for CLT sections; however, it is also important to base design recommendations on additional factors, such as those shown by comparing the effects of standard and natural fire scenarios on CLT panels.

2.4.4 Deflection

Deflection is a crucial parameter during experimental testing of structural elements under flexure bending and is often used as the control variable. Meaning tests are not carried out until total collapse but when the specimens can no longer sustain the applied loads. Or, when a particular deflection increasing rate has been reached, which for the study conducted by Wang et al. (2020), a deflection increasing rate of $L^2/9000d = 4.2$ mm/min (with L is the clear span of the CLT panel, and d is its total thickness) was used as the failure criterion. It should be noted that the acceptable level of deflection is much greater during a fire than at ambient temperature, where serviceability limits restrain structural elements' deflection under flexure bending. This is unlike the situation in the fire where the main objective is to allow enough time for occupants to evacuate the building and for firefighters to extinguish the fire.

From Mindeguia et al. (2021) the CLT panel midspan deflection rate correlated well with the rate of temperature increase. This good agreement is believed to be a consequence of the steep thermal gradients developed during the early stage of fire tests. It is also important to note that the third

natural fire scenario (Scenario 3) deviated significantly earlier than all other fire scenarios, mainly due to the progression of heat through the CLT panel, which resulted in its collapse at 108 minutes. The CLT panel exposed to the third natural fire scenario (Scenario 3) had the most significant increase in temperature, leading to the early deflection increase trend. In contrast, the CLT panels exposed to the first and second natural fire scenarios (Scenarios 1 and 2) did not collapse. Although the CLT panel exposed to the second natural fire scenario (Scenario 2) did not collapse during the fire development or the initial decay phase, it did experience a total collapse after 29 hr from the onset of heating. Due to the continued internal smouldering, which is a behaviour that needs to be studied further. It should be noted that no water was ever applied to the test assembly before failure occurred.

The midspan deflection values achieved by Wang et al. (2019) increased with time but formed a plateau after approximately 20 minutes in fire tests, and then, they continued to increase again but in more of an exponential trend. This can be attributed to the fact that the charring of the first strong layer (in the major strength axis) led to an upward shift in the location of the neutral axis of the CLT cross-section. As the char layer progresses into the second layer (in the minor strength axis), this delays the fire influence on the third strong layer (the very top layer in the case of a three-ply CLT panel). It is worth mentioning that the flexure bending strength of the CLT panels tested in the cited studies is governed mainly by the strong layers that are in the major strength axis, which in this case are aligned with the panel span, instead of the weak layers that are in the minor strength axis which are in the transverse direction of the CLT panel. Therefore, the increase in deflection is at a plateau as the char front progresses through the weak lamellas, which is why Wang et al. (2020) suggest that three-ply CLT panels should be avoided in the design of elements subjected to flexure bending with relatively high load levels. In other words, once the char front

has passed the first ply, there is not enough strength remaining in the CLT panel to sustain the applied loads as the CLT panel is basically down to only the top ply in the case of the three-ply panel.

2.4.5 Behaviour of Adhesives

Although using wood products instead of mass timber have benefits and is more economical, one of the disadvantages is the factors in determining their fire performance due to the behaviour of the adhesive used. That is why there is difficulty in modelling the fire performance of these sections due to the lack of knowledge on the behaviour of the bond when exposed to fire. One such study is by Okuni and Bradford (2020), who studied the behaviour of adhesives used on CLT and worked on developing the modelling of the temperature performance. It involved three wood species: Douglas Fir (DF), Southern Yellow Pine (SYP), and Spruce Pine Fir (SPF). As well included three different adhesives: melamine formaldehyde (MF), phenol resorcinol formaldehyde (PRF), and polyurethane (PUR).

Looking at the thermal-structural behaviour of the different wood species with the increase in temperature. The purpose of this was to act as a control experiment and to be able to compare with the results from the different adhesives. It is important to note that when designing EWP like Glulam and CLT, they are designed to have failed in the wood before failure occurs in the adhesive, which means understanding the best adhesive to use, we must know the strength that they must succeed. Comparing how the maximum stress and strain reduces with the temperature increase. When examining the maximum stress the SYP having the greatest values, followed by DF and SPF. Comparatively when studying strain versus temperature SPF had higher values followed by

DF and SYP (Okuni and Bradford, 2020). Showing that different tree species have different thermal-structural properties, and this need to be considered when designing members.

Next, look at the thermal-structural behaviour of the different adhesives when exposed to fire conditions. Likewise, the maximum strain reduces with the increase in temperature, with PRF having the highest values, followed by MF and PUR. The stress response of DF is also plotted to show that all adhesives are greater than the wood species. Thereby verifying that the failure will occur in the wood before the adhesives. Examining the differences in stress value can determine that MF and PRF have better thermal structural properties than PUR and therefore, should be recommended in the production of CLT panels (Okuni and Bradford, 2020). Furthermore, PUR has the highest strain, followed by PRF and MF. This implies that there are higher chances of delamination occurring for PUR than for PRF and MF. Therefore, the recommendation of types of adhesives to use is either MF or PRF as they have better thermal properties and are less likely of delamination occurring.

2.4.6 Numerical Analysis

The ability to simulate the fire behaviour of CLT panels through computer modelling is a challenging task to perform with a high level of accuracy. However, such an alternative approach to studying the fire behaviour of CLT panels is vital as fire testing is a very costly and time-consuming task to undertake. Through verified accurate simulations, it is possible to optimize the design of various CLT panels with different layup and thicknesses in fire conditions. Another advantage of finite element (FE) computer models is that they can be specific for each purpose and provide structural engineers with a performance-based approach in designing floor systems for most rapidly growing tall timber buildings. Nevertheless, the FE modelling of timber sections

is a complicated procedure due to the natural imperfections that are possible in the wood material and how this can influence the behaviour of timber members. Wood can also be characterized by three orthogonal planes of material symmetry: longitudinal, tangential, and radial. While this behaviour can be modelled, it is difficult to determine its mechanical parameters, and they usually have a wide variance in values. This is getting more complicated when dealing with the unique layup of each CLT panel with lamellas in opposite directions, accurate representation of charring rate, and behavioural changes due to the type of adhesive used. Two critical methodologies are available: (a) The Reduced Properties Method (RPM), which uses modification factors; and (b) The Effective Cross-Section Method (ECSM), which uses the zero-strength layer. Studies carried out by Schmid et al. (2018), Mindeguia et al. (2021), and Wiesner et al. (2021) all concluded that ECSM is favourable for CLT panels as the RPM can lead to uneconomic design in many cases. The zero-strength layer is a thickness added to the char layer to give the timber a total thickness that needs to be neglected when performing strength calculations due to fire exposure. Although the material next to the char front has not entirely burned, its strength has begun to degrade significantly. It is worth mentioning that the study conducted by Mindeguia et al. (2021) proposed a modification to this by considering a zero stiffness Layer.

The general structural analysis process and the bending capacity of the heated cross-section of CLT panels follows a typical process as illustrated by Schmid et al. (2018). The first to determine in that process is the temperature field of the thermal analysis and how heat transfers through the CLT cross-section. Next is applying the material properties to the layers in the major strength axis. As the strength and stiffness of the transverse layers (in the minor strength axis) are set to be negligible, it is assumed that the longitudinal layer account for the total flexure resistance of the CLT panel in the major strength axis. This assumption is justified due to the low wood strength

values in tension perpendicular to wood grain and the low rolling shear capacity. Next is the calculation of the area, and when the temperature in the CLT panel reaches 300°C (charring temperature), the charred cross-section area of the element is set to zero. When a segment is charred, it has lost almost all its strength and consequently can no longer sustain the applied loads. Lastly, the distribution of strains of all elements is calculated with respect to the equilibrium of the applied stresses and areas in the tension and compression sides of the CLT panel cross-section.

2.5 Concrete Behaviour under Fire

There are many factors when considering what type of concrete should be used when making TCC sections, as many different adjustments can be made in the mix design of the concrete matrix. It is these decisions that dictate the behaviour of the slab under fire conditions. Meaning the behaviour of the concrete is dependent on thermal, mechanical, and deformation properties and the phenomena of fire-induced spalling. The thermal properties determine the extent of heat transfer to the structural member. In contrast, the mechanical properties of constituent materials determine the extent of strength loss and stiffness deterioration of the member. The deformation properties, in conjunction with mechanical properties, determine the magnitude of deformations and strains in the structural member. In addition, fire-induced concrete spalling can play a significant role in the fire performance of reinforced concrete (RC) members (Kodur, 2014).

2.5.1 Thermal Properties

The thermal properties that influence the behaviour of the concrete include thermal conductivity, specific heat, and mass loss. These properties are significantly influenced by the aggregate type, moisture content, and composition of the concrete matrix. First, thermal conductivity is defined as the rate at which heat is transferred by conduction through a unit cross-section area of a material.

The variation in the data is mainly attributed to moisture content, aggregate, test conditions, and measurement techniques used in the experiment (Kodur, 2014). In general, can conclude that thermal conductivity decreases with the increase in temperature, and the amount of decrease depends on the concrete's mix design.

The second thermal property is specific heat, defined as the amount of heat required to raise the temperature of a material by a degree. When concrete is exposed to fire, it is susceptible to physical and chemical transformations. A factor is the moisture content as one of the many transformations includes the vaporization of free water at 100°C. The specific heat of concrete changes accordingly with the water-to-cement (w/c) ratio used. The aggregate types also have significant effects, as different minerals and rocks have various heat capacities. Carbonate aggregate concrete has a high heat capacity, which helps minimize spalling and enhance structural members fire resistance (Kodur, 2014). Specific heat is relatively constant up to 400˚C followed by a steep incline in the 700˚C range.

The last thermal property to consider is mass loss controlled by the concrete's density, and the concrete's density decreases with increasing temperatures. However, the aggregate type significantly influences the mass loss in concretes. This is shown by comparing the behaviour of concrete made with carbonate and siliceous aggregates. For siliceous based aggregate mixes, there is minimal mass loss even at 600°C. While with carbonate-based aggregates, there is significant mass loss once the temperature passes the 600°C mark. This is attributed to the dissociation of dolomite in carbonate aggregate at around 600°C.

2.5.2 Mechanical Properties

The mechanical properties that influence the behaviour of the concrete include compressive strength, tensile strength, and stress-strain response. Unlike the other properties, mechanical properties have been extensively researched and studied under fire conditions. However, a difficulty with these studies is that unlike testing in ambient temperature with specified specimen sizes as per the standards, the testing completed for fire performance is conducted on a wide range of specimens (Kodur, 2014). This is due to the lack of standardized testing when studying mechanical properties under fire conditions.

The first mechanical property that should be studied is compressive strength behaviour. This is important to understand, as the advantage of using concrete is its high compression resistance capabilities. There is a greater variation when looking at HSC compared to NSC. The reason for this is believed to be either fire-induced spalling, which will be discussed later or the testing apparatus's limitations. These variations can also be explained by the wide range of testing procedures and the changes in the heating, loading rates, specimen size and curing conditions at the testing (Kodur, 2014).

The second mechanical property when looking at the effects of fire on concrete is tensile strength. It is well known that concrete has approximately 10% tensile strength compared to compressive strength. TCC sections are designed with concrete only in the compression zone, so the loss in tensile strength should not influence the design. However, that is on the condition that the section acts as a composite, meaning it is still important to understand the changes in tensile strength to understand the section and material fully. Especially considering that the cracking that occurs in

concrete is typically due to tensile stresses and the structural damage of the member in tension is often generated by the progression in microcracking (Kodur, 2014).

Furthermore, this behaviour can become critical when Fire Induced Spalling behaviour occurs. Studies completed on NSC and HSC and the variation in results from various researchers where the loss in tensile strength is more gradual for NSC due to weaker microstructure allowing cracks to form. While with the HSC, the loss develops quicker because of the much stronger microstructure resulting in the build-up of pore water pressure causing spalling effects.

The final mechanical property that needs to be considered when studying the fire performance of concrete is the stress-strain response. This is important as stress-strain relations are often used as input data when designing models for evaluating the fire resistance of concrete structural members. Typically, with the decrease in compressive strength and increase in ductility of concrete, the slope of the stress-strain curve decreases with increasing temperatures (Kudor, 2014). The curves begin with a linear relationship followed by a parabolic response until reaching the peak stress and then a quick descent until the point of failure. It's important to note that until the temperature reaches $500^{o}C$ the peak stress reached before the descent is similar. As well as the increase in temperature, the peak stress corresponds to an increased amount of strain, especially 500˚C and higher. Therefore, it can be concluded that the stress-strain response is highly influenced by increasing temperature for both NSC and HSC.

2.5.3 Deformation Properties

The deformation properties that influence the behaviour of the concrete include thermal expansion, creep, and transient strains. Which are all highly controlled by the chemical composition, the type of aggregate, and the chemical and physical reactions that occur in the concrete during heating

(Kodur, 2014). The first of these properties is thermal expansion which is defined as the ability of matter to change in terms of shape, area, volume, and density, in response to a change in temperature. When concrete is subjected to fire conditions, it generally undergoes thermal expansion due to the aggregates and the cement paste, especially between the range of 20-700°C. Many factors change the effect thermal expansion has on concrete, including moisture content, chemical reactions, and microcracking resulting from nonuniform thermal stresses.

The other deformation properties that should be considered are creep and transient strains, which are highly enhanced at elevated temperatures under compressive stresses. Creep is defined as deformation under a sustained load and a long-term effect. Meaning that the older the concrete structure is when it experiences fire conditions will influence the behaviour controlled by creep. It is influenced by the movement of moisture in the concrete matrix. It is accelerated mainly by two processes: (1) moisture and dehydration of concrete due to high temperatures and (2) acceleration in the process of breakage of the bond (Kodur, 2014), while transient strains occur during the first time of heating and not during any successive heating. These strains are caused by different factors, including the chemical composition of concrete and mismatches in thermal expansion that lead to internal stresses and micro cracking in the concrete constituents (Kodur, 2014). Although there is limited research and information into how these factors affect concrete during fire conditions. Likely due to how these deformations form and their long-term effects when studies are typically analyzed in short-term duration.

2.5.4 Fire-Induced Spalling

Fire induced spalling is a phenomenon that is unique to concrete and can be the governing factor in determining the fire resistance of the section. It is defined as breaking up and falling off layers

of concrete when exposed to rapidly rising temperatures. As previously discussed, it is much more of a concern in the behaviour of the beam-type assemblies because the concrete slab is more exposed. Although there are studies completed on understanding this property, there are still conflicting statements. Some experiments reported explosive spalling occurring, while others reported little spalling observed. It is believed that the reason for this is the high number of factors and interdependency that control this behaviour. While there is no exact answer or explanation, there are two broad theories to explain this behaviour.

The first is pressure build-up of the pore pressure during heating caused by the vaporization of water, and the vapour cannot escape due to the high compactness of the matrix. It is theorized that this explains fire induced spalling because when the effective pore pressure exceeds the tensile strength of concrete, chunks fall off from the structural member (Kodur, 2014), which means following this theory as permeability decreases it effectively increases the effect of spalling. The second theory considers restrained thermal dilatation close to the heated surface. This leads to the development of compressive stresses, which are released, causing brittle fractures of the concrete or spalling. However, the onset of the instability is controlled by the pore pressure in the form of explosive thermal spalling (Kodur, 2014).

Therefore, many researchers seem to conclude that the primary causes are the low permeability of concrete and moisture migration in concrete at elevated temperatures (Kodur, 2014). Additionally, the effects of fire inducing spalling are significantly increased when examining HSC compared to NSC. This is because HSC has a lower permeability due to the dense microstructure, as it does not allow moisture to escape, resulting in a greater pressure build-up of pore pressure. When designing HSC, a significant decision and factor is the fire performance because of the dramatic results that

spalling can cause. Lastly, it's important to note that the current modelling that is being done does not include the effect of fire-induced spalling when examining TCC sections. Still, observations have been made when running experiments.

2.6 TCC Sections Behaviour at Ambient Temperature

The majority of currently completed studies are TCC sections studied in ambient temperatures. With the vast portfolio of different TCC sections that are possible in terms of sections, other timber and EWPs, and connections, there is an enormous amount of research on the topic. However, only a few investigations have been completed recently after streamlining to focus on sections utilizing CLT panels and STSs as shear connectors. Table 2.6 lists four studies conducted within the past six years. Many factors influence the design of the screw-type connections: overall dimensions, embedment, angle, and spacing. Those decisions alter the strength, stiffness, and general behaviour in flexure bending.

Table 2.6: Research on screw connections in TCC utilizing CLT

	(Gerber, 2016)	(Higgins et al., 2017)	(Mirdad & Chui, 2019)	(Salem and Virdi, 2021)
Type of Assembly	Slab Type	Slab Type	Slab Type	Slab Type
Test Method	Shear Tests and Flexure Bending	Flexure Bending, Orthotropic Stiffness, Full-Scale System Performance, and Long Term Creep	Shear Testing	Shear Testing
Dimension of Shear Tests	500 x 200 mm	-	400 x 200 mm	1000 x 600 mm
Dimension of Bending Tests	6000 x 600 mm	3048 x 610 mm	-	
Wood Component	CLT and others	CLT	CLT and others	CLT
Wood Dimension	3 ply, 99mm	5 ply, 175mm	5 ply, 175mm	3 ply, 105mm
Concrete Thickness	70mm	57mm	75mm	50mm
28-day Strength	Design: 30 MPa Tested: 45.5 MPa	Design: 34.4 MPa Tested: 37.5 MPa	Tested: 39 MPa	Tested: 30 MPa
Steel Reinforcement	Wire mesh for tensile cracking	#3 reinforcing bars spaced at 12 in. O.C.	Wire mesh for tensile cracking	-
Screw Arrangement	30° In line with bending profile, 45° Pairs	45° In line with bending profile,	30° Pairs 45° Pairs	45°
Spacing Longitudinal	150mm High Shear, 300mm Low shear	305 and 610mm	-	150 and 200mm
Transverse Spacing	200mm	305mm	-	2 screws: 400mm 3 screws: 250mm

Table 2.6: Research on screw connections in TCC utilizing CLT, Continued

	(Gerber, 2016)	(Higgins et al., 2017)	(Mirdad & Chui, 2019)	(Salem and Virdi, 2021)
Screw Length	240	219 mm	150 and 200 mm	100mm
Screw Embedment Length	100, 110, 150	133 mm	80 and 100 mm	65 mm
Screw Diameter	8 and 10 mm	8 mm	11 mm	8 mm
Insulation Layer Examined	Foamular® C-200 extruded polystyrene rigid, 25mm	-	Soundproofing layer made of polyester felt and elasto-plastomer bitumen 0, 5, 15 mm	-

2.6.1 Shear Testing

As previously mentioned, when studying TCC sections, a highly influential factor is the connection's behaviour in the system's success. Without first examining the various types of connections, it wouldn't be possible to design the overall section for in situ loading properly. But it is not just deciding between multiple types of connectors but the design specifications of each connector that influence the result. For STS, there are many design considerations, mainly the overall dimension in terms of length and diameter, inclination angle, longitudinal and transverse spacing, and inclusion of an interlayer between the timber and concrete material. Each has different pros and cons in the assemblies' behaviour and performance.

Work completed by Gerber in 2016 included an extensive experimental program studying different types of connections used in different timber materials and testing variances of each type of connector. Sections including STS can be seen in Figure 2.10, with (a) screws at 30 degrees, (c) screw pairs at 45 degrees, and (e) screw pairs at 45 degrees with an interlayer. Each resulted in

separate load-displacement curves Figures 2.10: (b), (d), and (f). The research included different screw lengths, two screw diameters, two inclination angles, and the inclusion of an interlayer. Alternatively, the work completed by Mirdad and Chui (2019) can be seen in Figure 2.9. The study included three different parameters. From the legend, each test was given a title naming the parameters, an example being L80-I0-45°, where (L) is the embedment length of the screw in the timber, (I) is the thickness of the insulation layer used, and lastly the degree of inclination to the horizontal. Figure 2.9 shows how much variance depends on which STS is used and confirms the importance of understanding the relevant relationships.

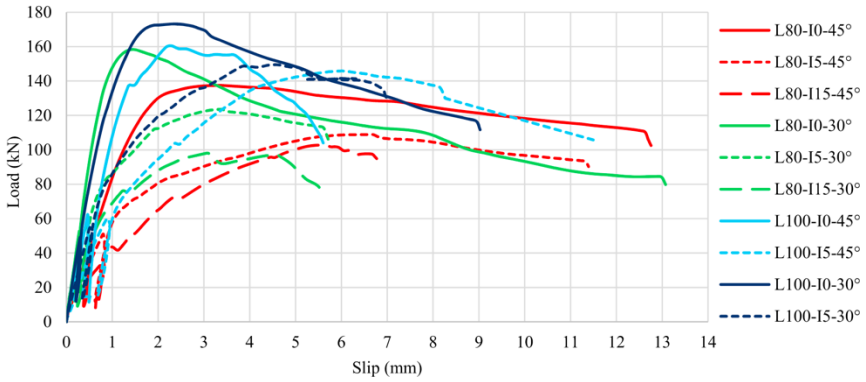

Figure 2.9: Load – Slip curves (adapted from Mirdad and Chui, 2019).

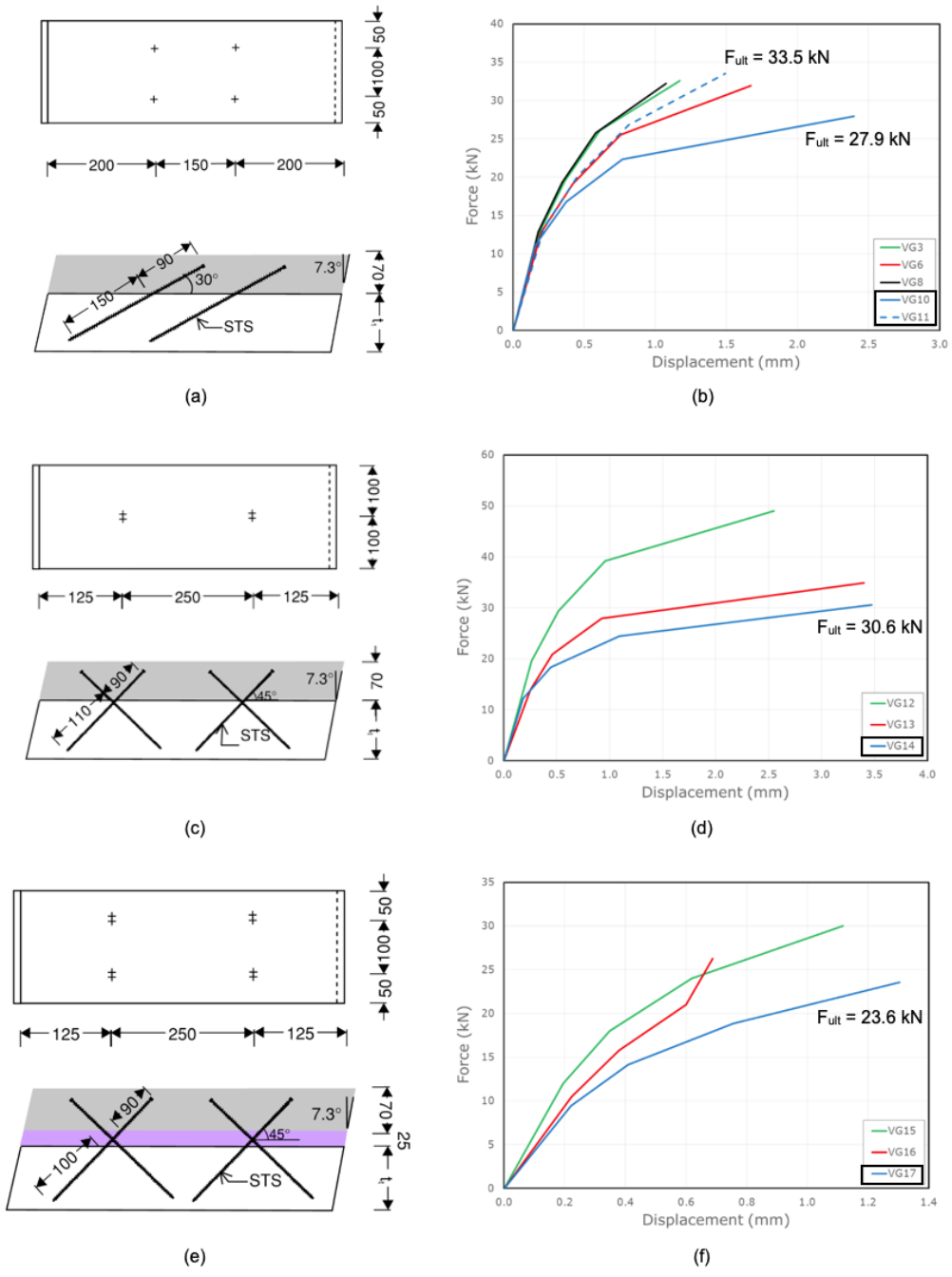

Figure 2.10: Specimen geometry and connector layout: (a) screws at 30°, (c) screw pairs at 45°, (e) screw pairs at 45° with insulation, averaged load slip curves: (b) screws at 30°, (d) screw pairs at 45°, (f) screw pairs at 45° with insulation (adapted from Gerber, 2016).

2.6.1.1 Overall Screw Dimensions

A starting point when designing STS connections for TCC sections is the overall dimension of the screws. This comes down to two key parameters: the screw diameter and embedment length in the timber. The influence of screw diameter is examined in work completed by Gerber (2016). It was found that the stiffness at the serviceability load levels was not impactful; however, the increase in strength was significant when increasing the screw diameter. While the cost per screw would be higher, it is expected to be cost-effective by installing fewer screws correlating to a reduction in labour hours. At the minimum would be able to break even by choosing a more expensive screw because of more efficient installation.

Like the effects the screw diameter has on the assembly's behaviour, the connection's strength is more sensitive to embedment length than stiffness. The two studies had separate observations for effect on stiffness. Whereas Gerber only observed a significant increase in stiffness at ULS levels of deformation. Figure 2.10 (b) shows the variance in peak load for each specimen; when the embedment length equals 150 mm, the peak load is 27.9 kN compared to 210 mm and peak load 33.5 kN. This means having a 40% increase in the embedment length equalled a 20% increase in the peak load. At the same time, Mirdad and Chui (2019) noted a significant influence on serviceability stiffness in all cases, Figure 2.9 and Table 2.7. The discrepancy could be related to the effects of the two different screw inclinations and arrangements. As for tests completed by Gerber (2016), the screws were single screws at 30 degrees, while Mirdad and Chui (2019) had pair screws placed at 30 and 45 degrees. Regardless, the difference there is a shown difference when altering the embedment length both for strength and stiffness. This is logical as it directly

correlates to extra length into the timber component and increases the withdrawal resistance. A greater load is required for the connection to fail and for the screw to be pulled out from the timber.

However, it is essential to note that other factors must be considered when choosing an embedment length. Firstly, the angle at which the screw is to be driven. As with a shallower angle, you gain greater embedment length for less embedment depth. Thereby affecting the strength and the stiffness of the connection. Secondly, don't want the screws to penetrate the bottom of the timber component. Especially when considering fire, as when the screw is exposed to the fire, the shear resistance provided is reduced proportionally to the remaining screw in uncharred timber. Thereby, a safe fire design would want adequate material between the end of the screw and the bottom of the section for the screw to protect against the damaging effects of fire for an appropriate duration in the fire event.

2.6.1.2 Screw Inclination Angle

From the completed research, the effects of altering the inclination angle can be seen. Three different arrangements were compared: STSs inclined to match the anticipated shear flow at both 30 and 45 degrees from the horizontal and STS screw pairs at 45 degrees with one driven in both tension and compression directions.

First, to compare the two different insertion angles. When single screws are used at each location, they are orientated to carry loads in tension and driven to follow the deflective shape of the floor. The results of the work completed by Mirdad and Chui (2019) show that as the insertion angle is decreased (closer to horizontal), the ultimate load-carrying capacity of the connection increases, regardless of the embedment length. Although connections included an insulation layer (I5 or I15),

the increase was much more insignificant when there was no insulation. Note that for tests, L100-30° had weaker concrete than L100-45°, which explains the variance in results.

Results from Mirdad and Chui (2019) when studying stiffness on the first and second loading cycle show the serviceability stiffness, an average 38% increase when the angle is 30 degrees compared to 45 degrees. This indicates that the overall stiffness of the connection is more sensitive to the angle rather than the strength. This is opposite to the influence of the diameter and screw embedment length, where strength is more influenced. Therefore, a smaller angle is a benefit as it increases the withdrawal strength and stiffness of the screw.

Secondly, the results comparing the difference between using two screws as composed to one can be seen in the work completed by Gerber (2016). Screw pairs mean there is no normal force generated between the materials. Thus, the stiffness and strength of the connection are purely controlled by the proportioning and spacing of the connectors. Also, having such an arrangement simplifies the installation process, as it is not necessary to anticipate the shear flow at every location. However, as previously mentioned having the screws at 45 degrees makes less efficient load-carrying capacity for a screw while simultaneously increasing the embedment depth for the corresponding embedment length.

2.6.1.3 Screw Spacing Arrangement

A decision when designing TCC connections is the overall layout and placement of the screws, both in the longitudinal and transverse directions, choosing between reducing spacing or increasing the number screws to provide a safe design. Each has reasonable limitations in terms of spacing and end distances that need to be accounted for. In addition, would want to achieve the most economical design possible to keep the number of screws required at a minimum, considering the

cost per screw and the labour required for installation. Work completed by Salem and Virdi (2021) examined three parameters: longitudinal spacing, quantity in the transverse direction, and age of concrete. Where spacing was reduced from 200 mm to 150 mm, increasing the quantity per row from two screws to three screws and concrete age at 14 and 28 days.

The maximum load was achieved with the three screws and the shorter distance of 150 mm. However, what was interesting was reducing the spacing or increasing the number of screws in the row resulted in a similar difference in maximum load. When you change from three screws to two screws at 200 mm spacing, the difference in maximum load is 59 kN. While keeping two screws and decreasing the spacing from 200 mm to 150 mm, the difference in maximum load is 54 kN. Proving minimal difference between the two alternatives. Although the authors recommended increasing the number of screws over decreasing the spacing as this allows a more uniform distribution of the shear stresses in the transverse direction of the composite section.

2.6.1.4 Influence of Interlayer

The motivation behind using insulation in composite slabs is strongly correlated to the advantages of the TCC section utilizing CLT panels instead of CLT panels on their own. That is the increased acoustic and thermal response. The resulting behaviour of the section depends on which type of material is used as the interlayer. While both Gerber (2016), Mirdad and Chui (2019) used interlayers in their respective studies, the findings were different as the behaviour is material dependent. Both studies, the screws were drilled through the insulation; the interlayer was a complete barrier between the CLT panels and the concrete.

Work completed by Gerber (2016) used Foamular® C-200 extruded polystyrene rigid insulation with a thickness of 25 mm. The arrangement for the screws was the 45-degree pairs; although

shown not the most efficient angle of inclination, having the compression screw means no additional compressive stress coming from the axial load in the screw, which tends to crush the insulation (Gerber, 2016). The difference is not significant by comparing results from the 45-degree cross pairs without and with insulation. Figures 2.10 (d) and (f) can see a reduction of approximately 29.6% in peak load by including insulation. But while there is strength loss, it is relatively similar. Adding insulation between the material improves acoustic performance and effectively increases the static moment arm of the elements relative to their centroids. This results in a stiffer overall panel with a weight reduction compared to an assembly without insulation, contingent on the connector maintaining reasonably similar strength and stiffness (Gerber, 2016).

Mirdad and Chui (2019) completed an in-depth study focused on the effect of having an interlayer in TCC assemblies. However, their research used a soundproofing layer made of polyester felt and elasto-plastomer bitumen. Each has a thickness of 5 mm, and three different amounts were studied: 0 mm (no interlayer), 5 mm (single layer), and 15 mm (three layers). Results can be seen for strength and serviceability stiffness changes in Table 2.7 and previously in Figure 2.9. Table 2.7, the reduction percentage is due to the presence of an insulation layer. The respective reduction is increased as the thickness of the insulation is increased. The strength is reduced on average by 17% for 5 mm and 34% for 15 mm. At the same time, stiffness is reduced by 35-50% for 5 mm and 55-60% for 15 mm. Results show that the stiffness of the section is more influenced due to the presence of the interlayer than strength. The exact relationship to how the inclination angle affects the STSs and the opposite of embedment length and screw diameter.

Therefore, the materials used for these two studies were different in material and corresponding mechanical properties, thereby the results are not directly comparable. Nevertheless, examining

this layer's influence on the section is essential to develop a complete understanding of the makeup of TCC slab assemblies. There are definite benefits of including interlayers in the design but must consider the type of material and not allow the section to be compromised in terms of overall and connection stiffness and strength.

Table 2.7: Connection test results per pair of screws (adapted from Mirdad and Chui, 2019)

Specimen	F_{ult} (kN)	Strength Reduce (%)	$K_{(0.4)1}$ (kN/mm)	Stiffness Reduce (%)	$K_{(0.4)2}$ (kN/mm)	Stiffness Reduce (%)
CLT-L80-I0-45°	33.61	0%	24.71	0%	56.35	0%
CLT-L80-I5-45°	27.70	15%	14.70	41%	31.78	44%
CLT-L80-I15-45°	24.27	28%	11.05	55%	25.89	54%
CLT-L80-I0-30°	41.88	0%	45.76	0%	92.76	0%
CLT-L80-I5-30°	31.55	25%	25.88	43%	52.49	43%
CLT-L80-I15-30°	25.04	40%	18.02	61%	43.79	53%
CLT-L100-I0-45°	44.23	0%	36.57	0%	80.45	0%
CLT-L100-I5-45°	35.85	19%	17.21	53%	38.42	52%
CLT-L100-I0-30°	39.66	0%	47.37	0%	83.27	0%
CLT-L100-I5-30°	36.07	9%	27.31	42%	53.15	36%

2.6.2 Flexure Bending

After the successful completion and understanding of the shear connectors, the subsequent step in testing is studying full-scale specimens under flexure bending. To replicate in situ loading and induce forces in the slab to observe behaviour. In terms of ultimate strength capacity and compare load vs. displacements curves. In Table 2.6, the experiment specifics can be seen for two studies that completed Flexure Bending programs. Gerber, in 2016 after extensive research of shear tests, used an efficiency equation to determine the relative achievement of composite action. With such, choose 9 with efficiencies in the 85-95% range and tested under four-point flexure bending. Including a TCC section using CLT with screws at 30 degrees orientated in the direction of shear flow; refer to Figures 2.10 (a) and (b) for shear test results. The spacing in the longitudinal direction alters, with a spacing of 150 mm in the high shear zone and 300 mm in the low shear zone. Refer to Figure 2.12(a) for a schematic of the bending specimen. Higgin et al. (2017) also conducted flexure bending tests as a part of their program. However, their samples were tested under three-point flexure bending. They utilized a screw connection with screws at 45 degrees orientated in the shear flow direction with two separate spacing arrangements. First, referred to as closely spaced screws where all spacings are kept at 305 mm, Figure 2.11 (a). The second was widely spaced screws, where high shear zone spacing was equal to 305 mm and low shear was 610 mm, Figure 2.11 (b).

While both types of flexure bending are widely used, the four-point flexure bending is often more favourable. As with the three-point flexure bending, the maximum bending stress occurs at a small, concentrated point under the loading point. As for the four-point flexure bending, the maximum region is spread between the two loading points. Common practice typically uses the three-point flexure bending when materials are homogenous and four-point flexure bending when

nonhomogeneous, such as wood and composites. Regardless, both are accepted forms of testing the flexure behaviour of the sections.

2.6.2.1 Bending Stiffness

While each previous parameter influences the strength and stiffness of the overall composite section and is necessary to design the composite properly, it ultimately comes down to the performance in flexure bending and the corresponding bending stiffness from the load-displacement curves. Results from Gerber (2016) can be seen in Figures 2.12 (b) and (c). The figure to the left is loaded up to service level, and to the right is the load applied until failure occurs. The test was duplicated, with the first reaching a peak load of 74.4 kN, while the second did not fail until 93.1 kN. This difference in ultimate values and load-displacement curves indicates the need for further testing and validation before being able to predict behaviour and the maximum capacity of the section.

Test results from Higgins et al. (2017) can be seen in Figure 2.11(c). The test results for closely spaced screws are in blue, and widely spaced screws are in green. Other tests of note are CB-CLT1 and CB-CLT2 in red, as these are the same tests on plain CLT panels, not TCC sections. To provide a direct comparison between variances in connectors and all the benefits of designing TCC sections themselves. However, the two specimens exhibited different stiffness and strength, showing the need for further testing. As for the results from the TCC sections, the values to the right of the figure show peak load and displacement at the time of peak load. Showing consistency between the repeated tests and minor differences in the spacing arrangements. The closely spaced screws increase the ultimate load by 14.9% from the widely spaced specimens.

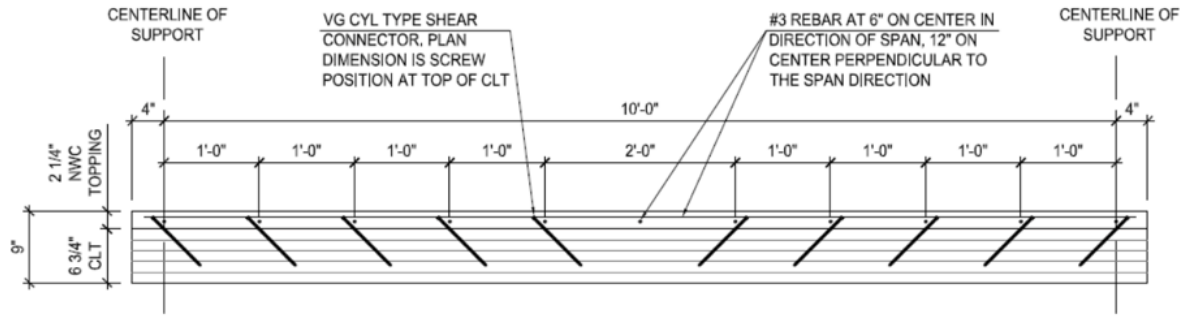

(a) Closely Spaced STS (CB-SC)

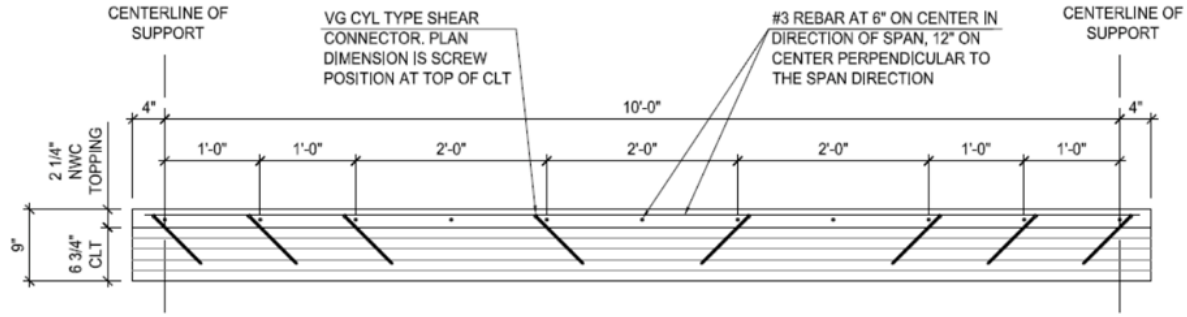

(b) Widely Spaced STS (CB-SW)

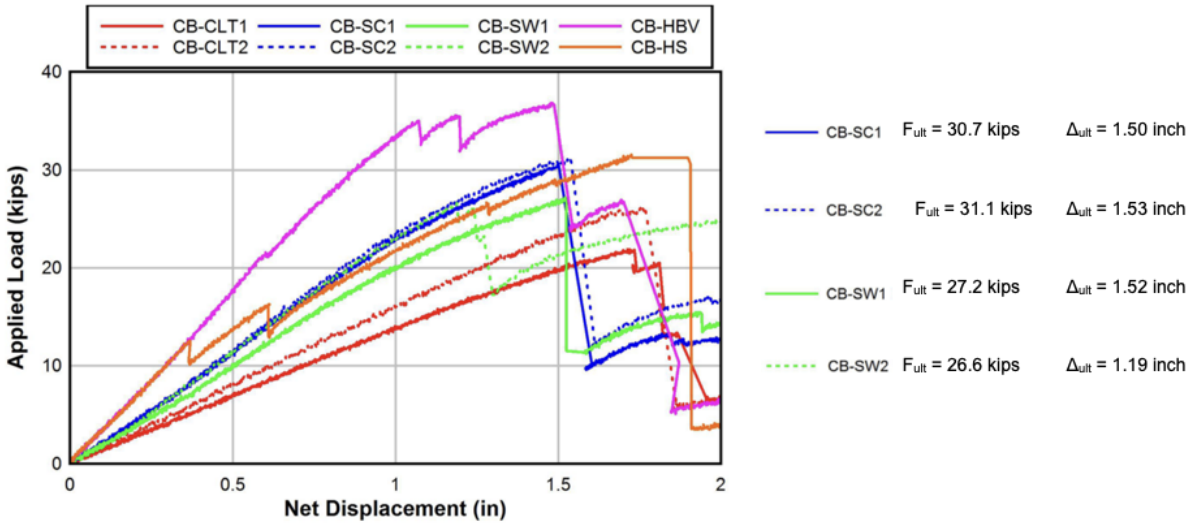

(c) Overall Midspan Displacement Response

Figure 2.11: Flexure bending results (adapted from Higgins et al., 2017)**.**

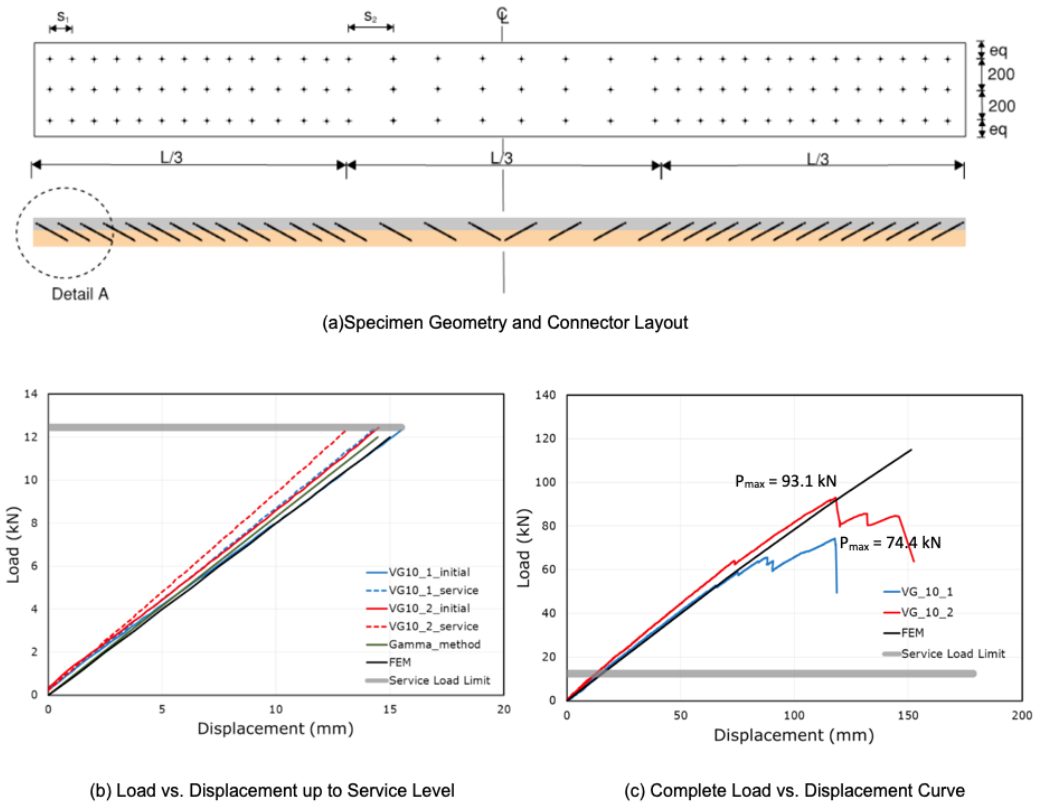

Figure 2.12: Flexure bending results (adapted from Gerber, 2016).

2.6.2.2 Failure Mode

The final parameter studied during any experimental testing is recording the failure mode of the section. Knowing the section's capacity is mandatory, but it is also essential to understand the failure mode. Typically, TCC sections, especially when considering slabs that utilize CLT panels and screw connections, resulting in a brittle failure mode. As observed in tests completed by Gerber (2016), all flexure bending specimens using screw connections and CLT have a brittle failure, specifically a timber facture. However, the author noted that the specimens that failed due to a brittle failure (concrete crushing or tensile fracture) occurred at much more significant applied loads than the sections that exhibited ductile failures (connector yielding or screw withdrawal).

This is important as while the panels did fail in a brittle manner, it would also be unlikely for the panel to reach such a load in a realistic loading condition, thereby providing safety in the overall design.

2.7 TCC Sections Behaviour under Fire

While TCC, when under ambient conditions, is more extensivity researched and studied both in terms of experimental and numerical analysis, there is lacking information when the fire conditions are involved. As previously mentioned, the need for further investigation when studying CLT panels when exposed to fire; the same goes for TCC sections. As for any TCC slab-type assembly, the behaviour of the overall floor is highly dependent on the behaviour of the timber component and the connections. Unlike the beam type assembly where both the timber and concrete are directly exposed to the fire and need to examine reactions in both materials. The slab type is where the concrete is protected from direct exposure to the fire until the timber material is gone. In most fire events, the temperature in concrete would not considerably change, as studies have shown minimal heat transfer from the connector to the surrounding concrete. Therefore, when assemblies that utilize CLT as the timber materials the principles of design are built from the core understanding of how the panel reacts. When a fire is considered, the material's ability to resist forces is affected due to the increased temperature and reduced timber area from the charring area. This loss in strength leads to a shift in the location of the neutral axis and, more crucially, the loss of stiffness from the connection. Complex thermal and mechanical responses must be considered when examining TCC sections exposed to fire, thereby increasing the challenge to develop both simple analytical methods and advanced numerical procedures to quantify the fire resistance according to the relevant codes (Hozjan et al., 2017). However, to develop such models, there is a

demand for more results to run comparative analysis to verify the reliability. Before forming such products there needs to be more material testing and more large-scale fire experiments on TCC sections. Table 2.8 summarises the completed research on screw connections in TCC assemblies when exposed to Fire. Note that limited data is available, as there are numerous ways to design TCC sections especially considering the type of sections, different wood materials, and various shear connection types.

Table 2.8: Research on STS in TCC exposed to fire (adapted from Shi et al., 2022)

	(Frangi et al., 2010)	(Caldová et al., 2015)	(Osborne, 2015), (Dagenais et al., 2016)	(Du et al., 2021)	(Shephard et al., 2021)
Timber Type	sawn and glulam	GLT	CLT, LVL	GLT	CLT
Connection	Screw (Ø6 x 150/100) oriented at ±45°	Screw (Ø7.3 x 150) oriented at 45°	STS (Ø8 x 180/100) oriented at 45°, Truss Plates, and lag screw (Ø13 x 152)	Screw (Ø12) oriented at ±45	Fully threaded screw (Ø9.35 x 200) oriented at ±45
Type of Test	Shear tests of TCC specimens; bending tests of TCC slab	Fire resistance tests of TCC floor	Fire resistance tests of TCC floor	Bending tests of TCC beam	Fire resistance tests of TCC floor
Calculation Method for Connection	Modification factor	-	-	Modification factor	-
Fire Numerical Modelling	-	3-D FE model	1-D FE model	3-D FE model	-

2.7.1 TCC with Screw Connections utilizing CLT Panels Under Fire

Limited research focused on the study of TCC sections using STS screws and having the timber component CLT. Two critical studies, from FPI Innovation and research completed by Shephard et al. (2021). See Table 2.9 for details of the assemblies, including specifics on each component of the TCC section and the relationships examined in the research. Results from each study show that using screws as the shear connector in TCC sections is effective.

Table 2.9: Research on screw connections in TCC slabs utilizing CLT when exposed to fire

	(Osborne, 2015) and (Dagenais et al., 2016)	(Shephard et al., 2021)
Type of Assembly	Slab Type	Slab Type
Test Method	Flexure Bending	Direct Shear and Flexure Bending
Dimension	4800 x 1829mm	4800 x 1200mm
Wood Component	CLT	CLT
Wood Dimension	5 ply, 175 mm	5 ply, 175 mm
Concrete Thickness	89 mm	57.2 mm
28-day Strength	30 MPa	34.5 MPa
Screw Arrangement	45° In line with bending profile	45° In line with bending profile
Spacing Longitudinal	406 mm	305 mm
Transverse Spacing	102 mm	305 mm
Screw Length	180 mm	200 mm
Screw Embedment Length	100 mm	150 mm

Table 2.9: Research on screw connections in TCC utilizing CLT when exposed to fire, Continued

	(Osborne, 2015) and (Dagenais et al., 2016)	(Shephard et al., 2021)
Screw Diameter	8 mm	9.53 mm
Other TCC sections	NLT with Truss Plates LVL with Lag Screws	NLT with Truss Plates
Fire Curve	CAN/ULC-S101	ASTM E119 Standard Fire
Loading Applied	Self-weight + 2.4 kPa	Distributed service load of 3.83 kPa
Relationships that are studied during experiments	Temperature Profiles, Charring, Deflection, Heat Transfer	Temperature Profiles, Charring, Deflection, influence of Panel-to-Panel Joint
Failure Criterion	Deflection	Deflection
Duration of Fire	214 min	187min

2.7.1.1 Temperature Data and Charing Behaviour

When studying any material or structural system exposed to fire, the critical data collection is temperature. Measuring the heat transfer rate from the side exposed to the top of the section. It is particularly interesting in TCC sections and learning to what level the connection transfers heat to the surrounding concrete. As previously discussed, research when examining CLT behaviour under fire when considering TCC utilizing CLT panels, the problem is as complex. Before confidently knowing the precise failure time, charring rate, or delamination effects, there still needs further investigation. However, comparing research done on either CLT panels alone or on TCC sections shows unmistakable similarities in behaviours and patterns.

For the panel studied by Osborne (2015), three key depths are important to note: the interface between the first three ply's (35 mm, 70 mm, 105 mm). The first ply was charred at 60 min, beginning to fall at 90 min, giving a char rate of 0.52 mm/min. The second ply was charred at 105 min, falling at 120 min, giving a charring rate of 0.68 mm/min. Then the third ply was charred at 150 min, falling at 180 min, giving a charring rate of 0.68 mm/min. Since the slab reached failure due to deflection at 187 min, the testing was terminated. Therefore, the charring rate began like that of the accepted European standard of 0.65 mm/min, but as the ply fell and delamination occurred, the charring rate further increased. Other temperatures of interest are at the interface, where there was only a slight increase of about 20°C and only 5°C at the mid-depth of the concrete. Last is the temperature of the screws, which increased by 93°C, but it's important to note that this didn't occur until the location of the screw tip reached a temperature of 100°C. The heat quickly transferred through the screw from the tip to the head and increased much more rapidly once the wood fell around the tip of the screw and was directly exposed to the fire. Although the temperature in the screw was raised, there was neglectable heat transfer to the concrete.

Similar patterns can be seen for the assembly studied by Shephard et al. (2021). The heat transfer from the exposed side to the interface (59°C) and into the concrete (72°C) was more significant. The charring rate since the first ply was 0.66 mm/min, and subsequent plys were 0.8 mm/min. Greater charring rates also lead to a greater loss of section with an average depth remaining 25 mm, which would be only the very top ply of the CLT panel. Unlike the previous study, where both the fourth and fifth ply remained. One reason for the difference could be that the adhesive that each panel is manufactured with, as previously discussed, affects the delamination occurrence. Although the placement of the screws and corresponding spacing is different, this would cause a

difference in the composite action behaviour and deflection, not the charring rate of the CLT panel. Another possibility is the influence that the panel-to-panel joint affects the performance of the floor. This is an area for future research, as the connection is the weak point when designing structural systems. If it is proven that having a panel-to-panel joint decreases the fire resistance time, then that would simultaneously affect the fire resistance for the entire flooring system, which is a much-needed topic for further exploration.

2.7.1.2 Deflection

Like testing CLT when exposed to fire when running tests on TCC section failure criterion is defection. As tests were not carried out until complete structural failure but when the sections were no longer load bearing. Additionally, for Shephard et al. (2021), this was two distinct times, first at 105 min when the loading was removed and then at 187 min when the floor could no longer carry self-weight. From Osborne (2015), the maximum defection before failure was 75 mm but rapidly increased to 210 mm after the structural failure occurred at 187 min.

CHAPTER 3: RESEARCH METHODOLOGY

While TCC sections have been studied for many years across various countries, limited testing and verification are completed in Canada. This shows that the possibility of TCC sections being implemented into the Canadian *Engineering design in wood* standard (CSA O86) requires more extensive experimental testing, computer modelling, and numerical analyses. Currently, TCC sections have only been designed using performance-based guidelines, as the prescriptive methods are still lacking in many of the published wood design standards.

After more data is obtained, trends can be studied and crossed examined. Thereby showing how the physical, mechanical, and thermal properties affect the structural behaviour of the TCC section and its overall design procedure. As previously discussed, several design parameters can affect the TCC sections' behaviour both at ambient and in fire conditions. For instance, assembly type, timber material, concrete properties, and shear connection type and dimensions are important design parameters. With such a wide variety of TCC sections having accurate design models not only simplifies the design procedure for structural engineers but is also cost-efficient, as experimental testing is expensive in terms of time and materials. Especially when considering fire testing, there is a faction of labs equipped to examine structural elements when exposed to fire. Therefore, when more experimental results are available, they can be used to validate computer models and analytical outputs, making it possible to exploit further and increase the use of TCC sections for floor systems in mass timber buildings across the country.

The reviewed literature highlighted a lack of research on TCC section's fire behaviour, especially when designed utilizing CLT panels as the timber component and STS as the shear connectors. Therefore, the experimental program of the current study was developed to investigate the

behaviour of TCC floor assemblies at elevated temperatures. The research carried out in this thesis is part of a larger research program being conducted on mass timber innovative structural systems at Lakehead University Fire Testing and Research Laboratory (LUFTRL) to study their behaviour when exposed to fire. This includes examining the different types of shear connectors utilized in TCC floor systems to enhance the fire resistance of such mass timber floor systems. Thereby providing comparative experimental results for further analysis and enriching the knowledge base for TCC floor systems in Canada.

3.1 Experimental Program

Following typical fire resistance design procedures, TCC floor assemblies were subjected to monotonic loading before being exposed to standard fire. Each floor assembly was exposed to CAN/ULC-S101 standard fire time-temperature curve for the fire tests of the research study presented in this thesis. In Canada, a minimum fire resistance rating of 45 minutes is required for structural timber components. However, considering the new era of erecting tall wood buildings and the introduction of EMTC, the goal has been changed to achieve a minimum fire resistance rating of 2 hours for buildings of more than six stories in height. Therefore, to accomplish the research objectives of this study, the following goals have been identified.

1. Achieving a 2-hour fire resistance for the TCC floor assemblies utilizing STS as shear connectors, thereby enhancing the fire performance of the CLT panels instead of being used separately as floor slabs.
2. Enhancing the understanding of the behaviour of TCC floor systems and their applications in Canada.

3. Verifying the actual charring rates and behaviour of CLT floor panels under one-dimensional heat transfer because of fire exposure.

3.1.1 Elevated Temperatures Testing

Fire endurance testing was carried out at Lakehead University Fire Testing and Research Laboratory (LUFTRL) located on the Thunder Bay campus, Ontario. The state-of-the-art facility, shown in Figure 3.1, accommodates a large custom-designed furnace with two natural-gas fed burners that can raise the furnace's temperature to 1300 °C. The furnace is equipped with a control panel that can be set to follow any fire time-temperature curve. The furnace compartment is within a large loading/supporting steel framed structure, Figure 3.2. The walls of the furnace include a strengthened heavy-steel plated exterior with thick Fiberfrax blankets lining the interior, Figure 3.3. The furnace is constructed so the large front door and roof panels can be removed using the 1-ton jib crane installed inside the facility. Thereby, allowing to install and then load different test specimens and assemblies with various configurations.

The roof panel is comprised of three separated strips that are joined together. As for this research, each of the 900-mm wide TCC floor slab was placed instead of the middle roof strip, thereby acting as a roof and being exposed to standard fire and thus, subjected to one-dimensional heat transfer from underneath, Figure 3.3. The overall dimensions of any TCC floor assembly are 5300 mm by 900 mm, with a clear span of 5000 mm. As the furnace itself is not load-bearing, the TCC floor slab rests on simple supports placed on the transverse beams of the exterior loading/supporting steel framed structure. Thereby, not the entire span (5000 mm) of the floor slab was exposed to fire, but rather a middle length equivalent to the interior length of the furnace chamber (3750 mm). This allowed 75% of the floor slab length to be exposed to fire as well as guaranteed keeping the

supports of the test specimens outside the furnace. Meanwhile, under the four-point flexure bending applied on the TCC floor slabs, the locations of the greatest shear, moment and deflection were always within the furnace chamber.

Additional vents on the furnace's floor and roof are present to facilitate the access of instrumentation and setup of fire tests. These furnace features allowed the fire tests to follow a similar experimental setup and methodology as that used during ambient temperature testing. However, for this experimental program, all instrumentation were installed from the top of the floor test assemblies and thereby located out of the furnace and not directly exposed to the increase in temperature.

Figure 3.1: Lakehead University Fire Testing and Research Laboratory – LUFTRL (Courtesy of Dr. Salem).

Figure 3.2: Large fire testing furnace accommodated at LUFTRL (Courtesy of Dr. Salem).

Figure 3.3: Interior of the testing furnace with one of the TCC floor test assemblies installed.

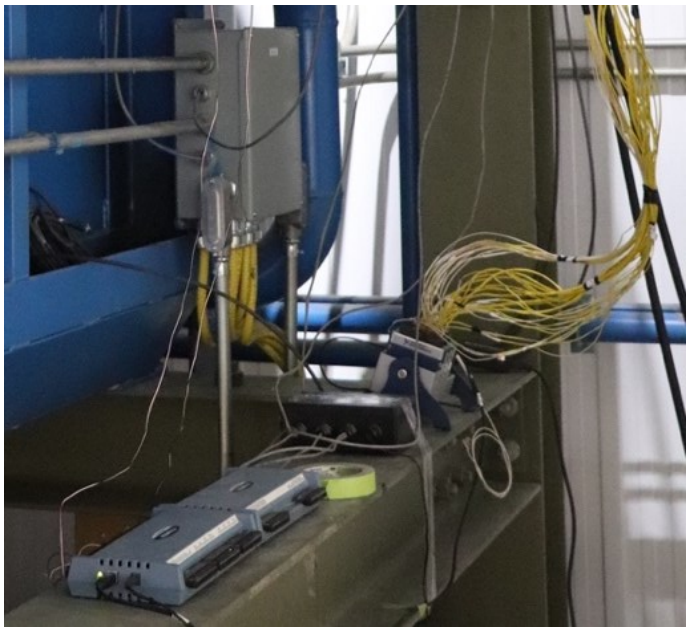

Figure 3.4: DAQ systems utilized.

3.2 Data Collection

To accomplish the objectives of this experimental study, measurements and experimental data are required to evaluate and quantify the performance of TCC sections when exposed to standard fire. Additionally, to study the behaviour of the STS connections utilizing the two different inclination angles and how well they affect ultimate behaviour. There are extensive studies examining TCC floor assemblies at ambient temperature; however, the influence of elevated temperatures on TCC's behaviour is still lacking. Also, it is essential to provide reference and insight into recorded visual observations of the floor assemblies as they were designed to achieve a fire resistance rating of 2 hours. Thus, fire tests were terminated shortly after reaching this fire resistance time mark. The critical data that needed to be captured were mainly temperature measurements and the overall deflections of the test assembly as the mid-span deflection was used as a control variable during experimental testing with the fire test being terminated once the assembly can no longer sustain the applied loading or the 2-hr duration has been achieved. Additionally thermal temperatures were

monitored to terminate the test once TC5 which is located at the interface between the third and fourth ply of the CLT panel reaches the wood charring temperature (i.e., 300˚C). Thermal measurements included furnace temperatures, external wood temperatures, internal wood temperatures, concrete temperatures, and screw temperatures.

3.2.1 Elevated Temperatures Testing

Test assemblies were loaded to the design load, including 2.0 kPa dead load (in addition to self-weight) and 2.4 kPa live load, to be representative of in situ loading for typically residential occupancy loading. Test assemblies were then exposed to elevated temperatures of the CAN/ULC-S101 standard fire time-temperature curve in the large-size fire testing furnace at Lakehead University's Fire Testing and Research Laboratory (LUFTRL). Each specimen was designed to achieve a 2-hr fire resistance, thereby doubling the fire resistance of the CLT panel as a standalone element as reported by the manufacture, Nordic Structures. The design of each TCC specimen and its shear connection was determined by adopting the clauses and equations in the Canadian Wood Design Handbook (2020), Design Guide for TCC Floors in Canada (Auclair, 2020), and European Design Code for screw capacity.

For the fire resistance testing, the failure criterion was determined when the mid-span deflection rate exceeded an acceptable rate. For this study, when the mid-span deflection rate reached an exceedance of $L^2/9000d$ = 11.92 mm/min or test duration exceeded 2-hr fire duration, the fire test was terminated. Therefore, it was essential that loading and corresponding deflection data were collected accurately to determine when the TCC section failed. In addition, during fire testing, the applied load must remain constant with respect to time. This way, the assembly would represent realistic conditions, deflect more because of the fire exposure, and show the decrease in load-

carrying capacity. Due to the highly elevated temperatures, placing any displacement transducer inside the fire-testing furnace at temperatures that could easily reach 800 – 900°C in about 30 minutes is impossible. Instead, displacements were measured at three locations along each slab, at the midpoint and at the location of the two-point loads, using three draw-wire displacement transducers installed above the furnace away from the elevated temperatures.

In addition to the mechanical measurements, thermal measurements must be captured during fire endurance tests. The furnace's control panel uses the temperature data from the furnace compartment to control the fire and allow the test to follow the corresponding standard fire time-temperature curve, Figure 3.5. It operates by taking the temperatures from the thermocouples installed in the furnace. This data in turn controls the flow of gas to lower or raise the temperature to regulate the temperature in the furnace compartment to follow the profiles of pre-programmed time-temperature curves.

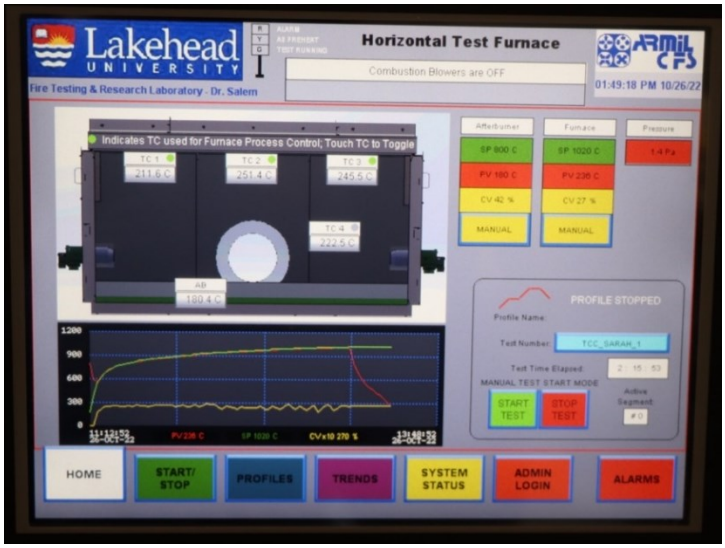

Figure 3.5: Human-Machine Interface (HMI) touch screen of the furnace's control panel (Courtesy of Dr. Salem).

Additional temperature measurements were required to monitor the temperatures of each test assembly. Thus, high temperature insulated Type K thermocouples were used at specific locations in the CLT panel, concrete slab, and on the STS connection. In total there were 37 thermocouples inserted into each slab at specified depths that are discussed in the following sections of this chapter. This data provides information on the transfer of heat through the specimen and the temperature of different components at a given time during the test and thus, can be used to observe the relationship between time, temperature, and the depth into the floor assembly cross-section. Measuring the temperature throughout the section is even more critical when studying EWP compared to concrete or steel specimens, as it is needed to examine the charring rate and loss of area resisting applied loading. Unlike other materials, EWP's charred section is permanently lost, not just a reduction in mechanical performance, thereby leading to a significant loss in strength and stiffness.

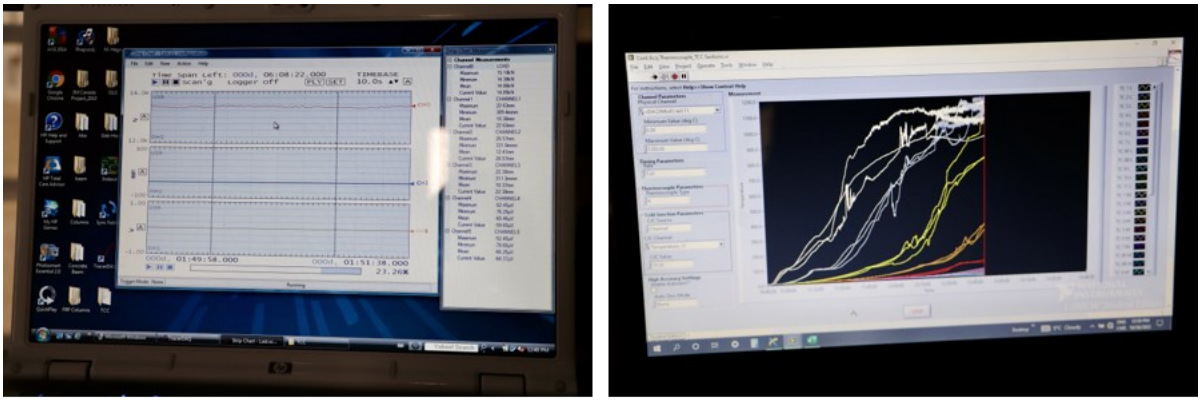

(a) Mechanical Measurements (b) Thermal Measurements

Figure 3.6: DAQ systems setup.

3.3 Materials

When designing TCC sections, the proper design of its three components significantly influences the overall section's behaviour. That being the timber, concrete, and shear connection components.

Each affects the design of the other components simultaneously, and all must be considered before reaching a final design of the TCC section.

3.3.1 CLT Panels

Designing TCC sections starts with a selection of timber material and assembly type. As previously mentioned, this research project utilized CLT panels supplied by Nordic Structures. The principal mechanical properties of the sections summarized in Tables 2.2 and 2.3 in section 2.1.6 of this thesis were provided by the manufacturer and verified by the Canadian Construction Materials Centre (CCMC) in Evaluation Report CCMC 13654-L (CCMC, 2022).

While there are many differences in layup thickness and quantities for CLT to choose from, it is clearly shown in the literature review that when considering fire design, 5 ply or greater is recommended due to charring behaviour and strength resistance provided by the ply oriented in the major strength direction. Therefore, a 5-ply CLT panel was chosen when considering the experimental setup, overall specimen dimensions, and applied loading. As Nordic Structures provides two 5-ply CLT panels, one with all ply thickness being 35 mm, giving an overall depth of 175 mm, and one with major strength plys 35 mm while the minor strength direction plys are 19 mm, giving an overall depth of 143 mm. The slenderer one was chosen to align with the research objectives.

The primary motivation is to achieve a 2-hr fire resistance time using TCC sections instead of only having the CLT panel. Figure 3.7 shows the fire resistance of panels provided by Nordic Structures. Showing the 175 mm panel already achieves a 90-min fire resistance rating considering specimen dimensions and loading (clear span of 5000 mm, 1.0 kPa dead load, and 2.4 kPa live load). While the 143 mm panel only reaches a 60-min fire resistance rating; therefore, taking the slender CLT

panel and designing it for 2-hr fire resistance rating results in doubling the time for the panel as a standalone. This simultaneously meets the other research objectives as it improves the framework for the TCC sections in Canada and verifies the panel's behaviour while under standard fire exposure.

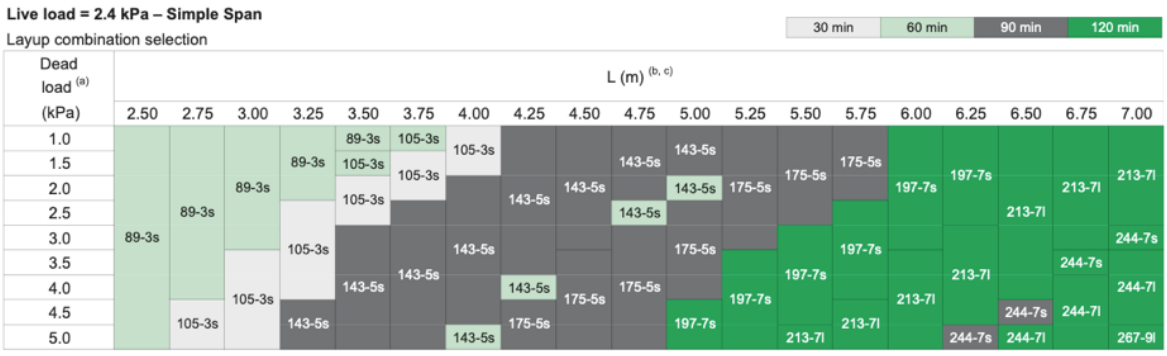

Figure 3.7: Fire resistance time of the CLT panels produced by Nordic Structures (adapted from Nordic Structures, 2020)**.**

3.3.2 Concrete

After determining the timber aspect of a TCC section, the next step was evaluating the concrete portion. However, for this it is essential to not only design for strength properties but also consider the overall design of the section. How the material best work together and dimensions of the shear connectors to be able to provide adequate cover. Therefore, an impactful parameter is the thickness of the concrete slab that is used. Based on the literature review for TCC sections with STS as shear connectors, typical concrete thickness ranged from 50-89 mm, with an average value of 66 mm.

When deciding on concrete thickness, two essential aspects of the design of the TCC section must be considered. First, the overall concept of TCC sections is to have the concrete located entirely in the compressive zone and timber in the tensile zone. Therefore, common sense dictates that the section's neutral axis be situated at the interface between the two materials. However, while

studying fire conditions, it is favoured to have the neutral axis located in the timber material. However, when the char front progresses, the neutral axis is shifted upward due to the cross-section loss. If considering elevated temperatures, it is recommended to have the neutral axis even below the interface. Second is the type and dimension of the shear connectors used. As previously mentioned, the shear connectors used in this research is STS, meaning that concrete cover needs to be considered at the end and from the top of the slab. Therefore, the screw dimensions need to be compared against not only the embedment into the timber but also into the concrete.

The concrete used in this research is normal strength concrete. See Table 3.1 for mix design for 1one cubic meter of concrete as well as its design properties. Coarse aggregates were dolomite based with a maximum aggregate size of 16 mm and a nominal diameter of 13 mm. Smaller-diameter aggregates are common in TCC sections as it allows for the mix to adequately flow and bond around the shear connectors. Water-cement ratio used was approximately 0.56 and no additives were used in the concrete mix. Additionally, the minimum reinforcement ratio of 0.002 of the concrete slab cross-sections was achieved by placing a wire mesh with 150 mm grid of 6 mm steel. This is mainly to control tension cracking due to shrinkage.

Table 3.1: Concrete mix design

Component	Quantity (kg)
Coarse Aggregates	1121.2
Fine Aggregates	852.5
Cement	310
Water	175.7
Compressive Strength	30 MPa
Modulus of Elasticity	25000 MPa
Density	2400 kg/m^3

Additionally, due to the seen benefit of including insulation layer at the interface with respect to increasing the moment arm between the timber and concrete components, decreasing overall weight, and increasing the thermal and vibration characteristics, a layer of insulation was added to all four specimens. However, due to the less desirable effects when placing STS directly through the installation layer with the decrease in strength and stiffness as the screw tends to twist and buckle, the insulation was only placed in between the screws row, Figure 3.8. Also, the thickness of the concrete layer was reduced where the insulation layer is located; however, the concrete layer full thickness was maintained at the shear connectors. Therefore, the thickness of concrete is 90 mm around the STS, 65 mm over the insulation layer, with average concrete thickness of 79 mm. Type of insulation was FOAMULAR CodeBord XPS Insulation cut to strips of 200 mm wide and placed intermediate between screw rows.

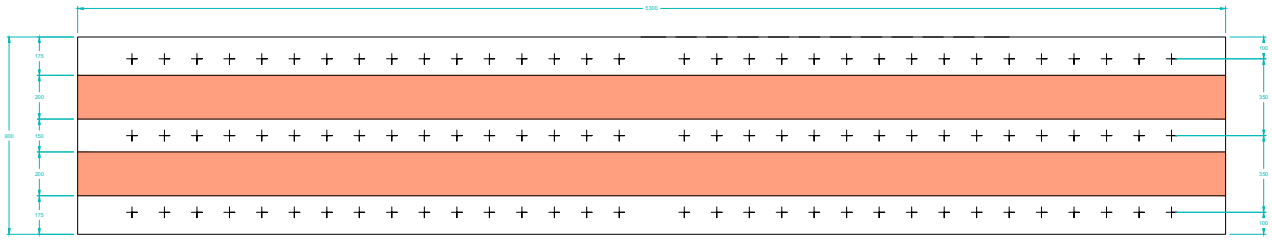

Figure 3.8: Insulation layout (top view).

3.3.3 Self-Tapping Screws

The properties of the screws investigated in this research are shown in Table 3.2 and Figure 3.9. The product evaluation report provides the technical specifications of the screws (CCMC 13677-R, 2020). Screws were inserted at two different inclination angles to compare their influence on the fire performance of the different TCC floor assemblies. The first two slabs had screws at 45°

and the other two had them at 30° (measured to the horizontal). Thereby giving a difference in the vertical and horizontal projection of the screw into each of the material (i.e., concrete and timber).

Table 3.2: STS properties (CCMC 13677-R, 2020)

Diameter (mm)	Length (mm)	Concrete Embedment Length (mm)	Wood Embedment Length (mm)	Bending Strength (MPa)	Tensile Strength (kN)	Shear Strength (MPa)
8	240	90	150	1015	18.9	641

Concrete Embedment (mm)		
	45 Degrees	30 Degrees
Horizontal Projection	64	78
Vertical Projection	64	48
CLT Embedment (mm)		
	45 Degrees	30 Degrees
Horizontal Projection	106	130
Vertical Projection	106	75

Figure 3.9: SWG ASSY VG plus cylindrical head.

3.4 Design Calculations

As previously mentioned, two calculation methods need to be considered when designing TCC sections: the γ-method and the EPM. While the first is more appropriate for brittle connectors, and EPM is designed for ductile connection, both need to be calculated to determine the minimum estimated value. Both methods result in three equations for determining bending moment capacity and four equations for shear resistance. All must be calculated during ambient temperatures for standard and long durations and fire conditions for short durations. The design calculation

procedure followed was from the Design Guide for TCC Floors in Canada (Auclair, 2020) and European Code to determine screw capacity (COST Action FP1402, 2018).

3.4.1 Screw Capacity

The shear resistance of the STS connector significantly impacts their quantity and layout arrangement. When designing connections using STS, calculations were completed following the Design of timber-concrete composite structures by COST Action FP1402/WG4, that utilized equations from EN 1995-1-1 and ETA – 13/0029 to determine the Load-Carrying Capacity per ASSY plus VG screw and a check to verify the behaviour of screws in the transverse direction. Table 3.3 has the final calculation results with the screws orientated at 45° and 30° and at ambient and fire conditions. Refer to Section 3.4.4.2 for adjustments required for determining the shear resistance of screws when exposed to elevated temperatures. Equations 3.1 through 3.5 show the calculation procedure that is required to follow.

Table 3.3: Calculated shear resistance per screw

$F_{Rk} = V_{r,conn}$ (kN)	45°		30°	
	Ambient Temperature	Fire Condition 2-hr Duration	Ambient Temperature	Fire Condition 2-hr Duration
	14.44	6.59	15.49	9.99
Difference in Resistance	45.6%		64.5%	

Note: F_{Rk} is from Euro Code 5 standard, $V_{r,conn}$ is from (Auclair, 2020), both are Shear resistance of a single connector in the span direction

Equation 3.1: Load on screws in a row (EN 1995-1-1)

$$F_1 = \frac{\gamma_t E_t A_t a_t s}{(EI)_{eff}} V_f$$

where:

$$\gamma_t = \frac{1}{1+\frac{\pi^2 (EA)_t}{L^2 \quad K}}$$

where:

$K = \frac{k_s n}{s_{eff}}$

where:

k_s = Shear stiffness of a single connector in the span direction for serviceability limit state

n = Number of screws rows in the transverse direction

s_{eff} = effective spacing of the connector

L = clear span distance (mm)

E_t = Young modulus of timber component (MPa)

A_t = Cross-section area of timber component (mm^2)

$a_t = \frac{\gamma_c (EA)_c r}{\gamma_c (EA)_c + \gamma_t (EA)_t}$

where:

$(EA)_c$ = Axial stiffness of concrete layer (N), refer to Equation 3.7

$(EA)_t$ = Axial stiffness of timber layer (N)

$r = 0.5h_t + t_{eff} + 0.5h_{c,\,eff}$

where:

t_{eff} = Effective gap between the concrete and the timber layer (mm).

$\gamma_c = 1$

s = spacing of the connector along the span (mm)

$(EI)_{eff}$= Effective Bending Stiffness ($N.mm^2$), refer to Equation 3.7

Equation 3.2: Characteristic Load-Carrying Capacity per ASSY plus VG screw (ETA-13/0029)

$F_{Rk} = \min (F_{Rk,1},\, F_{Rk,2})$

where:

α=30° or α=45°

$F_{Rk,1} = (cos\alpha + \mu sin\alpha)F_{ax,\,a,\,Rk}$

$F_{Rk,\,2} = (cos\alpha + \mu sin\alpha)f_{ten,k}$

where:

μ = Friction coefficient; for direct contact between timber and concrete μ= 0.25; otherwise μ= 0

$F_{ax,\,a,\,Rk} = \left(\frac{f_{ax,k}dl_{ef}}{1.2cos^2\alpha+sin^2\alpha}\right)\left(\frac{\rho_t}{350}\right)^{0.8}$

where:

$f_{ax,k}$ = Withdrawal Parameter (refer to Table 3.4)

d = Screw diameter in mm

I_{ef} = is the embedment depth of the ASSY plus VG screw in the timber member in mm

ρ_t = is characteristic timber member density in kg/m^3

$f_{ten,k}$ = Tensile Capacity (refer to Table 3.4)

Table 3.4: Properties of ASSY plus VG Screws (adapted from ETA-13/0029, 2017)

ASSY plus VG Screw	Diameter = 8 mm	Diameter = 10 mm
Yield Moment $M_{y,k}$ (Nm)	20	36
Tensile Capacity $f_{ten,k}$ (kN)	7	32
Withdrawal Parameter $f_{ax,k}$ (N/mm^2)	11	10

Equation 3.3: Effective Number of Screws (EN 1995-1-1)

$n_{ef} = n^{0.9}$

where:

n= number of screws per location; 1 of single and 2 for pair arrangements

Equation 3.4: Design Load Bearing Capacity of the Screws in a row

$F_{Rd} = \frac{n_{ef}k_{mod}F_{Rk}}{\gamma_M}$

where:

k_{mod} = Refer to EN 1995-1-1 Table 3.1

F_{Rk} = Load-Carrying Capacity per screw (Refer to Equation 3.2)

γ_M = Refer to EN 1995-1-1 Table 2.3

Equation 3.5: Verification of Fasteners

$$\frac{F_1}{F_{Rd}} < 1$$

Note that connectors need to be checked at both serviceability and ultimate limit states for standard/short and long duration, as well as if there is a difference in screw spacing or significant changes in shear load profile.

3.4.2 Bending Moment Resistance

After knowing all the behaviour properties of the three components: timber, concrete, and shear connectors, it is possible to calculate the overall behaviour of the section under flexure bending. Following the γ-method must check with timber being the limiting factor (Equation 3.8) and the other when concrete (Equation 3.9) is the limitation. Then an additional analysis following EPM (Equation 3.10) where the connector has assumed to be yielded. After conducting all three investigations, the final moment resistance is the minimum value from the three equations (Equation 3.6). The calculation results can be seen in Tables 3.5 and 3.6, and equation details for γ-method in section 3.4.2.1 and EPM in section 3.4.2.2. Calculating the section Effective Bending has been studied both in terms of duration and for Serviceability Limit States (SLS) and Ultimate Limit States (ULS), as the overall deflection must be checked following SLS.

As for moment resistance, both short/standard term, long-term, and fire conditions have been examined. The section utilization factor follows standard design procedure where in fire conditions

typically the utilization factor of the section is almost doubled compared to that for the ultimate design capacity of the section at ambient condition. Note that the values for the equations following the γ-method are equal for both screw insertion angles, as the equations are not related to the shear connection's properties but the timber and concrete properties. In contrast, EPM considers the shear resistance of screws and alters the moment resistance when it changes. The reason for the difference as the screw orientation changes will be discussed later in detail; refer to section 3.4.4.2.

Equation 3.6: Bending moment resistance of the composite section

$$M_r = \min\left(M_{r,\gamma,t};\ M_{r,\gamma,c};\ M_{r,EP}\right)$$

Table 3.5: Calculated effective bending stiffness of composite section

Effective Bending Stiffness $(EI)_{eff}$ (N.mm^2)				
Serviceability Short and Standard Term	Serviceability Long Term	Ultimate Short and Standard Term	Ultimate Long Term	Fire Conditions Ultimate Short Term
7.4138 x 10 ^{12}	2.713 x 10 ^{12}	6.326 x 10 ^{12}	2.350 x 10 ^{12}	1.5303 x 10 ^{12}

Table 3.6: Calculated bending moment resistance of composite section

Bending Moment Resistance M_r (kNm)				
Screw Orientation		Short and Standard Term	Long Term	Fire Conditions 2 hr Duration
45°	$M_{r,\gamma,t}$	118.52	65.00	51.18
	$M_{r,\gamma,c}$	91.99	107.77	30.47
	$M_{r,EP}$	137.29	108.90	37.71
	$M_r = \min$	**91.99**	**65.00**	**30.47**
	M_f	26.23	19.14	18.29
	$M_r \geq M_f$	√	√	√
30°	$M_{r,\gamma,t}$	118.52	65.00	51.18
	$M_{r,\gamma,c}$	91.99	107.77	30.47
	$M_{r,EP}$	113.97	113.29	52.20
	$M_r = \min$	**91.99**	**65.00**	**30.47**
	M_f	26.23	19.14	18.29
	$M_r \geq M_f$	√	√	√

3.4.2.1 γ-Method

Equation 3.7: Effective Bending Stiffness $(EI)_{eff}$

$$\boldsymbol{(EI)_{eff} = (EI)_c + (EI)_t + \gamma_c (EA)_c a_c^2 + \gamma_t (EA)_t a_t^2}$$

where:

$\gamma_c = 1$

$\gamma_t = \frac{1}{1+\frac{\pi^2}{L^2}\frac{(EA)_t}{K}}$, refer to Equation 3.1

$(EA)_c = E_c b_c h_{c,\,eff}$

where:

E_c = Young modulus of concrete (MPa)

b_c = width of concrete (mm)

$$h_{c,eff} = \sqrt{\alpha^2 + \alpha(h_t + 2h_c + 2t)} - \alpha \leq h_c$$

where:

$$\alpha = \frac{\gamma_t (EA)_t}{\gamma_c E_c b_c}$$

h_c = height of concrete (mm)

h_t = height of timber (mm)

$$(EI)_c = E_c \frac{b_c h_{c,eff}^3}{12}$$

$$a_c = \frac{\gamma_t (EA)_t r}{\gamma_c (EA)_c + \gamma_t (EA)_t}$$

where:

$$r = 0.5h_t + t_{eff} + 0.5h_{c,eff}$$

where:

t_{eff} = Effective gap between the concrete and the timber layer (mm)

a_t = Distance between the centroid of timber and the neutral axis of the concrete layer, refer to Equation 3.1

Equation 3.8: Bending moment resistance of TCC using γ-method limited by timber layer

$$M_{r,\gamma,t} = \frac{(EI)_{eff} T_{r,t} M_{r,t}}{\gamma_t (EA)_t a_t M_{r,t} + (EI)_t T_{r,t}}$$

where:

$(EI)_{eff}$ = Effective Bending Stiffness (N.mm^2) refer to Equation 3.7

$T_{r,t}$ = Tension resistance of the timber element (N)

$M_{r,t}$ = Bending moment resistance of the timber element (N)

γ_t = Non-dimensional factor for composite action for timber layer, refer to Equation 3.1

a_t = Distance between the centroid of timber and the neutral axis of the concrete layer, refer to Equation 3.1

$(EA)_t$ = Axial stiffness of timber layer (N), refer to Equation 3.1

$(EI)_t$ = Bending stiffness of layer (N·mm^2), refer to Equation 3.1

Equation 3.9: Bending moment resistance of TCC using γ-method limited by concrete layer

$$M_{r,\gamma,c} = 0.9\phi_c f_c' S_c$$

where:

ϕ_c = Resistance factor of concrete

f_c' = Specified compression strength for the concrete

$S_c = \frac{(EI)_{eff}}{E_c(0.5h_{c,eff}+\gamma_c a_c)}$

where:

$(EI)_{eff}$= Effective Bending Stiffness (N.mm^2) refer to Equation 3.7

$h_{c,eff}$ = Effective height of the concrete layer by neglecting the concrete in tension, refer to Equation 3.7

$\gamma_c = 1$

a_c= Distance between the centroid concrete and the neutral axis of the concrete layer, refer to Equation 3.7

3.4.2.2 Elasto-Plastic Method (EPM)

Equation 3.10: Bending moment resistance of TCC section calculated with the EPM

$$M_{r,EP} = N\left(\frac{h_t}{2} + t + h_c - \frac{h_{c,eff}}{2}\right) + \sigma_{b,c}\frac{b_c h_{c,eff}^2}{6} + \sigma_{b,t}\frac{b_t h_t^2}{6}$$

where:

$N = mF_{Rk} \leq \min(T_{r,\,t};\ 0.9\phi_c f_c' A_c)$

where:

m = Number of connectors between the zero moment and the critical cross-section

F_{Rk} = Characteristic Load-Carrying Capacity, refer to Equation 3.2

h_t = height of timber (mm)

t = Height of gap between the concrete and the timber layer

h_c = height of concrete (mm)

$h_{c,\,eff}$ = Effective height of the concrete layer by neglecting the concrete in tension, refer to Equation 3.7

$$\sigma_{b,\,t} = \left(1.0 - \frac{N}{T_{r,\,t}}\right)\frac{6M_{r,\,t}}{b_t h_t^2}$$

where:

$T_{r,t}$ = Tension resistance of the timber element (N)

$M_{r,t}$ = Bending moment resistance of the timber element (N)

b_t = width of timber (mm)

$$h_{c,\,eff} = \sqrt{\frac{NE_t h_t}{E_c \sigma_{b,\,t} b_c}} \leq h_c$$

where:

E_t = Young modulus of timber component (MPa)

h_t = height of timber (mm)

E_c = Young modulus of concrete (MPa)

b_c = width of concrete (mm)

$$\sigma_{b,\,c} = \frac{N}{b_c h_{c,\,eff}} \leq 0.45\phi_c f_c'$$

3.4.3 Shear Resistance

The next step is to calculate the shear resistance of the cross-section. Resembling determining bending moment resistance, there are equations following γ-method and EPM. However, both have

two equations where the timber limits the first and the other is limited by concrete. Which means what is expected to fail first between the materials. Following the predicted behaviour of the section and failing due to the timber component before the concrete. The overall shear resistance can be determined using Equation 3.11, with calculation procedure for γ-method as per Equations 3.12 and 3.13 and EPM Equations 3.14 and 3.15.

Values from each of the equations can be seen in Table 3.7, considering short/standard, long-term, and 2-hr fire duration. Shows that the equations limited by timber are critical considering either method. Additionally, as previously mentioned the γ-method is consistent at ambient condition but different considering elevated temperatures, unlike EPM, which changes regardless of the thermal environment. This gain relates to the variables in the equations and the difference when γ-method is for the shear connectors in elastic behaviour, while EPM is after the connector is already yielded and becomes within its inelastic behaviour region.

Equation 3.11: Shear resistance of the composite section

$$V_r = \min\left(V_{r,\gamma,t};\ V_{r,\gamma,c}; V_{r,EP,t};\ V_{r,EP,\,c}\right)$$

Table 3.7: Shear resistance of composite section

Shear Resistance V_r (kN)				
Screw Orientation		Short and Standard Term	Long Term	Fire Conditions 2-hr Duration
45°	$V_{r,\gamma,t}$	57.68	34.92	52.30
	$V_{r,\gamma,c}$	190.97	243.49	80.87
	$V_{r,EP,t}$	59.41	41.11	34.18
	$V_{r,EP,c}$	268.75	320.35	181.58
	$V_r = \min$	**57.68**	**34.92**	**34.18**
	V_f	20.98	15.31	14.64
	$V_r \geq V_f$	√	√	√
30°	$V_{r,\gamma,t}$	57.68	34.92	52.30
	$V_{r,\gamma,c}$	190.97	243.49	80.87
	$V_{r,EP,t}$	60.08	41.77	44.85
	$V_{r,EP,c}$	245.49	315.82	96.53
	$V_r = \min$	**57.68**	**34.92**	**44.85**
	V_f	20.98	15.31	14.64
	$V_r \geq V_f$	√	√	√

3.4.2.1 γ-Method

Equation 3.12: Shear resistance using γ-method limited by timber layer

$$V_{r,\gamma,t} = \frac{(EI)_{eff}}{(EI)_t + 0.5\gamma_t (EA)_t (h_t + t) a_t} V_{r,t}$$

where:

$(EI)_{eff}$ = Effective Bending Stiffness (N.mm^2), refer to Equation 3.7

$(EI)_t$ = Bending stiffness of timber layer (N·mm^2)

γ_t = Non-dimensional factor for composite action for timber layer, refer to Equation 3.1

$(EA)_t$ = Axial stiffness of timber layer (N)

h_t = height of timber (mm)

a_t = Distance between the centroid of timber and the neutral axis of the concrete layer, refer to Equation 3.1

$V_{r,t}$ = Shear resistance of timber layer

Equation 3.13: Shear resistance using γ-method limited by concrete layer

$$V_{r,c} = 0.21\phi_c\lambda\sqrt{f_c'}b_c h_c$$

where:

ϕ_c = Resistance factor of concrete

f_c' = Specified compression strength for the concrete

λ = 1 for Normal strength concrete

b_c = width of concrete (mm)

h_c = height of concrete (mm)

3.4.2.2 Elasto-Plastic Method (EPM)

Equation 3.14: Shear resistance of the composite section calculated with the EPM limited by timber

$$V_{r,EP,t} = \left(V_{r,t} - \frac{mV_{r,conn}}{L_m}\frac{h_t+t}{2}\right)\frac{(EI)_0}{(EI)_t} + \frac{mV_{r,conn}}{L_m}r$$

where:

$V_{r,t}$ = Shear resistance of timber layer

m = Number of connectors between the zero moment and the critical cross-section

$V_{r,conn} = F_{Rk}$ = Characteristic Load-Carrying Capacity, refer to Equation 3.2

L_m = Length between the critical cross-section and one point of zero moment

h_t = height of timber (mm)

t = Height of gap between the concrete and the timber layer (mm)

$(EI)_0 = (EI)_c + (EI)_t$

where:

$(EI)_c = \frac{E_c b_c h_c^3}{12}$

where:

E_c = Young modulus of concrete (MPa)

b_c = width of concrete (mm)

h_c = height of concrete (mm)

$(EI)_t$ = Bending stiffness of timber layer (N·mm^2)

$$r = \left(\frac{h_t}{2} + h_c - \frac{h_{c,eff}}{2} + t\right)$$

where:

$h_{c,eff}$ = Effective height of the concrete layer by neglecting the concrete in tension, refer to Equation 3.6

Equation 3.15: Shear resistance of the composite section calculated with the EPM limited by concrete

$$V_{r,EP,c} = \left(V_{r,c} - \frac{mV_{r,conn}}{L_m}\frac{2h_c - h_{c,eff} + t}{2}\right)\frac{(EI)_0}{(EI)_c} + \frac{mV_{r,conn}}{L_m}r$$

Refer to Equation 3.12

3.4.4 Elevated Temperatures Considerations

When considering elevated temperatures for calculating the shear and moment resistance of the composite section, two key differences must be understood and calculated: the CLT panel's altered capacity; and the reduced shear capacity of each screw in the connection. The design would be unsafe and unrealistic in situ conditions without reducing the timber and shear connector components.

3.4.4.1 CLT Capacity

As discussed in Section 2.4 with CLT behaviour under fire, many variables influence the panels' behaviour, particularly the charring rate and delamination of lamellas. Additionally, the inherited design properties of the panels with the ply in the major strength direction, taking a significant

portion of the applied loading, influence how to design for CLT under fire. Therefore, following the WDM, the capacity of CLT under fire is determined by first calculating the moment of inertia of the panels only in the direction of applied stress, (i.e., d_1 and d_2) after subtracting the expected loss of cross-section (x_r) due to charring (x_c) and heated wood layer(x_t), Figure 3.10. After determining this, the corresponding moment, shear, and tensile resistances can be calculated. These values are then input into the calculations from the previous section to evaluate the performance under fire exposure since each fire time relates to different char depths. Thus, evaluation of lamellas remaining in the major strength direction to determine the moment of inertia and corresponding resistances for the section becomes important. For this research study, when performing the design calculations, a charring rate of 0.73 mm/min was used, based on the average charring rate from the previously discussed studies when CLT is exposed to standard fire. Although it exceeds the standard from the European Code of 0.65 mm/min, it accounts for delamination and provides an additional margin of safety.

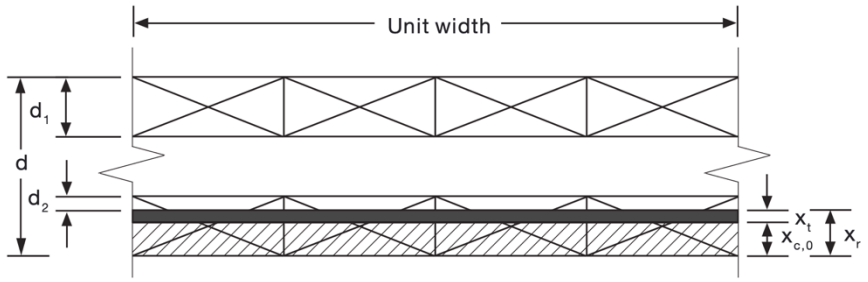

Figure 3.10: CLT in fire condition calculation (adapted from CWC, 2020, p. V1-882)

For moment and shear resistance equations refer to Section 2.1.6, Equations 2.1 and 2.3.

Equation 3.16: CLT - Tensile Resistance in the Major Strength Direction

$$T_{rn,\,fi} = \phi F_t A_n$$

where:

$\phi = 1$

A_n = Net cross-section of CLT, of remaining timber in both major and minor strength directions

$$F_T = f_t(K_D K_H K_{Sb} K_T K_{fi})$$

where:

f_t = specified tensile strength of laminations in the longitudinal layers (MPa) (refer to Table 2.2)

3.4.4.2 Screw Capacity

As previously discussed, it is critical to know the resistance of the shear connectors when designing TCC sections, especially when exposed to fire. From values for both bending moment and shear resistance of the section, a clear difference can be seen depending on if the screws are orientated at 45° (Slabs 1 and 2) or 30° (Slabs 3 and 4). The reason for this is as follows; when determining shear resistance per screw, it is multiplied proportionally to the percentage of the depth of the screw remaining in the CLT panel from the original screw embedment length. Logic follows as Slabs 1 and 2 have a steeper angle and, therefore, greater vertical projection into the CLT (Table 3.2) that the screws at 45° will be exposed to fire first compared to those at 30°. Approximately, 51 min into the fire, the screws in Slabs 1 and 2 will start being affected by the increased temperature compared to the screws in Slabs 3 and 4 that would not until around the 93 min mark. This is a huge difference in fire resistance and structural performance. Therefore, at the goal of 2-

hr fire resistance time, the shear resistance per screw is at 45% for the 45° inclined screws, while at 64% for the 30° inclined screws. This is a significant difference in the strength of the connection design. Accordingly, while the shear resistances of the STS at the two insertion angles are comparable at ambient condition, they are greatly influenced when considering fire exposure, especially for longer durations, such as 2 hours.

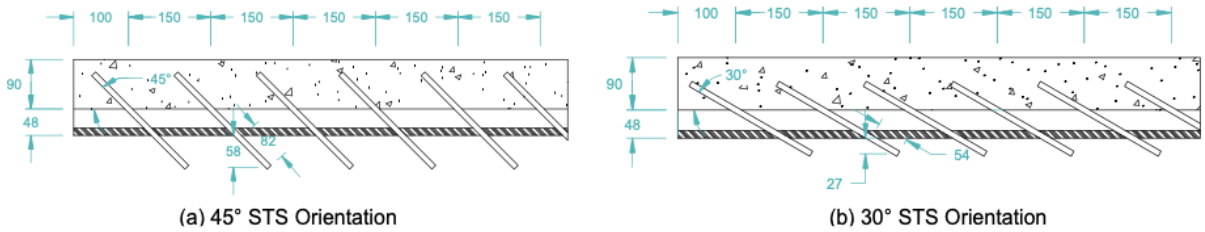

Figure 3.11: Screws exposed to 2-hr standard fire.

3.5 Fabrication Process and Details

Due to the complex nature of TCC sections, it is a multi-step process that must be followed to fabricate each test sample. Both before, during, and after cast concrete on the CLT panels and the STS shear connections. Special care was taken to ensure accurate measurements of the thermal data during testing. This step is vital as it directly reflects results and conclusions drawn. Slabs 1 and 2 have 45° STS orientation, and Slabs 3 and 4 have 30° STS orientation.

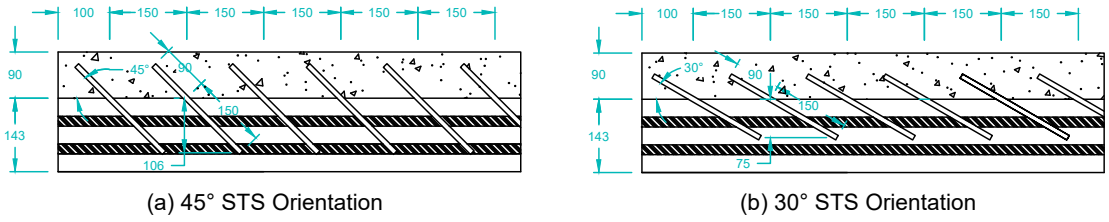

Figure 3.12: TCC slab cross-sections.

3.5.1 Thermocouples Layout and Installation

(a) (b)

Figure 3.13: Thermocouple installation process.

Thermocouples located in the CLT panel:

- Used a portable electrical drill with a drill guide to ensure holes were straight and perpendicular to the surface of the CLT. Holes with near the diameter of a typical Type K thermocouple wire,
- Three thermocouples line were used, left of center, centerline, and right of center,
- Specified depths were selected at the interface between each ply and the mid-depth of the major ply,
- This resulted in a total of 21 thermocouples located in the CLT for each test specimen.

Thermocouples located at the interface:

- At each of the three thermocouple lines (left, center, right), there were two thermocouples stapled to the interface. Note that thermocouples were installed prior to casting concrete,
- This is a critical location; therefore, the reason for the duplication,
- This resulted in a total of 6 thermocouples located at the interface between materials.

Thermocouples located in the concrete:

- At each of the three thermocouple lines (left, center, right), a thermocouple was situated at the same depth of concrete where the steel mesh was placed., which was mid-depth of the concrete over the layer of installation. Note that thermocouples were placed prior to casting concrete,
- Additionally, one thermocouple is located at the top of the concrete, only in the center of the slab,
- This resulted in a total of 4 thermocouples located in the concrete for each slab.

Thermocouples located on the STS connectors:

- At each of the three thermocouple lines (left, center, right), there were two thermocouples located on the screws. Note that thermocouples were placed prior to casting concrete,
- The left and right lines were placed on the outside screws (transverse direction) that were in line with the other thermocouples,
- For the center, as there are no screws located on the center line, thermocouples were placed on the middle screws on the ones just left and right of center,
- This resulted in a total of 6 thermocouples located on the STS connectors for each slab.

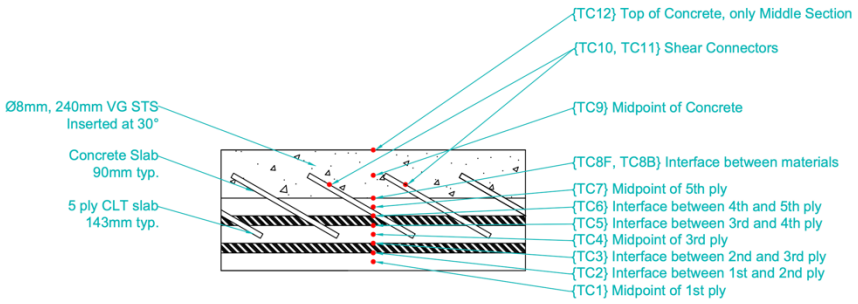

Figure 3.14: Thermocouple locations – Front View.

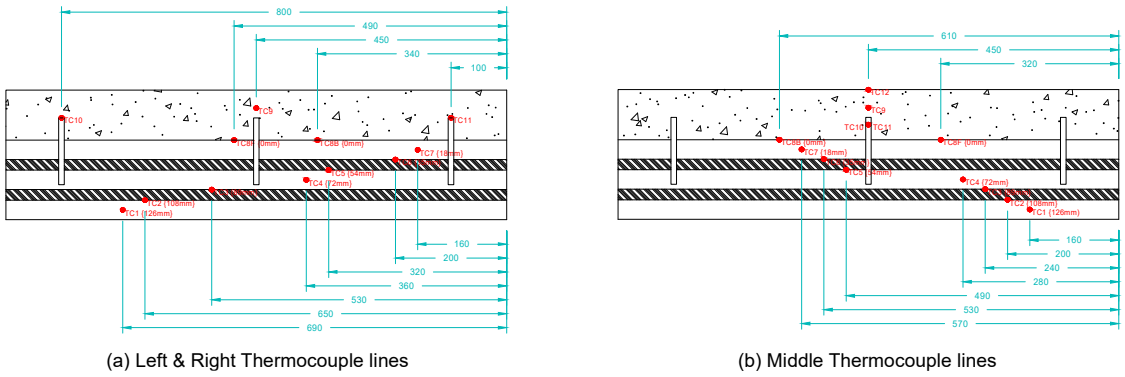

(a) Left & Right Thermocouple lines

(b) Middle Thermocouple lines

Figure 3.15: Thermocouple locations – Side View.

3.5.2 Screw Connections

3.5.2.1 45° Screw Connections Installation

- Using a portable electrical drill and drill guide adjusted to 45°, with a small diameter bit, a guide hole was first made at each of the screw locations, Figure 3.16 (a),
- All screws were taped to mark the embedment depth of the screw in the CLT. Note that the tape was removed after installation to provide good bondage of the concrete to the screws,
- Using a portable electrical drill with the guiding arm placed at 45,° the screws were drilled partially into the CLT, Figure 3.16 (b). Note that this tool cannot insert the screws at full

depth but ensure they are inserted at the correct angle for portion of the targeted embedment length,

- For the final distance, an electrical impact drill was utilized, providing enough torque and power to place the screws at the full 150 mm embedment depth in the CLT, Figure 3.16 (c),
- Figure 3.16 (d) shows the screws were placed with an acceptable level of tolerance from the 45°.

Figure 3.16: 45° screw connection installation.

3.5.2.1 30° Screw Connections Installation

- 30° connection was more challenging to install due to the shallow angle to the horizontal and drilling tools could not be adjusted to an inclination angle less than 45°. Therefore, the installation method was slightly altered,
- The drill guide was set at 60° and entirely rigged to be rotated to 90°. Thereby, having the drill bit adjusted to insert at 30°. With a small diameter bit, a pilot hole was first made at each of the screw locations, Figure 3.17 (a),
- All screws were taped to mark the embedment depth of the screw in the CLT. Note that the tape was removed after installation to provide good bondage of the concrete to the screws,
- Dependent on the pilot hole a portable electrical drill was used to partially insert the screws into the CLT, Figure 3.17 (b). Note that the previous tool for this stage could not be set to 30°,
- For the final distance, an electrical impact drill was utilized, providing enough torque and power to place the screws at the full 150 mm embedment depth in the CLT, Figure 3.17 (c),
- Figure 3.17 (d) shows the screws were placed with an acceptable level of tolerance from the 30°.

Figure 3.17: 30° screw connection installation.

3.5.3 Concrete Preparation and Casting

Concrete preparations:

- Temporary formwork was attached to each slab set to the required concrete depth of 90 mm, Figure 3.18 (a),
- Insulation boards were cut in strips of 200 mm width and placed in intermediate spaces between the STS rows and then glued in place to prevent movement when casting concrete.

Note that cut offs were made around the thermocouple wires to avoid noise in thermal readings during fire testing, Figure 3.18(b),

- Wire mesh, 6-mm gauge steel with 150 x150 mm grid, was placed and secured to some of the installed STS to prevent uplift and shift in concrete. Mesh was placed at approximately 57 mm from the CLT surface, which is mid-depth of the concrete over the insulation layer, Figure 3.18(c),
- Steel threaded rods were inserted at the corners of the slab to act as supports during concrete casting/curing and used as the lift points to move the slab. Note that the said rods were secured to the CLT with nuts and thick washers from underneath, Figure 3.18(c), before casting concrete, and Figure 3.19 (e) after curing,
- Additionally, two eyebolts were placed just to the side of the outer thermocouple lines to connect safety chains secured between the slab and the loading/supporting steel frame during fire testing, Figure 3.18 (e) before casting, and Figure 3.19 (f) after curing.

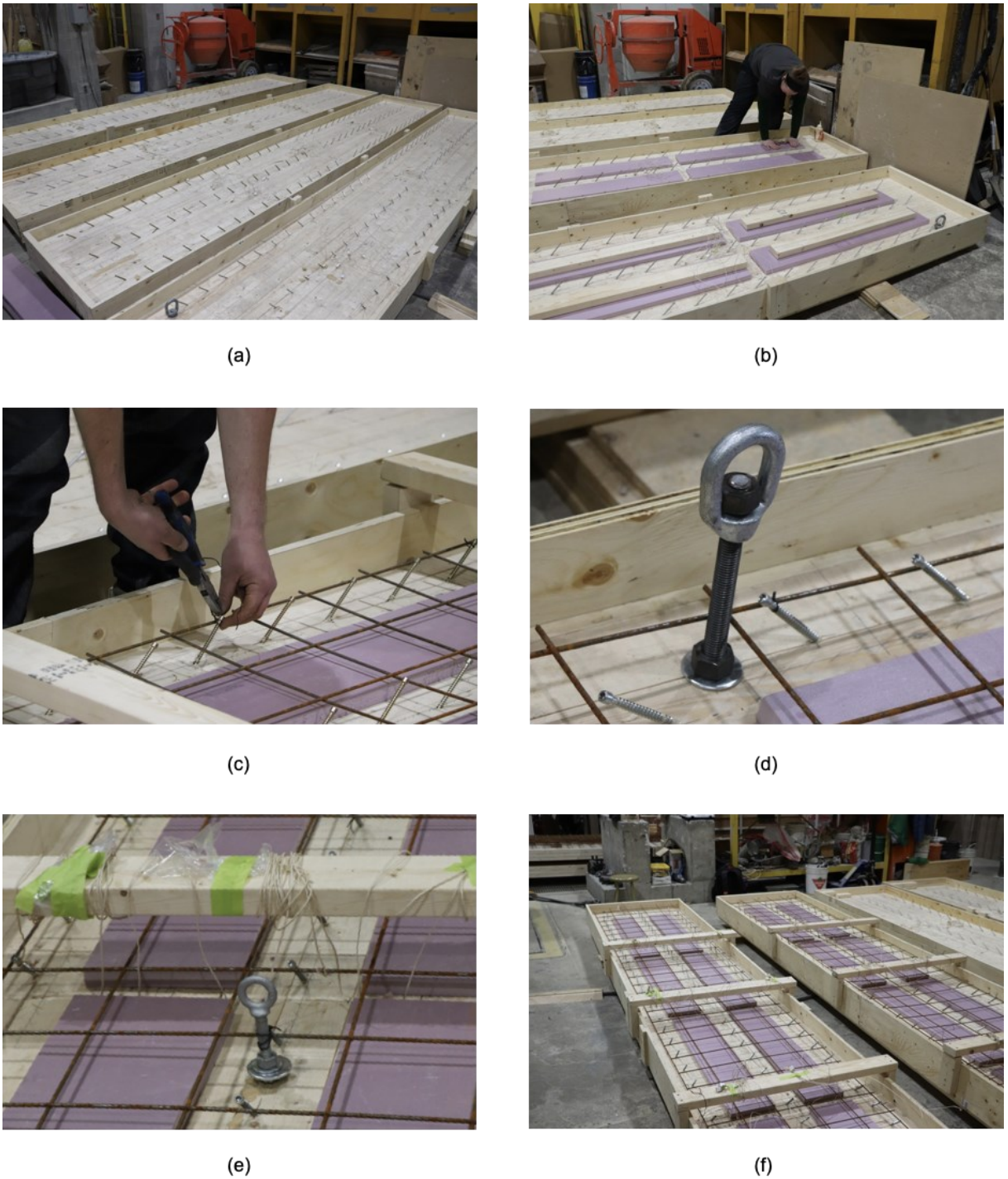

Figure 3.18: Preparation for concrete pour.

Casting concrete details:

- Figure 3.18 (f) shows slabs ready for concrete casting. Note that 2" x 4" pieces were placed across the slabs to wrap the thermocouples around, keeping them safe and dry during casting,
- Concrete was cast for each slab separately, each with approximately 0.5 m^3 of concrete,
- Casting concrete followed the standard procedure for pouring concrete slabs: mixing, slump measuring, distributing evenly, vibrating, and smoothing accordingly,
- For each slab, three compression cylinders were taken for both 7 and 28-day testing, Figures 3.19 (a) through 3.19 (d). Additionally, density bucket was taken and measured,
- Slabs were covered with plastic to aid in moisture retention and prevent rapid shrinkage in the early stages of curing. Additionally, slabs were watered for initial days and formwork was removed after 7days, Figures 3.19 (d) through 3.19 (f),
- Minimal shrinkage was evident after removal of formwork, on average 2-3 mm on the sides.

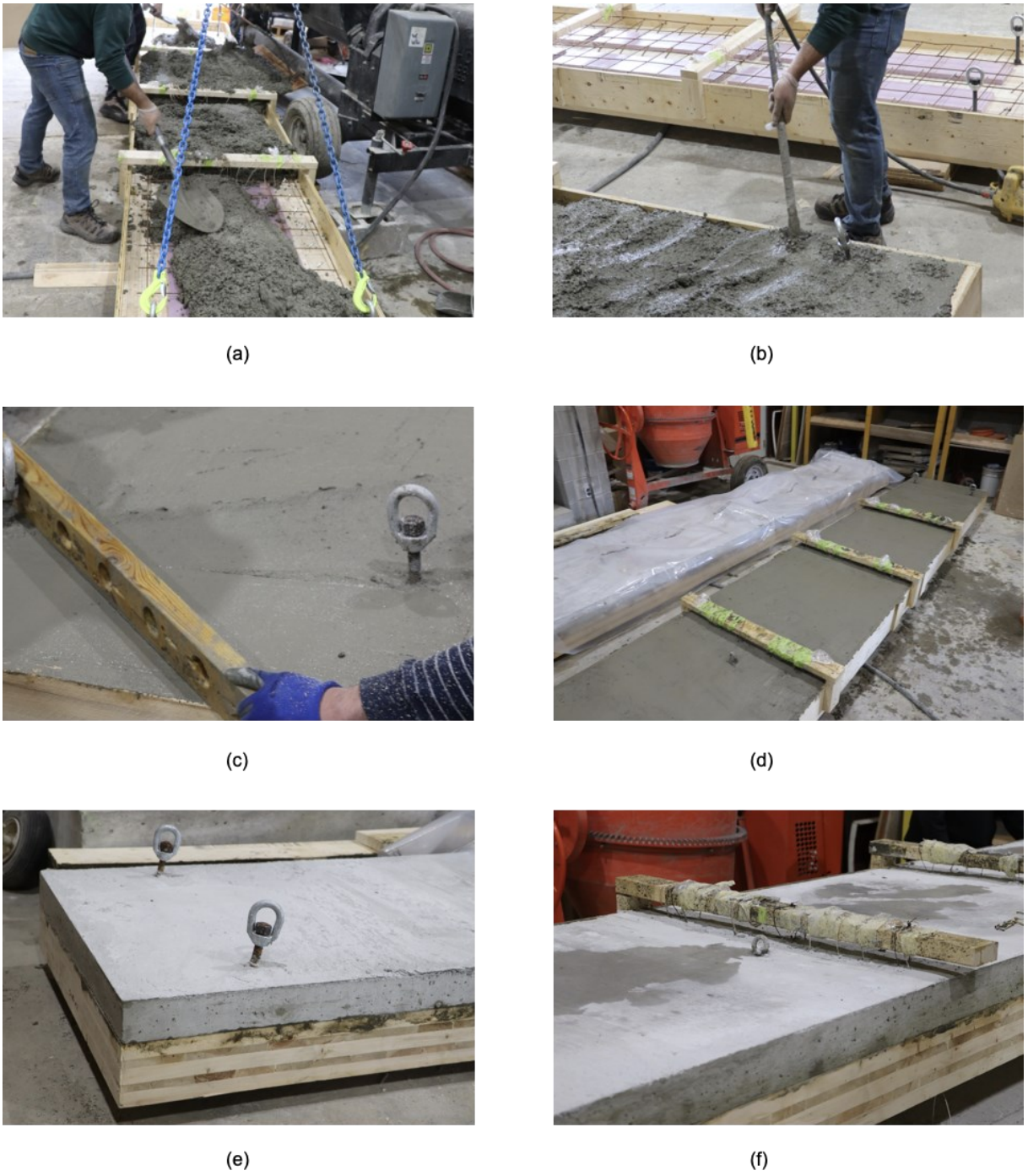

Figure 3.19: Concrete casting.

3.6 Test Set-up and Procedure

The test set-up schematic can be seen in Figure 3.20, with a top view of the furnace and a general specimen placed, showing the dimension and placement of all mechanical and thermal measuring devices. As previously discussed, there are three thermocouple lines with 12 thermocouples on the left, 12 on the right, and 13 at the center, Figures 3.14 and 3.15. Thus, a total of 37 thermocouples were installed in each test specimen to capture the temperatures and to monitor the overall performance of the specimen. Additionally, three draw-wire displacement transducers were installed at the location of the two-point loads and at the center. Comparing the left and right to each other and the center where the maximum deflection is located can determine if the slabs are deforming symmetrically about its center.

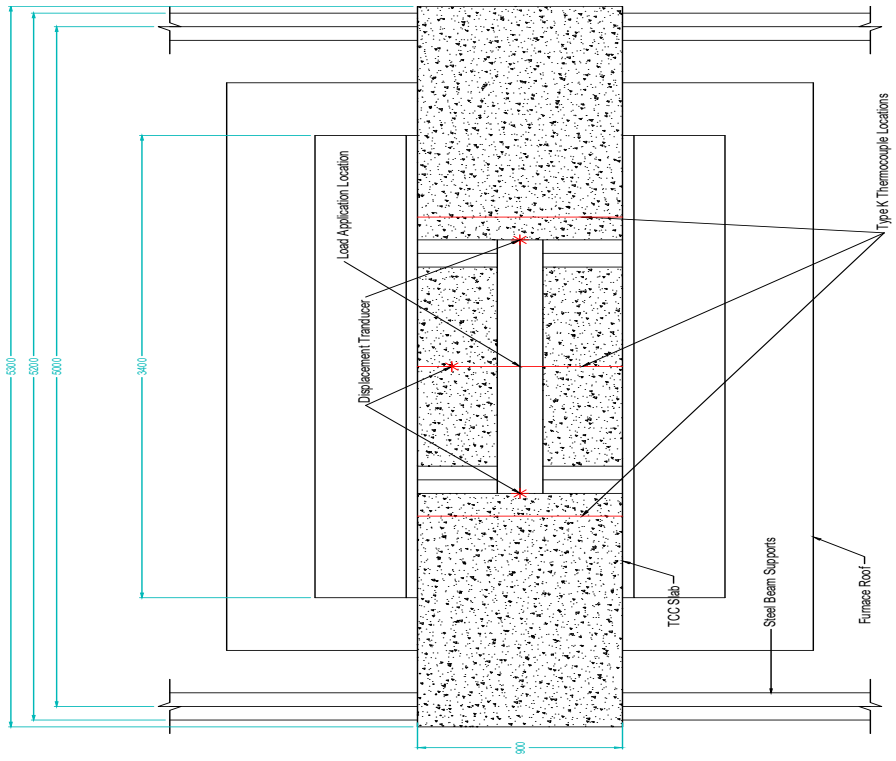

Figure 3.20: Test set-up with a general test assembly placed – Top View Schematic.

Figure 3.21: Test set-up with a general test assembly placed.

The total load was applied in four increments, 25% each, and then was maintained for at least 30 minutes before the start of the fire test in conform with CAN/CSA-S101 fire endurance testing standard. According to the current testing capabilities, it was only possible to apply the desired load over two-equal line loads to follow that of four-point flexure bending. However, in situ conditions, the load would be uniformly distributed (UDL) for floor slabs. To overcome this difference and test to realistic situations, loading was chosen to create equal moment magnitude from that of a UDL but be applied as a two-equal point loads.

The standard fire exposure was controlled and monitored by an HMI system that allows one to follow the desired fire time-temperature curve. During testing, deflections and temperature changes throughout the section were monitored. All tests were terminated when either TC5 (located between the third and fourth ply) reached the charring temperature or exceeded the critical deflection rate. Additionally, as each slab was duplicated to verify experimental results, the fire

test was terminated soon after the 2-hr time mark. However, the other duplicated specimen continued to show behaviour that does not dramatically drop quickly after the 2-hr fire exposure. As post-test analysis, the charred wood layers on the specimens were removed, thereby uncovering the remaining CLT panel with structural integrity. Only slabs that were exposed to only 2-hr test duration were examined to determine the critical value of residual section after charring. Thereby, giving comparative results to previous research and the influence of the inclination angle of the STS on the charring rate of the CLT slabs.

Figure 3.22: TCC section with CLT exposed to standard fire.

CHAPTER 4: EXPERIMENTAL RESULTS AND DISCUSSIONS

All TCC floor assemblies were exposed to one-dimensional heat transfer due to elevated fire temperatures while being subjected to four-point flexure bending. Loading was maintained throughout the duration of the fire test to follow standard fire endurance testing procedure, noting that the loads applied throughout fire testing were specified loads (not factored).

Measurements recorded included vertical displacements at the location of point loads and midspan and extensive thermal readings throughout three sections along the length of each test assembly. Experimental results can evaluate the thermal and mechanical performance of TCC sections with CLT and STS shear connectors throughout the test duration. Meaningful relationships to study are the measured temperatures with respect to time, the charring behaviour of the CLT panel and how this influences the TCC section, and overall deflection. Four samples were tested, with the first two having STS orientated at 45° and the last two having STS orientated at 30° from the horizontal.

4.1 Concrete Testing

Before completing fire testing on specimens, the concrete properties were examined, including slump, density, and compressive strength at seven and 28-day testing. As each slab was casted on a different day from separate batches, the consistency shown is essential. The mix and TCC sections were designed considering concrete with compressive strength equal to 30 MPa. Test results show an average seven-day strength of 29.86 MPa and 28-day strength of 38.27, each with minimal standard deviation. As the fire testing did not occur until about five months on average after casting, the concrete compressive strength continued to increase during this time. However, from previous research studies, the rate concrete compressive strength increases after the concrete age passed the 28 days is significantly reduced. Thus, the 28-day testing achieves most of the

concrete compressive strength; although the inherent nature of concrete, the strength will continue to increase as time progresses. From separate testing on the same concrete mix design, the strength would have increased by approximately 4-5 MPa by the time of fire testing (approximately after five months).

It is important to note that although the concrete strength is higher at the fire testing time and that of the original design, it would not influence the fire resistance of the TCC section. As previously discussed, when calculating bending moment and shear resistance, there are multiple calculations following the γ-method and EPM. Each considers the limiting property being either the timber or concrete components. Increasing the strength of concrete could make the design not limited by that equation but doesn't increase the overall performance as the timber strength properties have not been altered.

Table 4.1: Concrete strength properties

Sample Number	1 - 45°	2 - 45°	3 - 30°	4 - 30°
Slump (mm)	45	120	70	65
Density (kg/m^3)	N/A	2440	2467	2430
Compressive Strength 7-Day (MPa)	27.98	29.36	30.40	31.84
	28.87	29.62	32.65	26.78
	29.06	29.20	31.61	31.00
Average	28.64	29.39	31.55	29.87

Table 4-1: Concrete strength properties, (continued)

Sample Number	1 - 45°	2 - 45°	3 - 30°	4 - 30°
Compressive Strength 28-Day (MPa)	38.34	35.46	39.23	40.29
	39.15	38.35	37.86	40.08
	37.67	40.50	34.87	37.40
Average	38.39	38.10	37.32	39.26
Strength Comparison	75%	77%	85%	76%
Curing Time	169	159	161	151

4.2 Measured Temperatures

During any fire endurance testing on structural elements, it is essential to monitor and study the thermal behaviour of the sections, even more so when considering combustible materials like CLT or any other EWP to understand the rate of heat transferred and charring of the section. Unlike other materials where structural integrity is only diminished, with wood products, this occurs in addition to the loss of cross-section. Thereby significantly influencing the ultimate capacity and loss that is unrecoverable. Examining CLT when exposed to fire conditions is complex but extremely important to designing TCC with slab-type assemblies and providing adequate reliability in fire conditions.

Samples were tested following the CAN/ULC S101 fire endurance testing standard and its time-temperature curve to provide equivalent exposure times. Thus, comparing behaviours and performance of various assemblies and materials, including results from this research, and able to relate with other experimental programs. Figure 4.1 shows the actual fire time-temperature curves

applied throughout the four fire tests, and a direct comparison to the standard time-temperature curve that was followed. Thereby, establishing consistency and validity of the fire curves used during testing with the standard fire curve, as all profiles nearly overlap. Figures 4.6 through 4.9 show the averaged thermocouple readings and the fire time-temperature curve corresponding to each test (which will be discussed in greater detail in section 4.2.1). Exhibiting the development of temperature corresponding to the fire curve and heat transfer through the slabs against time.

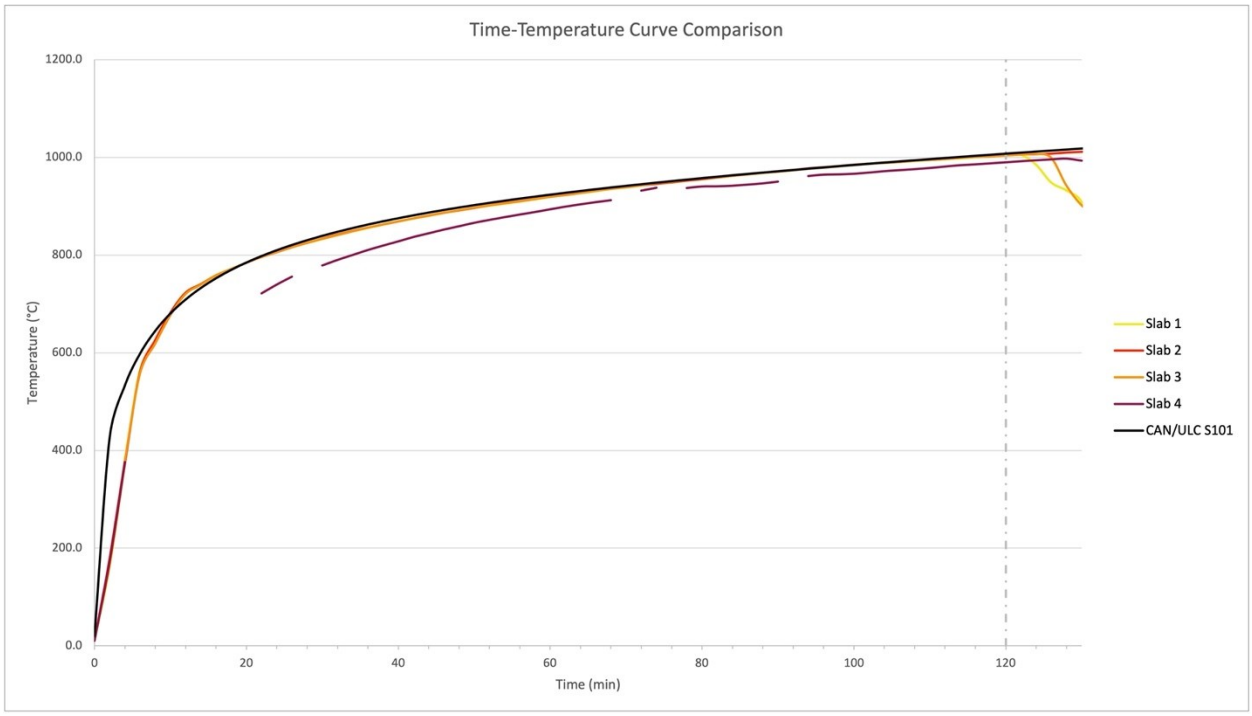

Figure 4.1: Time–Temperature curve comparison

Results were analyzed in two distinct ways. First compared the slabs against themselves by looking at the overall sections and studying the differences with the three separate thermocouple locations: left side, midspan, and right side. The left and right lines are just offset from the location of the point-loading application. Then next is comparing the slab against each other, tracking if duplicate samples are consistent and studying differences when comparing Slabs 1 and 2 with Slabs 3 and

4, where the inclination of the STS for shear connectors changed. Refer to section 3.5.1 and Figures 3.14 and 3.15 for specifics of the thermocouple layout. Concisely, thermocouples TC1 to TC7 were in the CLT panel, TC8 at the interface between materials, TC9 at the mid-depth of concrete, TC10 and TC11 around the STS, and TC12 on the concrete surface.

4.2.1 Temperature Profiles

Temperature profiles were developed for each slab; from studying all figures, they are in good agreement with each other and very comparative in terms of rate and heat transfer through the slabs. The first five thermocouples are the most critical, with TC1 being 17.5 mm inward, TC2 being 35 mm, TC3 being 54 mm, TC4 being 71.5 mm, and TC5 being 89 mm, as they are first to experience the effects of fire, and the rate at which they heat dictates the overall performance of the TCC floor assembly. Additionally, TC5 was used as a test termination to protect the utmost major strength ply of the CLT panel.

All slabs safely achieved the threshold of two-hour standard fire exposure, with Slab 1 and 3 tests being terminated at 125 min, while Slab 2 and 4 continued until 145 min. Thereby, all slabs were able to sustain the applied loads for the time required, if not exceed, and have a minimum of two-hour fire resistance rating. Furthermore, charred depths and behaviour at two-hour standard fire exposure were determined to show that failure does not occur shortly after the specific two-hour time mark.

Figures 4.2 through 4.5 show the entire test duration and measurements of all thermocouples implemented in each test specimen. Comparing the trends in how each of the different depths and locations increases temperature can evaluate how the specimens were burning. Each thermocouple number is the same colour, with the three separate locations having different line types: left side

dotted, middle solid and right side dashed. Having multiple locations can have a better representation of the slab and be able to distinguish if it is burning at similar rates across the furnace. This is further demonstrated when examining the charring rate and depth discussed in subsequent sections. While Figures 4.6 through 4.9 show temperature profiles of data averaged for thermocouple numbers to better examine the overall performance of the slabs and compare them against each other more simply. All presented time-temperature curves show relatively smooth profiles with a more gradual increase in temperature, i.e., no sudden jumps in increased temperature. This is attributed to the very minimal delamination experienced by the CLT panels during fire tests. As there are no sudden spikes in thermal behaviour, no significant amount of charred timber fell during testing on the furnace floor. Delamination is a critical issue for CLT panels in fire conditions.

It should be noted that Figures 4.5 and 4.9 are for the fourth slab and have shown gaps in the thermal data resulting from a testing complication and the inability to run the test continuously. Complete data was stitched together, showing the time and duration of the stops. The HMI setup allows staggering the starting point of the standardized fire curve. Therefore, the slab was still tested following the same standard time-temperature curve. There is a minimal difference when comparing the results from the previous test as it is only needed to consider that the time in fire and total duration are not equal. The temperatures changed more during the time stops after the point of charring as the thermocouples would be fully exposed to the fire and more influenced when the furnace stopped. Compared to still being in the timber material, even when the fire stopped, it did not extinguish the timber; instead, there was continuous burning and smouldering. Thereby, not giving a difference for the short durations of the time stops. For this test, the two hours of fire exposure occurred at 148 min into the total duration.

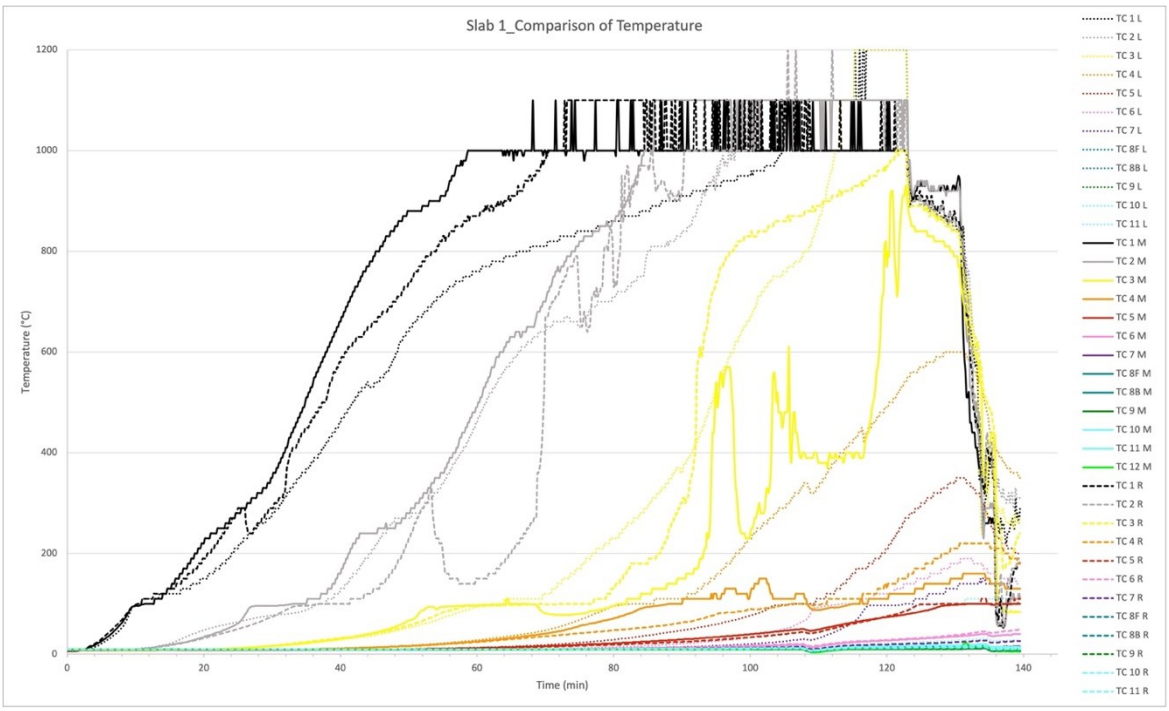

Figure 4.2: Slab 1 comparison of temperatures.

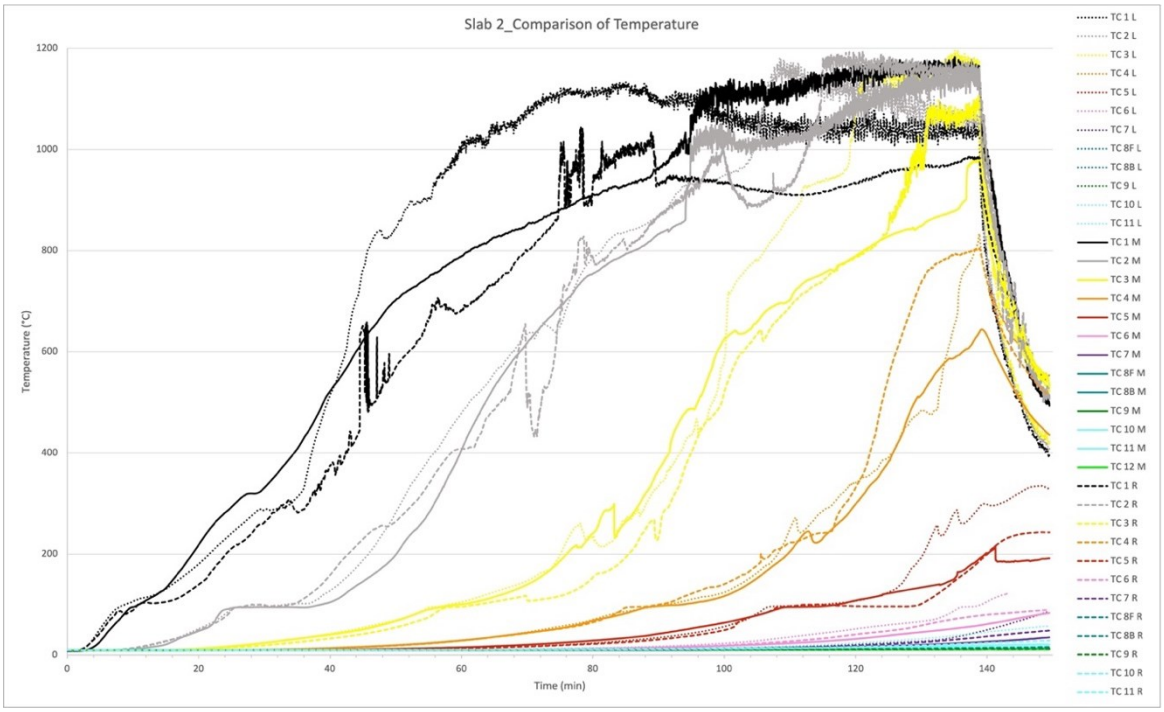

Figure 4.3: Slab 2 comparison of temperatures.

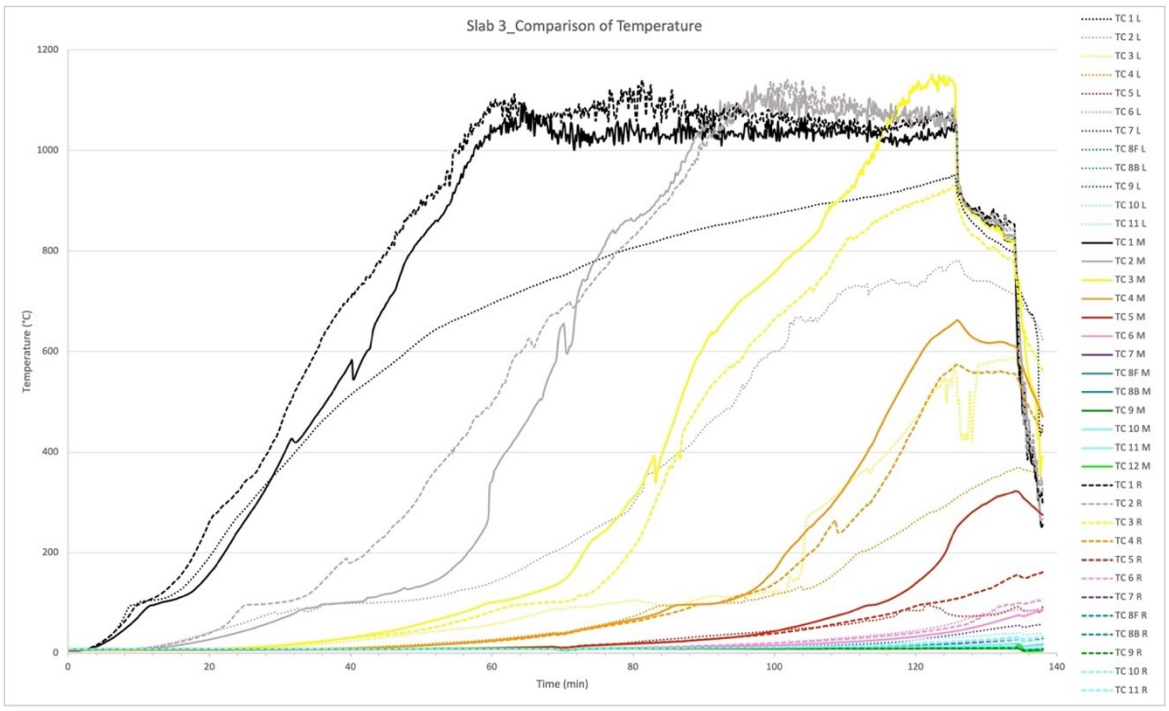

Figure 4.4: Slab 3 comparison of temperatures.

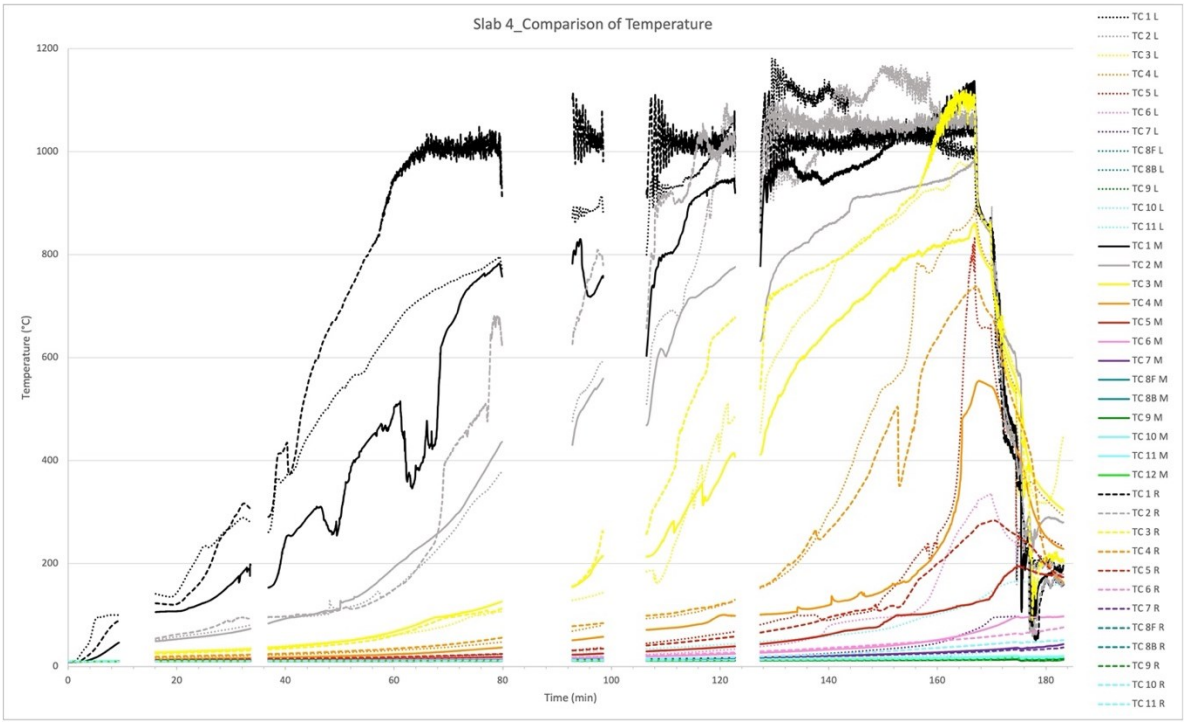

Figure 4.5: Slab 4 comparison of temperatures.

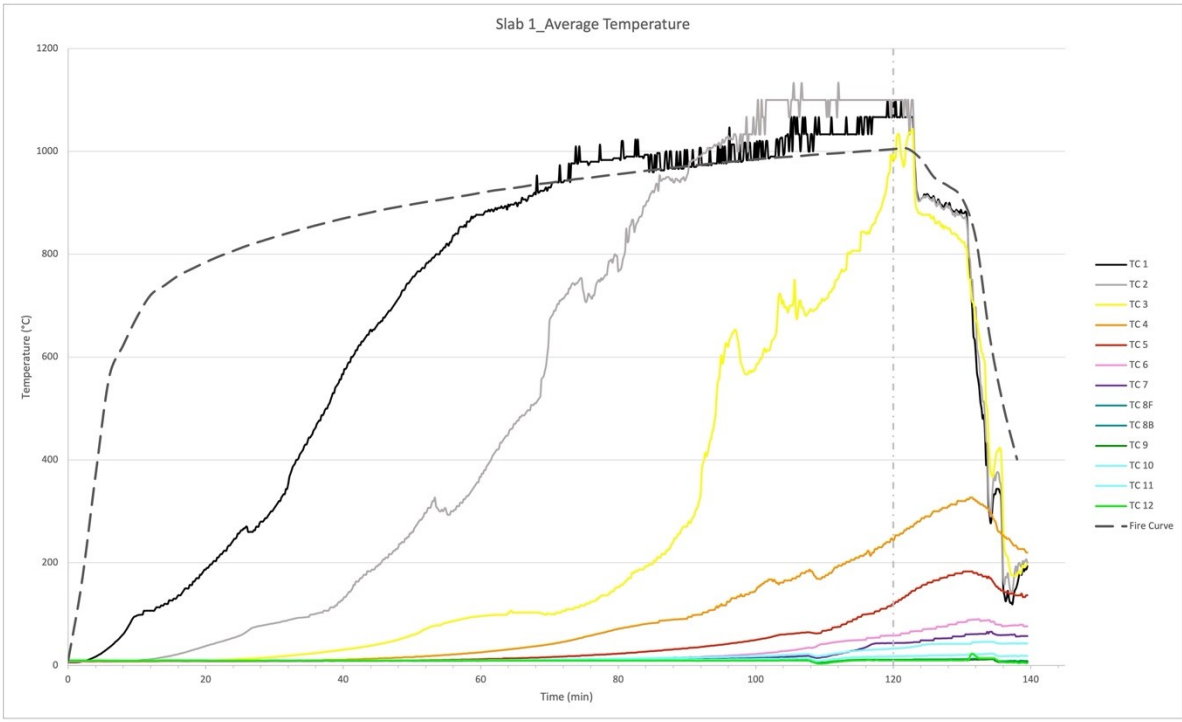

Figure 4.6: Slab 1 average temperature readings.

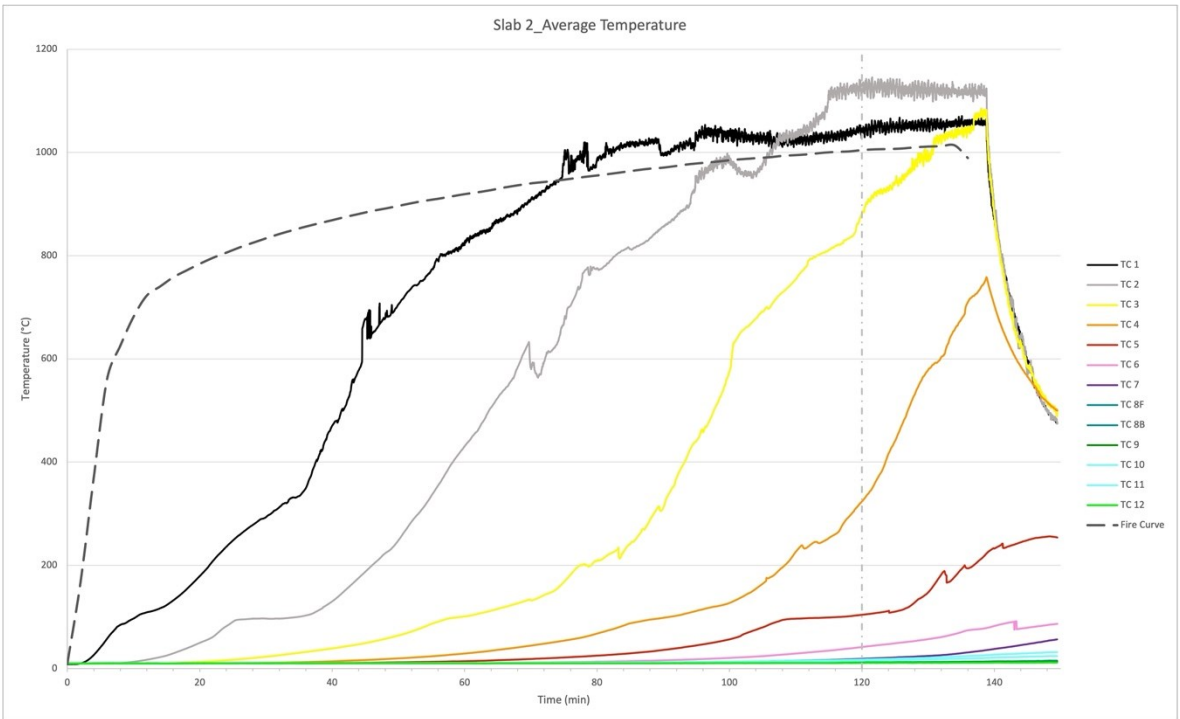

Figure 4.7: Slab 2 average temperature readings.

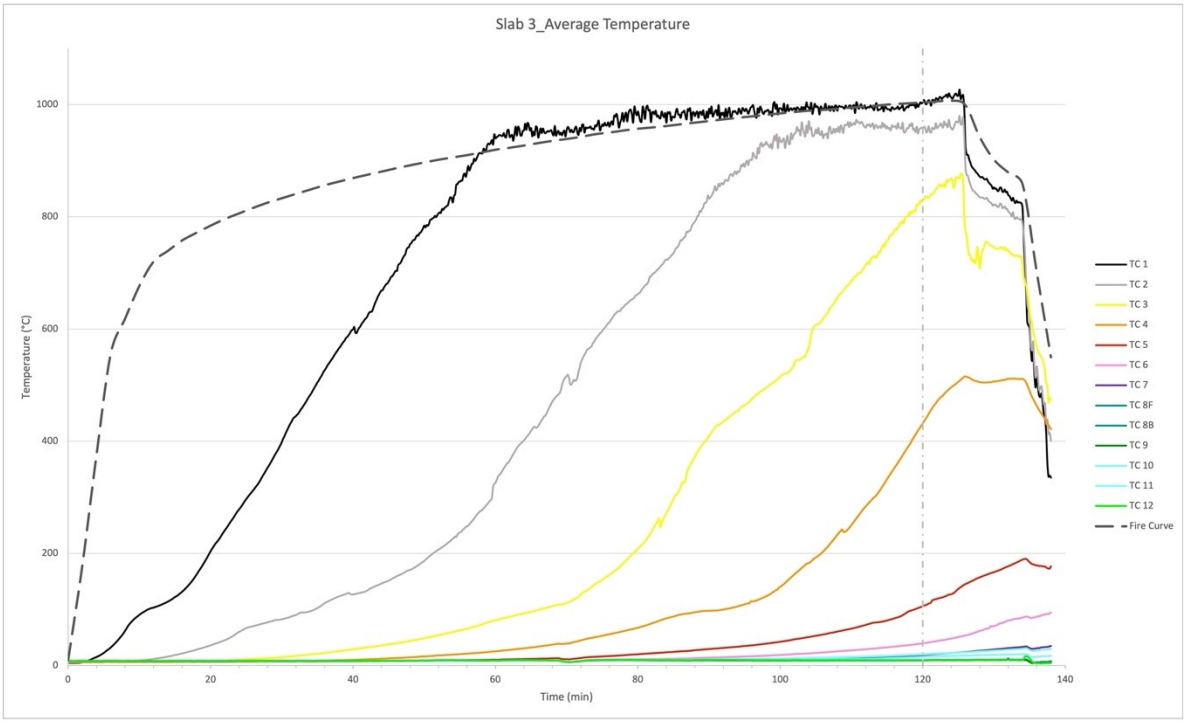

Figure 4.8: Slab 3 average temperature readings.

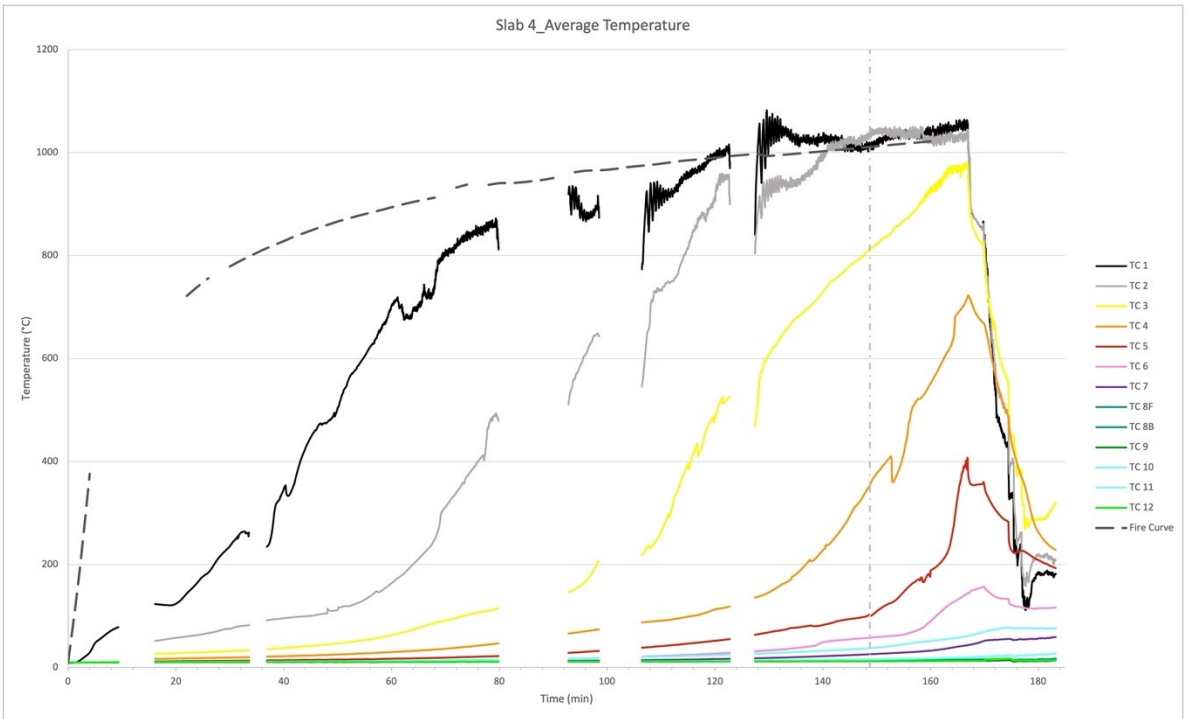

Figure 4.9: Slab 4 average temperature readings.

4.2.2 Critical Thermocouple Temperatures Comparison

The most critical thermocouple (TC5) was carefully monitored throughout fire tests. The measurements of the said thermocouple were used to terminate the fire test. The said thermocouple (TC5) is located at the interface between the third and the fourth ply of the CLT panel, thereby having this thermocouple not reaching the charring temperature allowed for this minor-strength direction ply to protect the utmost and final major-strength direction ply. As previously stated, only the major-strength direction plys resist the applied loading and were used in determining the strength properties of the CLT panel under fire exposure. Therefore, it was critical to ensure that the very top ply remained to ensure the integrity of the TCC floor assembly and the safety while removing the fire-damaged assembly from the furnace after terminating the fire test.

As can be seen in Figures 4.10 through 4.13, the temperature profiles for thermocouple (TC5) from each location: the left, the right, and the middle; additionally, the averaged profile for each slab are shown. After examining the profiles at the fire test's two-hour duration, the measurements of TC5 reach approximately 100-150°C. Therefore, the location is undoubtedly experiencing the effects of the fire but not at the point where full strengths of wood were lost.

It should be noted that the temperatures continued to increase for all test specimens after the two-hour mark, even for the first and third slabs with a test duration of 125 min. This is the effect of internal smouldering of the CLT panels and shows that once a combustible material ignites, even though the fire is stopped does not directly correlate to the extinguishment of the sample. Furthermore, due to the test setup and procedure, it took, on average, another 15 minutes to extinguish the samples after the furnace was shut off. Therefore, the thermocouples that were directly exposed to the fire, i.e., TC1, TC2, and TC3, as seen in previous figures had sudden drops

in temperature due to the dramatic change in the fire environment by shutting off the furnace and removing the fuel supply to the fire. However, more internal thermocouples still protected by previous charred layers remained insulated and continued burning and charring upward.

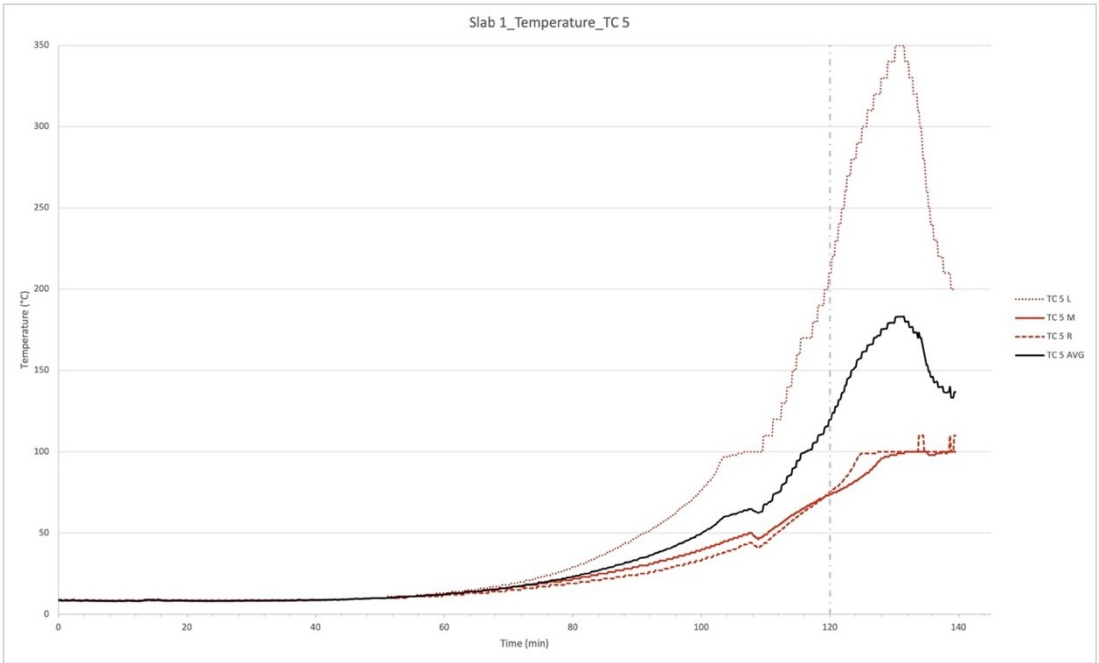

Figure 4.10: Slab 1 temperature examination of TC5.

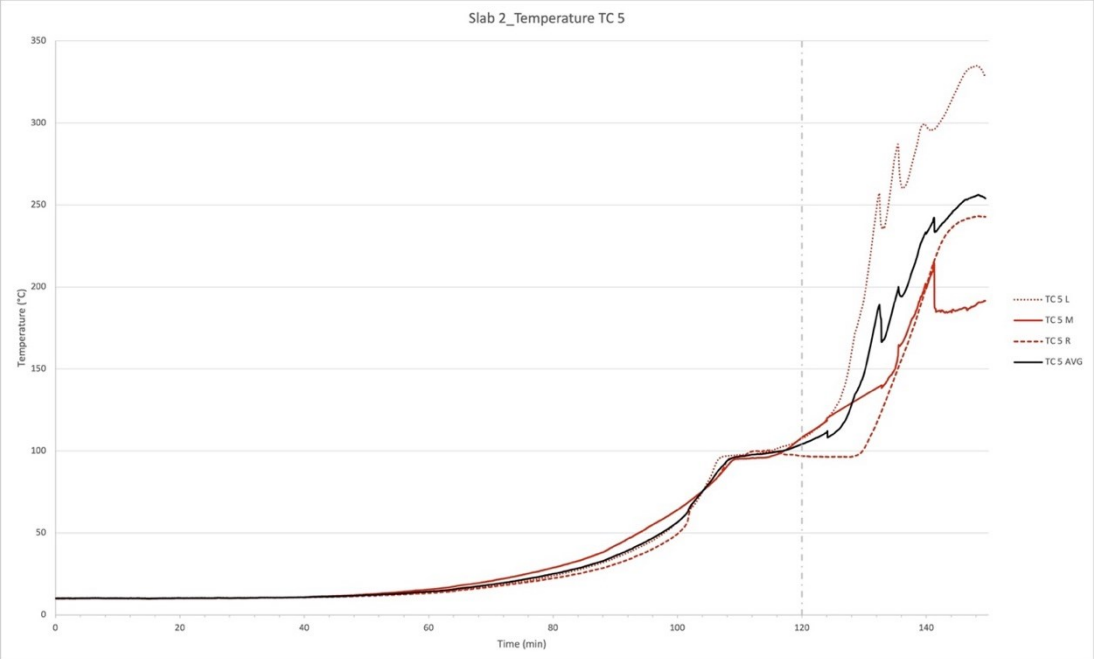

Figure 4.11: Slab 2 temperature examination of TC5.

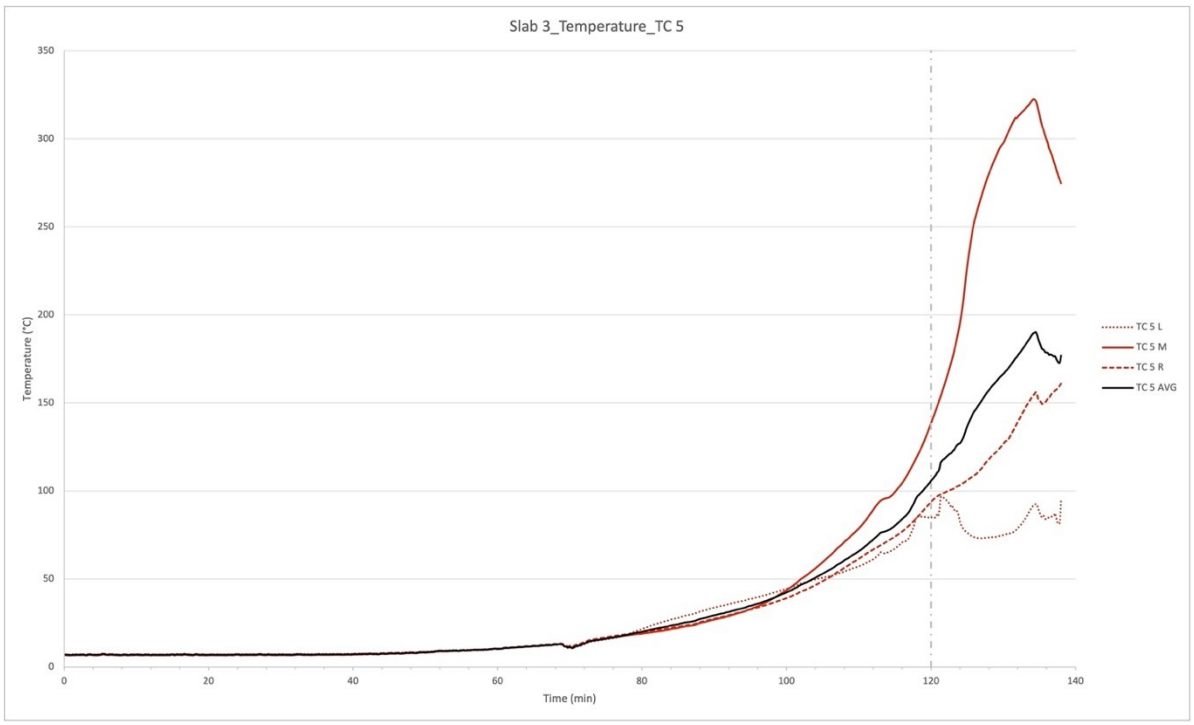

Figure 4.12: Slab 3 temperature examination of TC5.

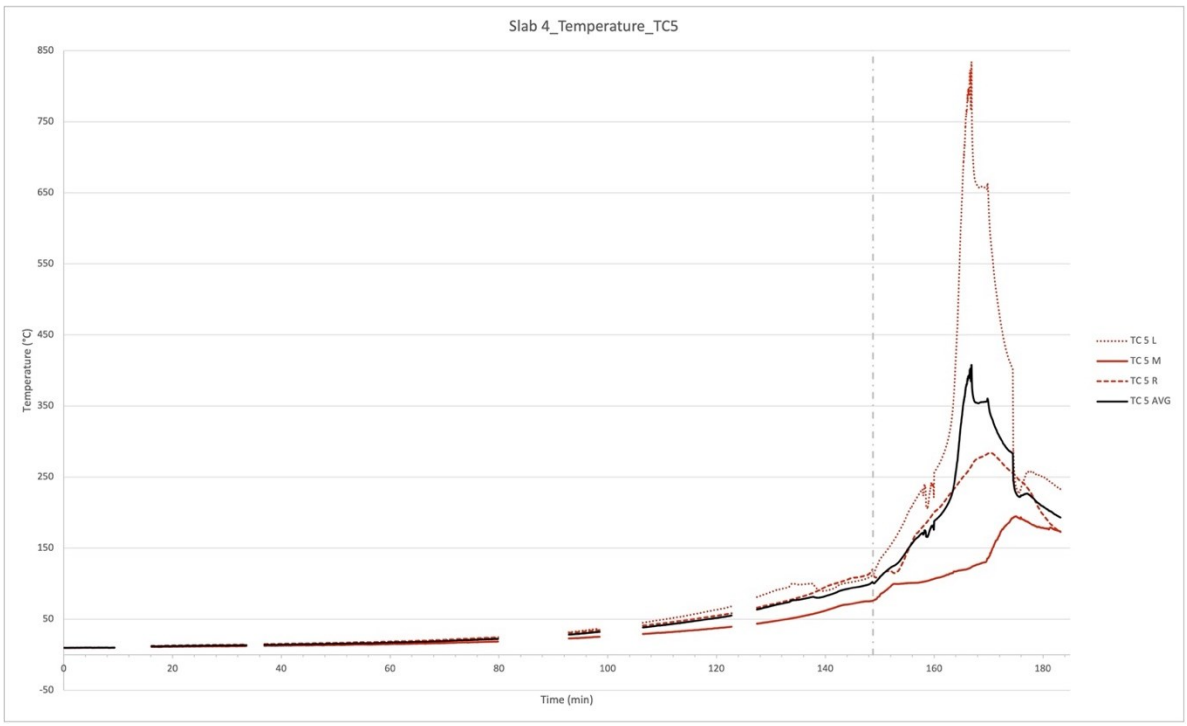

Figure 4.13: Slab 4 temperature examination of TC5.

4.2.3 Heat Transfer Through Slab

Monitoring the fire development and charring progression of the sections throughout the fire testing comes down to evaluating how heat transfers through the slabs. Apart from the thermocouples that are exposed initially and others not until near the end of the fire test, it is essential to examine the locations that are protected from previous layers of wood and ones located in the concrete. These temperature profiles can be seen in Figures 4.14 through 4.17, where thermocouples TC6 through TC12 are shown for each slab.

Where TC6 and TC7 in the CLT, TC8-F and TC8-B are at the interface between materials, TC9 and TC12 in the concrete, and TC10 and TC11 around the STS. Examining the profiles shows that very minimal temperature increase occurred above the temperatures measured by TC5. Meaning a lack of heat transfer to the top of the slab, although the bottom is experiencing a fire temperature of approximately 1000°C. Proving a lack of heat transfer through the slab as most thermocouples do not reach temperatures higher than 40°C after the two-hour fire duration. It also should be noted that those that measured an increased temperatures are mostly TC6 and TC7, which are still located in the CLT panel. Comparatively, the ones found in the concrete and at the interface between materials barely increased (approximately 10°C) from the initial starting temperature before the fire test began.

As for the thermocouples at the STS screws, the measured data concluded that they do not represent the temperature of the screws themselves; during testing, they were directly exposed to the full heat of the fire. Instead, they represent the concrete proximity to the screws. Once any steel material is exposed to high temperatures, there is near-immediate heat transfer through the metal. Therefore, these thermocouples do not show the temperatures of the STS but show that though the

connectors are heated, they do not correlate with heat transferred directly to the concrete's surroundings. However, CLT is a combustible material, which could influence the wood around the screw after the screws are exposed to the heat of the fire. For future examination, it is recommended to weld the thermocouple beads directly to the screw instead of wrapping the thermocouples around. That way would accurately represent how quickly the screws experience elevated temperatures through conducted heat.

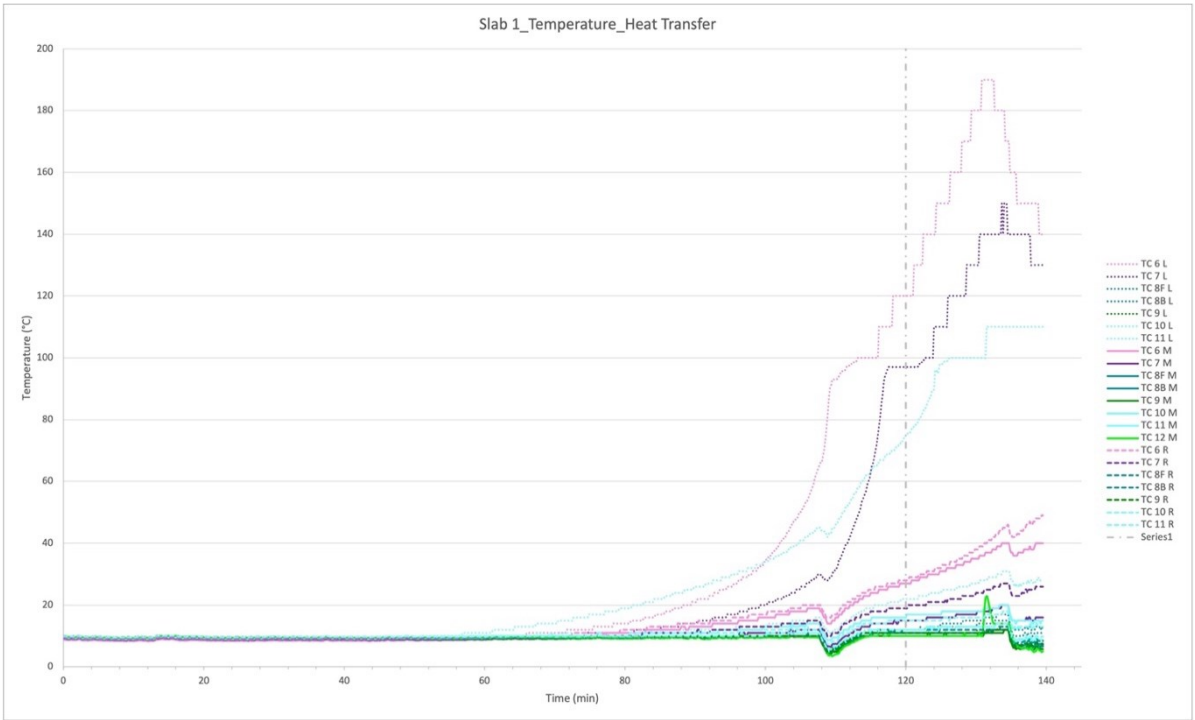

Figure 4.14: Slab 1 heat transfer to unexposed thermocouples.

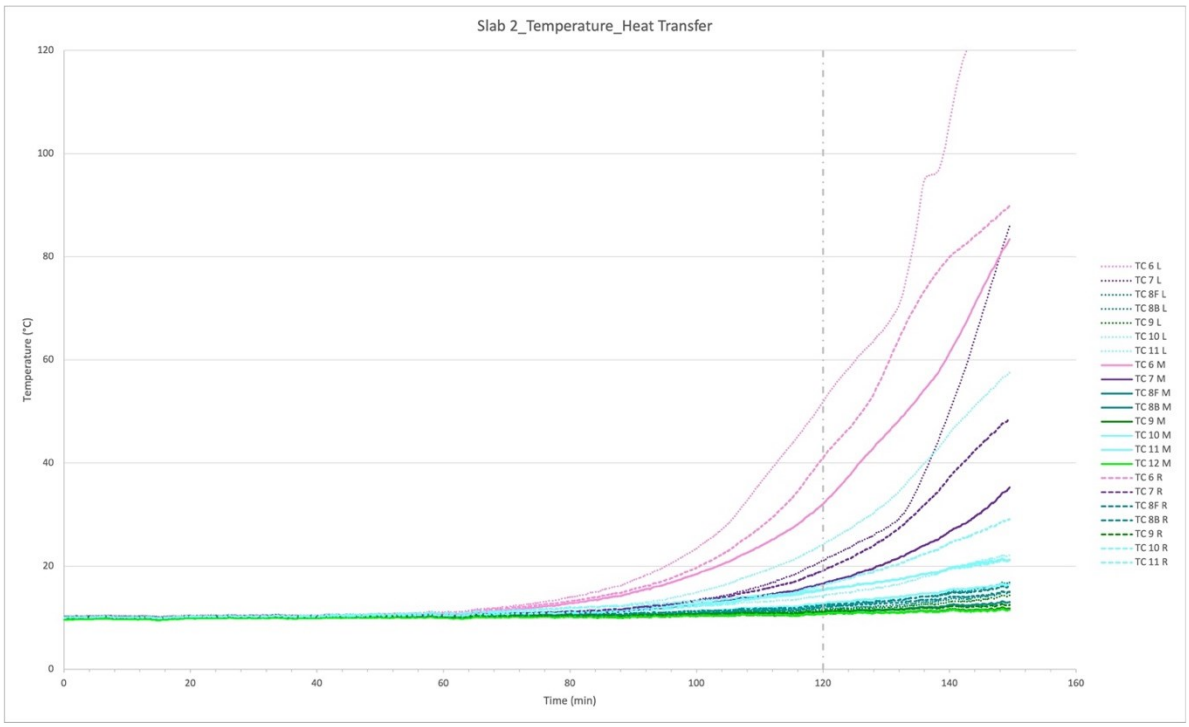

Figure 4.15: Slab 2 heat transfer to unexposed thermocouples.

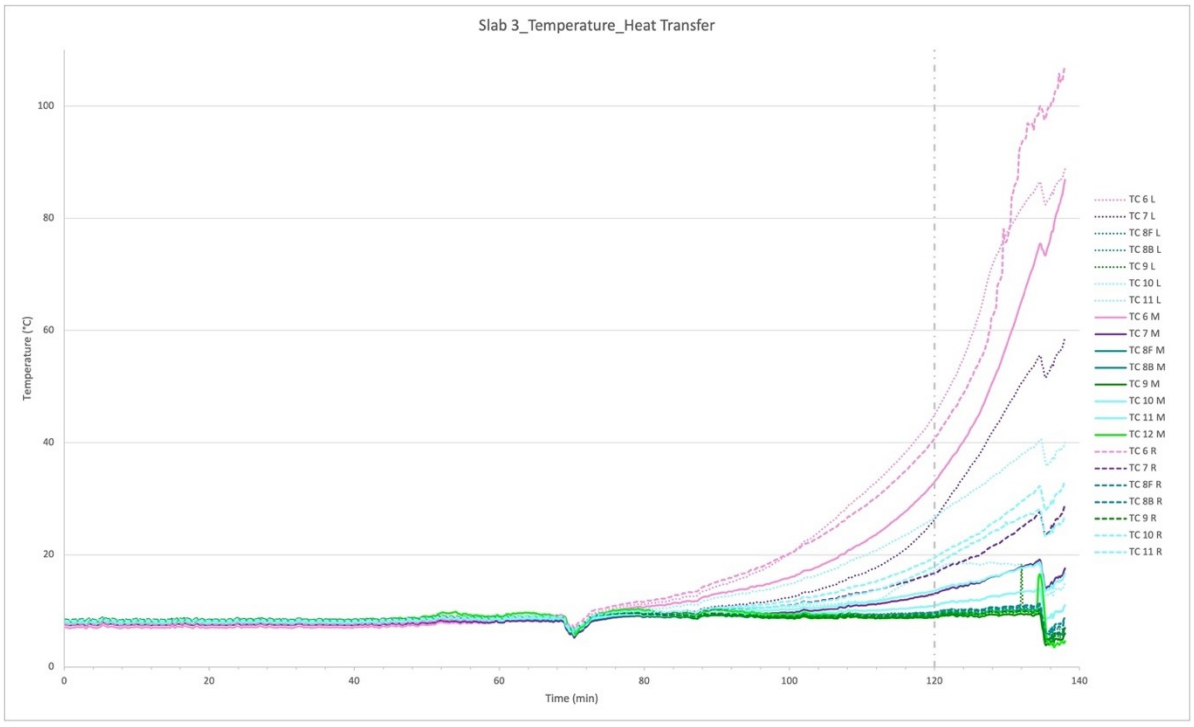

Figure 4.16: Slab 3 heat transfer to unexposed thermocouples.

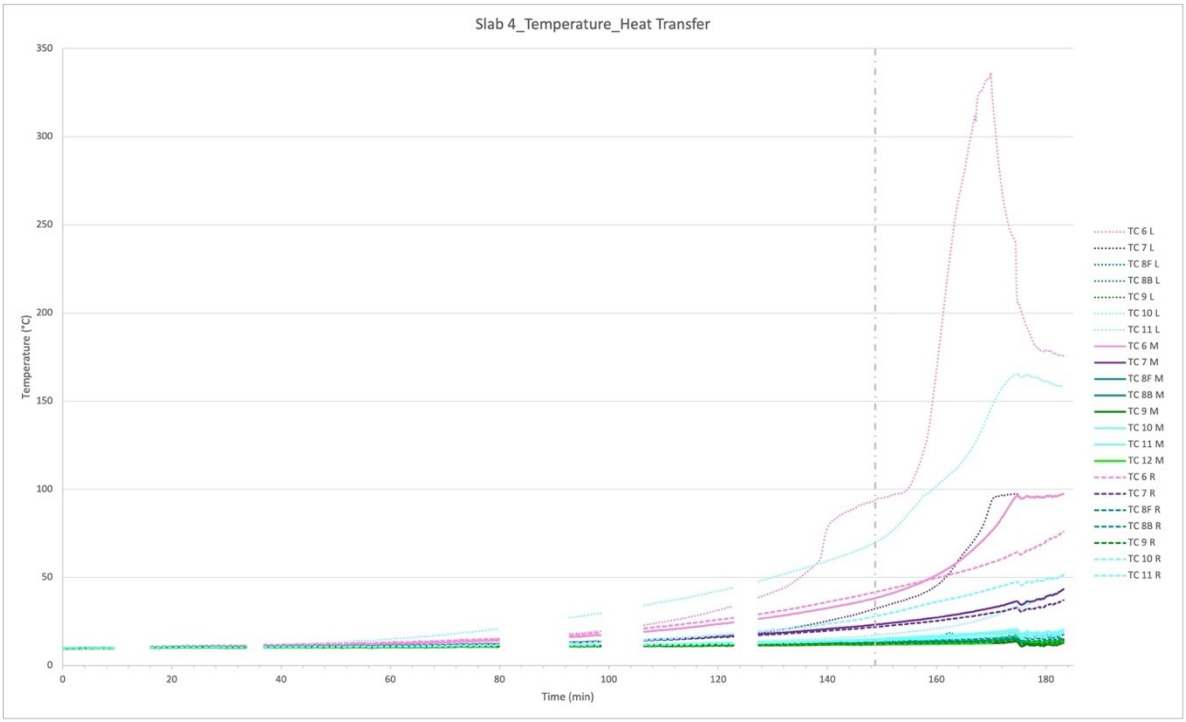

Figure 4.17: Slab 4 heat transfer to unexposed thermocouples.

4.3 Deflections

Apart from thermal measurements, the fundamental measurement monitored throughout the fire tests is the vertical deflection of the TCC floor assemblies, resulting from the applied loads and the effect of fire exposure. As loading was maintained throughout the test duration, Figures 4.18 through 4.21 show the deflection measurements due to fire exposure's effects. In addition, Figure 4.22 directly compares deflection profiles measured at midspan for all four samples tested. Providing consistency and reliability in results as all tests followed very similar results and no sudden jumps or drastic deviations during the testing.

One of the benefits of the slab-type assembly in designing TCC sections is that the timber material can be used as permanent formwork for the concrete portion. As a result, this causes an initial deflection for the slabs due to the weight of wet concrete and, ultimately, the self-weight of the specimens before any loading is applied. The resulting values were as follows: for Slab 1, 4.77

mm; for Slab 2, 6.57 mm; for Slab 3, 6.02 mm; and for Slab 4, 7.83 mm. These values are not represented in the figures but important to note the additional deflection the slab experiences and resists.

By examining Figures 4.18 through 4.21, it can be noticed that deflections followed a similar trend for all four test specimens. There is no sudden increase in values; therefore, none of the samples approached the test termination criteria of exceeding an acceptable deflection rate and did not reach failure. It also should be noted that during the test for Slab 3, there was trouble collecting deflection data at the midspan for the initial hour of the fire test. However, following the typical trend of differences between the midspan and point load locations, an approximation was generated as there was usually a difference of 1-2 mm. The problem was corrected and the most crucial deflection data from 67 mins onward (near the end of the fire test) was successfully collected.

Toward the end of each test, there was an increase in the deflection rate and the most significant difference in behaviour when studying the different STS inclination angles. This increased deflection rate correlates to the time after the first ply (the very bottom one) was completely charred at approximately the 1-hour mark to when the third or the second major ply began charring. Subsequently, after the third ply continues to burn, the deflection was evermore increasingly more quickly until the completion of the test. This difference in deflection and increased rate correlating to the time of charring is analysed in more detail in section 4.4.2.

Additionally, Slab 1 had more significant deflections than those experienced by Slabs 2, 3 and 4. This shows that as the CLT burns near-uniformly, this corresponds to similar deflection rates and profiles. Although Slab 1 had more significant deflection than other samples, reducing the

inclination angle consistently kept the deflection results at reduced values. As expected, once the screws are exposed to the effects of the fire and thereby decrease in stiffness, the section deflects at an increased rate. It's important to note that the change in impact is not constricted to the inclination angle of the screw but, more significantly, when considering the fire exposure, the reduction in embedment depth of the STSs in the samples. As with the screws orientated at 45°, they are exposed to the heat of fire earlier and start losing their strength quicker and to a greater extent at the two-hour test duration. Finally, consider the angle of inclination and the embedment depth when studying elevated temperatures. This behaviour matches the results from the literature and expected performance when looking at the effects of the inclination angle on the fire performance of TCC sections with STS. Therefore, the reduced angle and embedment depth would be recommended over the 45° STS.

However, a benefit of having a greater embedment depth is the ability of the STS to aid in keeping the CLT panel cohesive and potentially prohibiting the damaging effects of delamination of the lamellas during fire exposure. It should be kept in mind if CLT delaminates; it can severely affect fire performance and achievable fire resistance rating. From temperature profiles, deflection results, and observations, no samples experienced global delamination during testing; this also correlates with the change in using a more thermal resistance adhesive during manufacturing. Although if there is a concern or question regarding delamination, then be mindful of not only the inclination angle performance but also the embedment depth and to which ply the screws are secured.

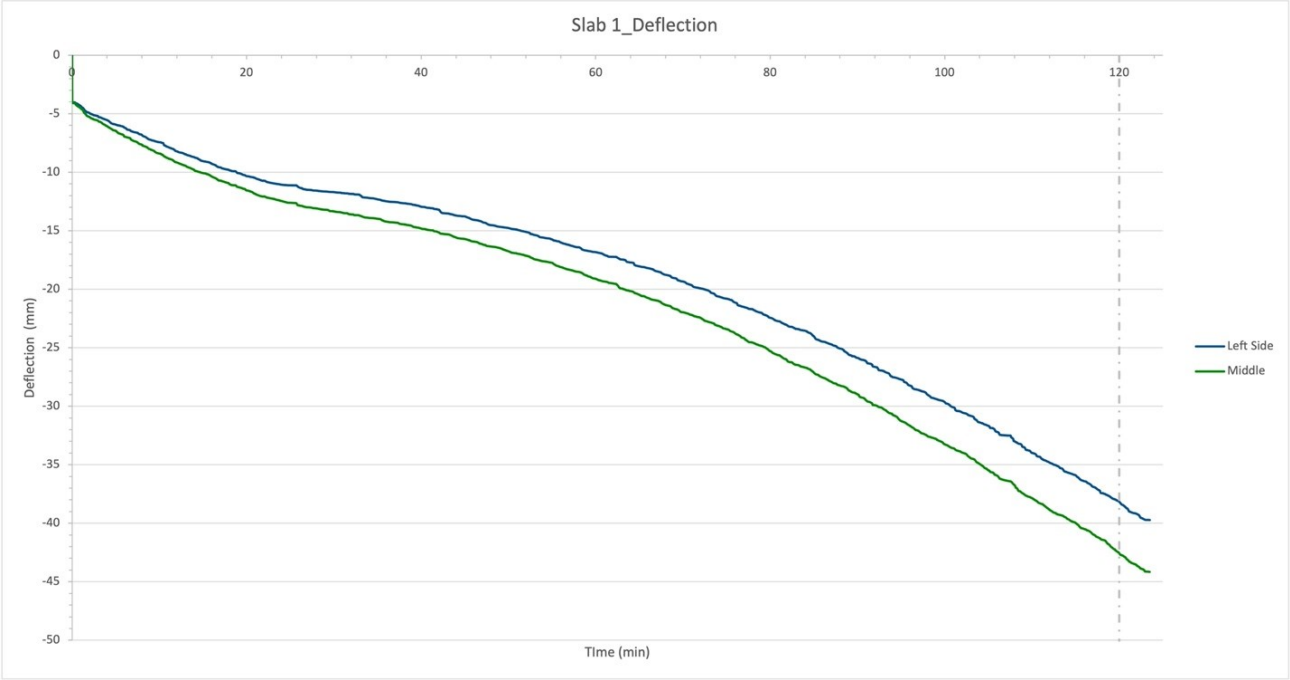

Figure 4.18: Slab 1 deflection vs. time curve.

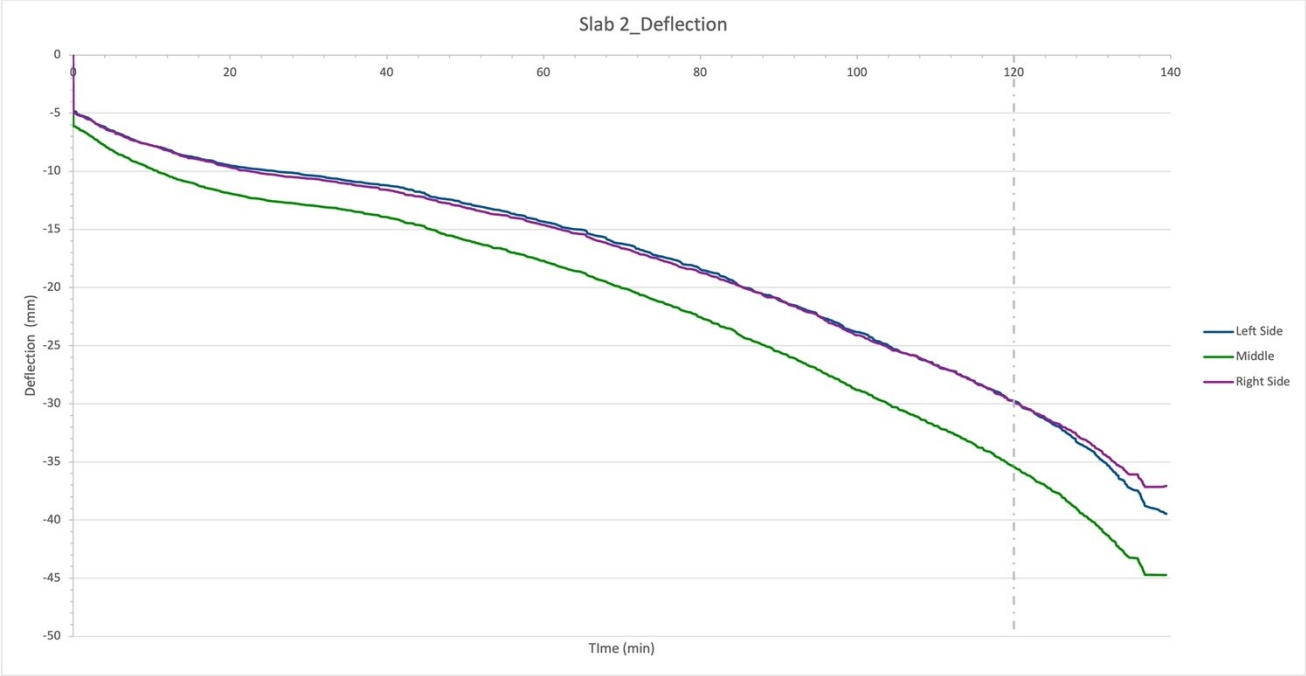

Figure 4.19: Slab 2 deflection vs. time curve.

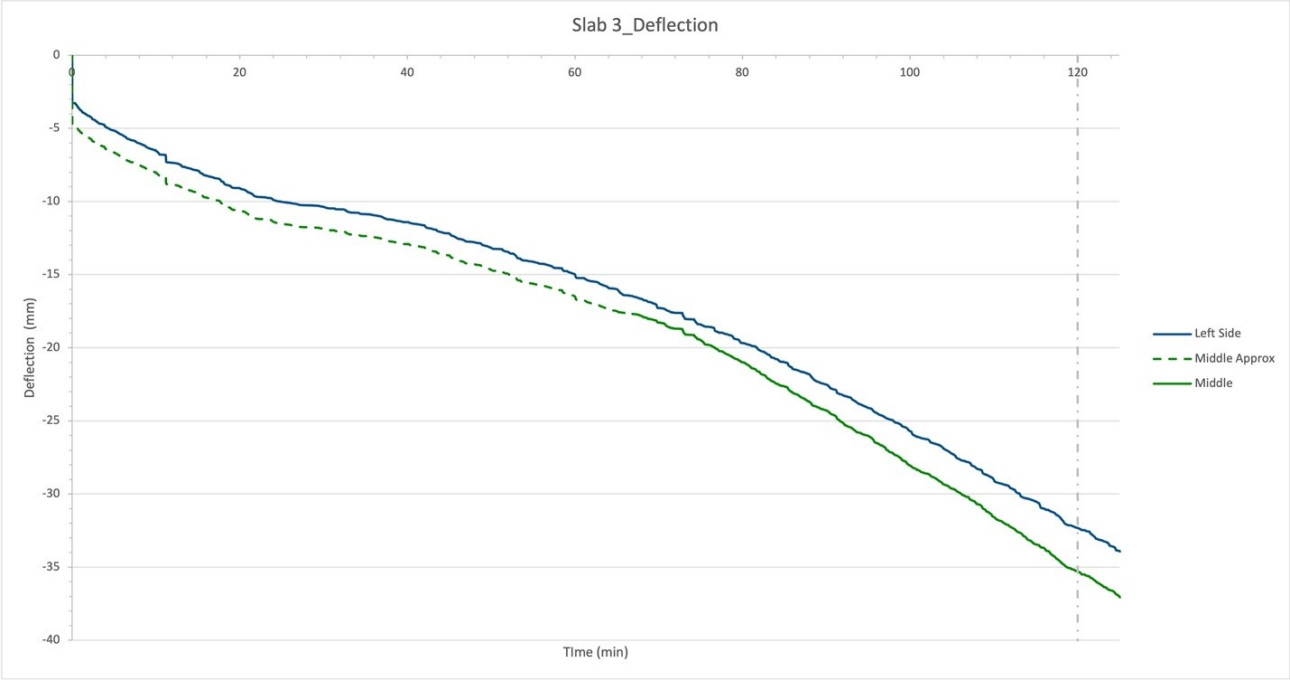

Figure 4.20: Slab 3 deflection vs. time curve.

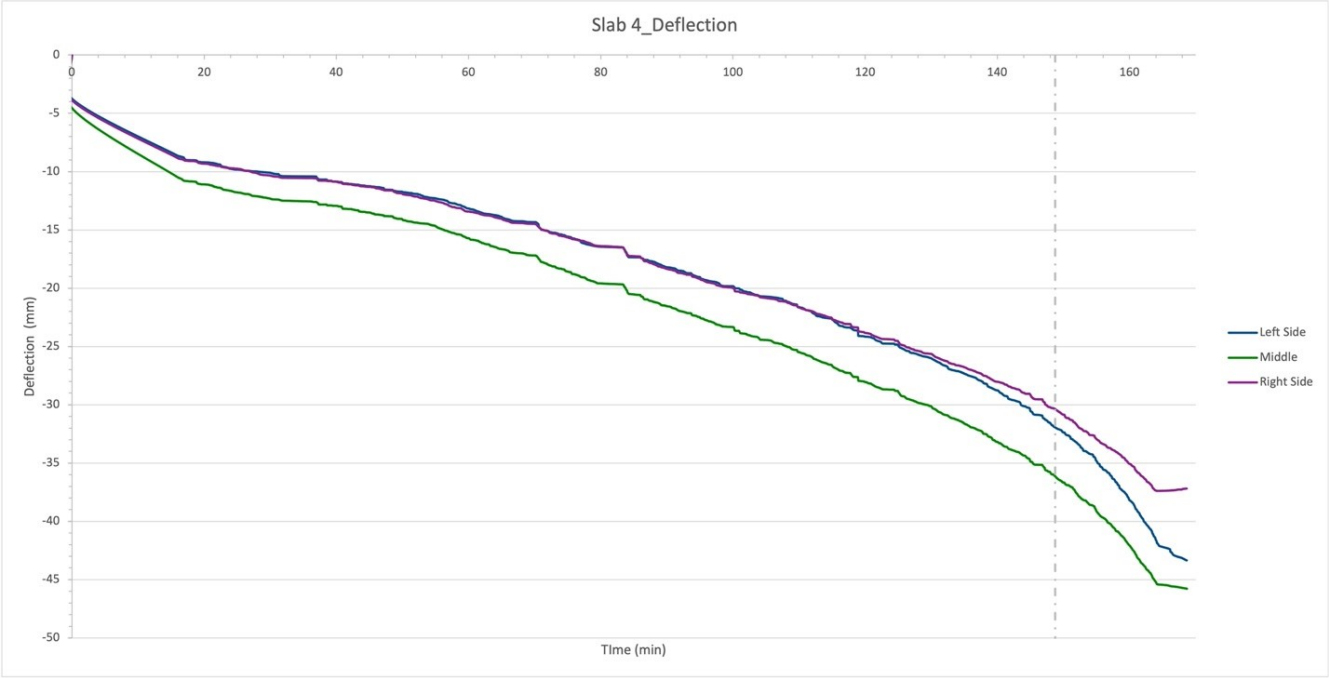

Figure 4.21: Slab 4 deflection vs. time curve.

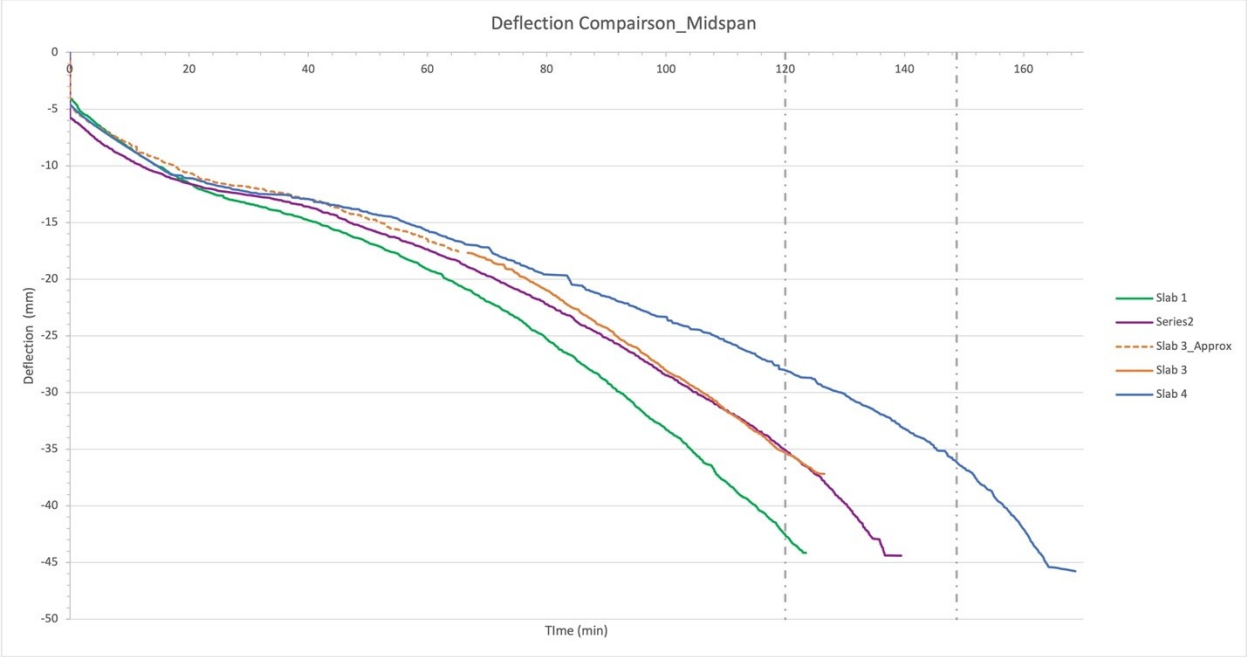

Figure 4.22: Midspan deflection vs. time curves comparison.

4.4 Charring Behaviour

A crucial step in studying the behaviour of timber materials when exposed to fire is the rate and development of the charred front. As described previously in section 2.4.3, when studying the behaviour of CLT under fire, all strength properties are affected more severely as temperature and fire exposure duration increase. Although this relationship is further exaggerated with timber materials, with the loss of properties once wood becomes heated a total loss of the wood strength occurs once its temperature reaches 300°C. This is a critical point and key when examining thermal data obtained from. Charring behaviour are studied in four ways: the time when temperatures reached 300°C, the deflection at those corresponding times, the rate that charring occurred, and the measured residual depth of the section.

While compared to contemporary theories and reasons for the hesitation when increasing the construction of tall timber buildings, these combustible products perform very well in fire

conditions. Heat transfer through the different plys that form a CLT panel takes a significant amount of time. Figures 4.14 through 4.17 show that even when the exposed side is at temperatures over 1000°C, the utmost ply has barely changed. Proving the insulation properties of the material, and while the temperature threshold of loss of strength is low, it takes an extended period while exposed to an elevated temperature to reach this point.

4.4.1 Charring Time

The measured temperature data for each test specimen was studied and evaluated when the thermocouples reached 100°C and 300°C, represented in Figures 4.23 through 4.27, shown in a stacked bar chart where the first level is when that thermocouple at that location reached 100°C and then the next level when reached 300°C. The first four charts show all thermocouple data for each slab, respectively. Conversely, Figure 4.27 directly compares all tests using the averaged values in temperature from the three locations for each depth, giving one value for each depth.

From studying the behaviour, the typical behaviour with 120 min is that TC1 through TC5 reach 100°C and typically, TC1 through TC4 charring temperatures with TC4 getting there at the end of the duration. This means that at the two-hour fire duration, only the top ply of the CLT is resisting the applied loads.

It is clearly shown in Figure 4.27 that all test specimens were charred at similar times for each thermocouple location regardless of the inclination of the STS. This makes sense as the shear connectors affect the deflection and mechanical performance of the slabs but does not alter how the wood material burns.

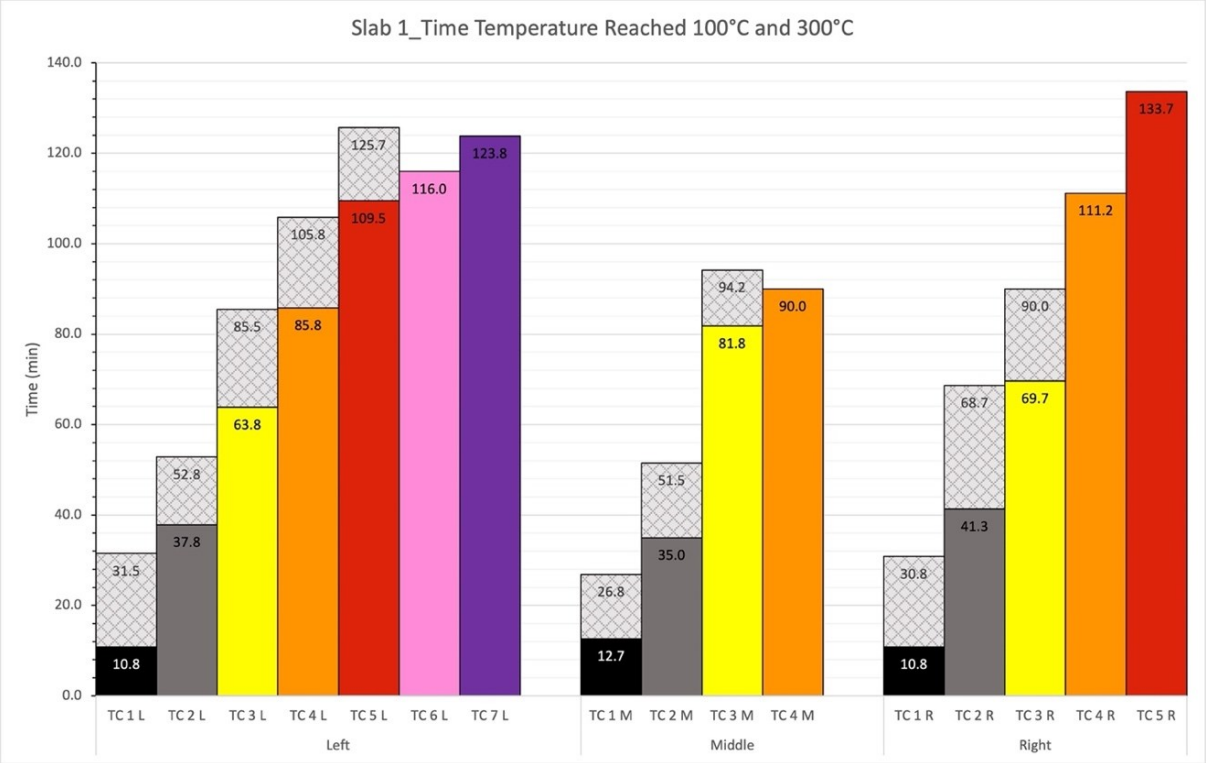

Figure 4.23: Slab 1 time when thermocouples reached 100°C and 300°C.

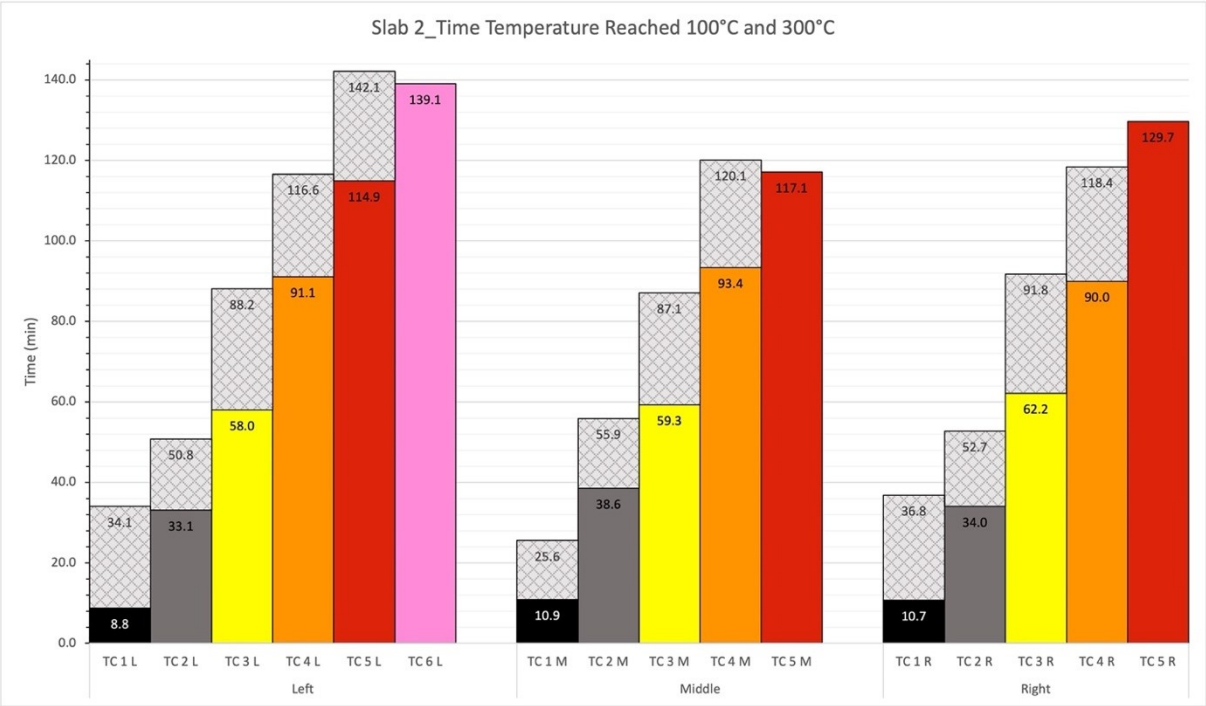

Figure 4.24: Slab 2 time when thermocouples reached 100°C and 300°C.

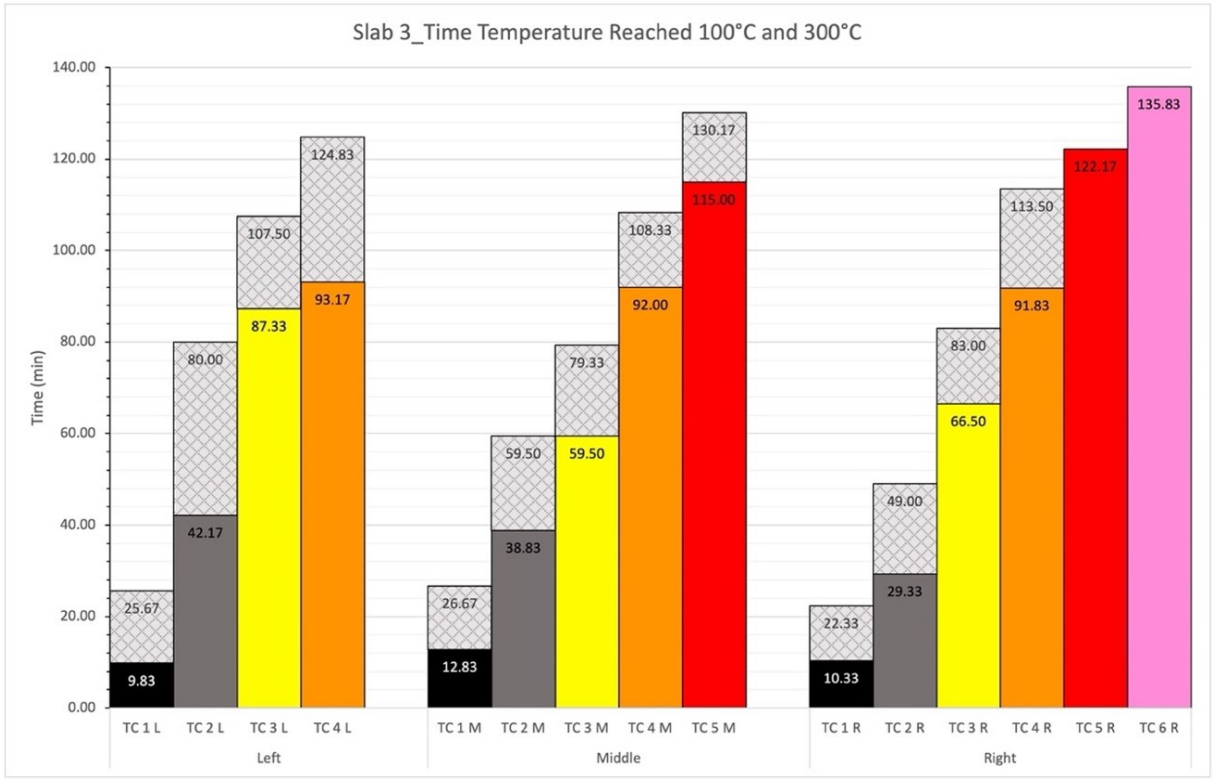

Figure 4.25: Slab 3 time when thermocouples reached 100°C and 300°C.

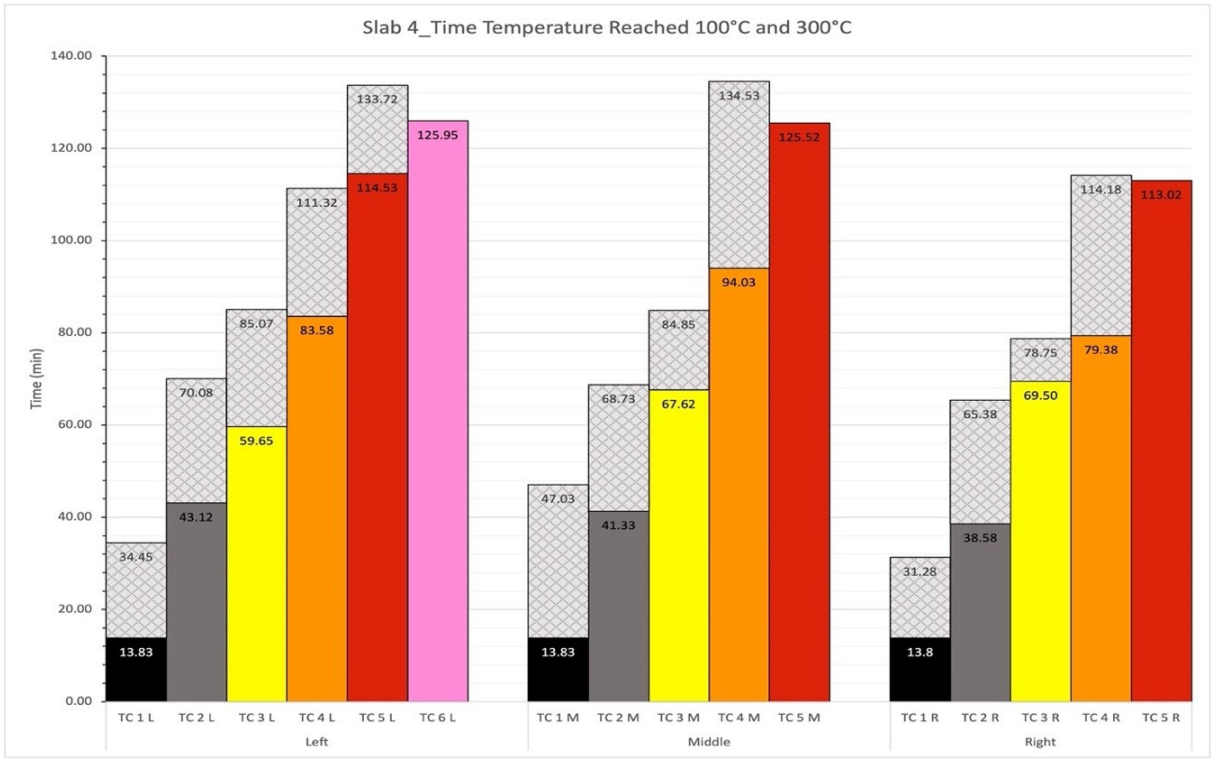

Figure 4.26: Slab 4 time when thermocouples reached 100°C and 300°C.

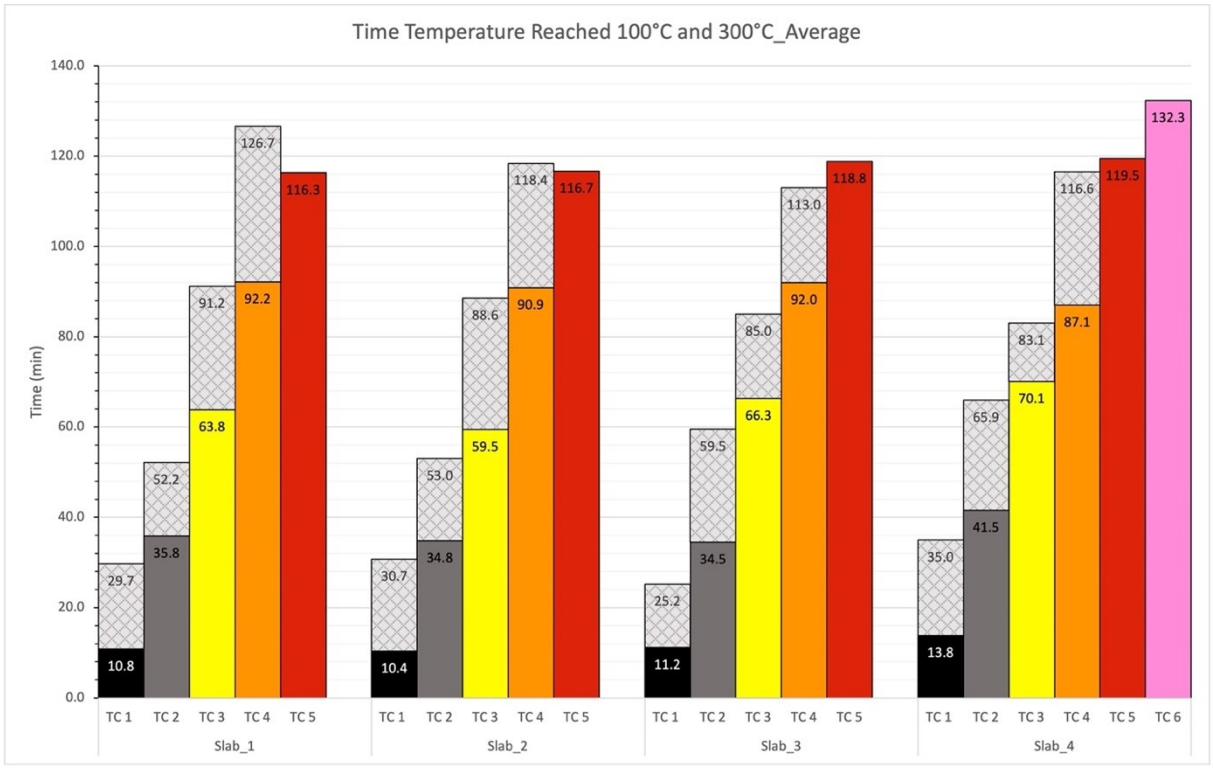

Figure 4.27: Time when thermocouples reached 100°C and 300°C using averaged temperatures.

4.4.2 Deflection at Charring Temperature

Now it is important to relate the time when the measured temperatures reached the wood charring temperature to the resulting deflection values to examine the coupled thermal and mechanical effects on the TCC floor assemblies. Figures 4.28 through 4.31 show results for all thermocouples in each test specimen that reached charring temperature, while Figures 4.32 through 4.35 use the averaged values for each thermocouple impediment depth from the CLT bottom surface, thereby being able to compare across each test specimen and relate specimens to each other.

It can be noticed that much of the time the test specimens were deflecting equally with respect to the similar readings from the left and right deflection values. This is clearly shown in Figures 4.29 and 4.31 where the left and right-side deflection values are reasonably equal. Also, it was observed

that the center deflection values were consistently greater than those of the two side displacement transducers located where the applied line loads.

From Figure 4.30, the left-side displacement transducer measured more significant deflection values than the center transducer measured. However, it is essential to note when the thermocouples measured the charring temperature. It is worth mentioning that the left side of the test specimen burned slightly slower, so once the 300°C was reached later in the fire test and thus, this was corresponded to more significant deflections later. Therefore, the test specimen was not deflected unsymmetrically but did not have consistent charring behaviour when comparing its left side to the center. This can also be seen in Figure 4.25, where the left side of the test specimen was charred at a slower rate than both its center and right side. This was the only specimen where this behaviour occurred and could result from a difference in delamination compared to the other three test specimen.

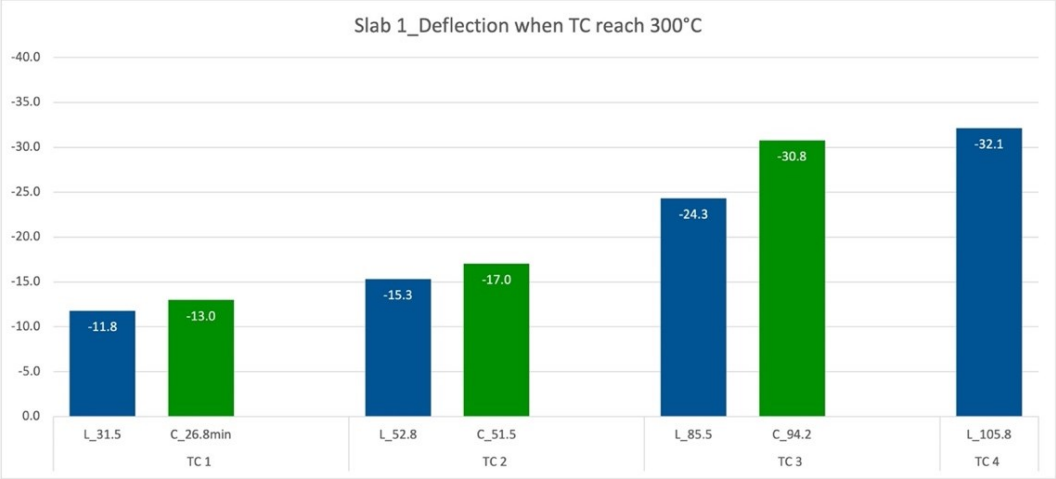

Figure 4.28: Slab 1 deflection when thermocouples reached charring temperature.

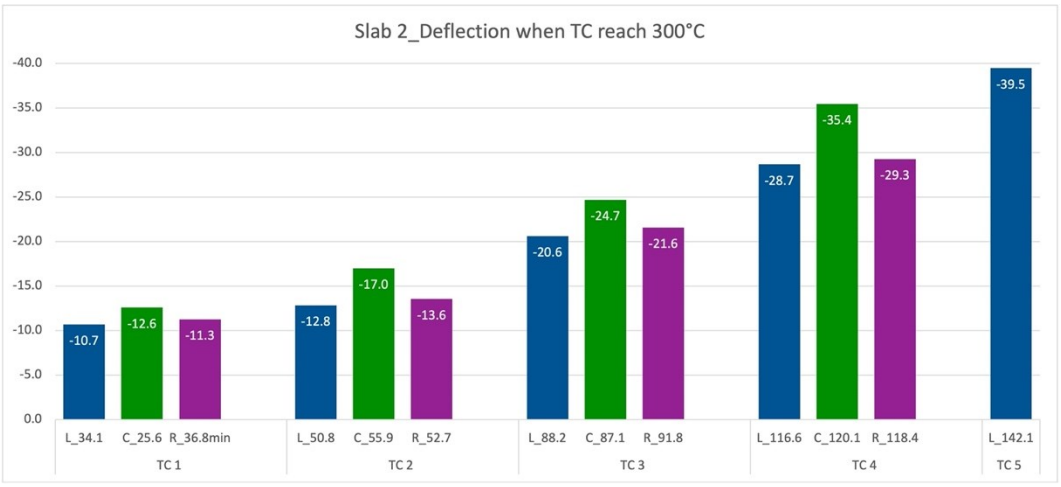

Figure 4.29: Slab 2 deflection when thermocouples reached charring temperature.

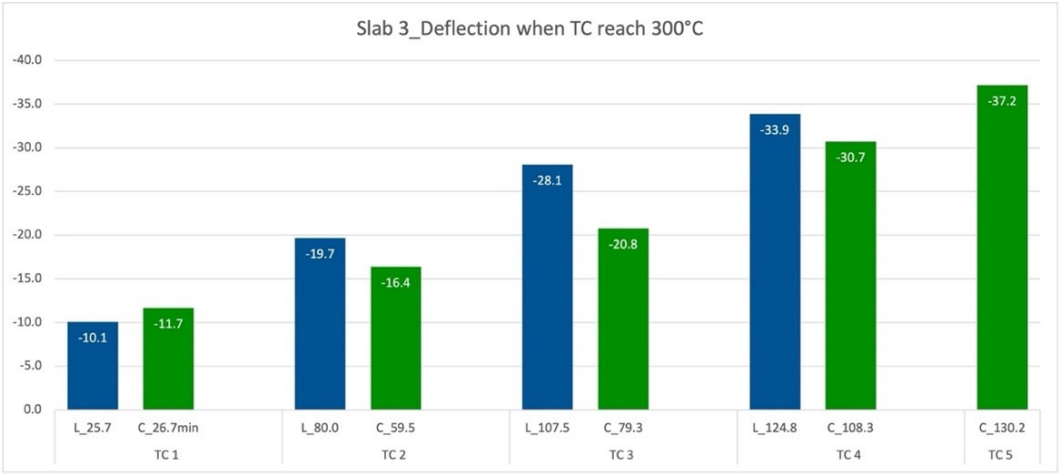

Figure 4.30: Slab 3 deflection when thermocouples reached charring temperature.

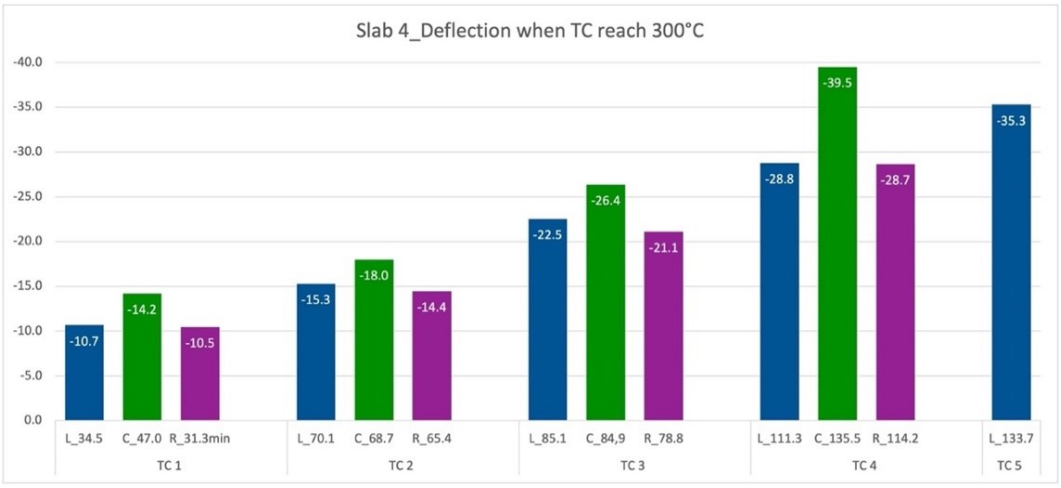

Figure 4.31: Slab 4 deflection when thermocouples reached charring temperature.

Inspecting Figures 4.32 through 4.35 can compare the test specimen's behaviour against each other. It is also noticed that test specimens deflected in very similar trend and consistently between test duplication and test parameter, due to minimal difference in all four samples. Each thermocouple reaches the charring temperature and experienced relative deflection values.

Comparing those figures shows the difference between the test specimens with STS oriented at 45° and those with STS at 30°. The deflections were relatively similar at TC1 and TC2, but afterward, deflections continued to diverge more. After this point, the 45° screws would begin being exposed to the fire while the 30° screws were still protected. The shear capacity of the STS in Slabs 1 and 2 are starting to be altered while the 30° screws were still the same as an ambient condition until further into the fire test. They result in a minimal difference between the two inclination angles of the STS; however, as previously mentioned, the 30° screws consistency kept the deflection values reduced compared to the results from Slab 1 with the approximately 10mm deflection increase. It showed the improvement in behaviour and response of the shallower angle over the 45° screws. Due to the less embedment depth, this is the expected performance but requires further experimental investigation to prove and evaluate the difference.

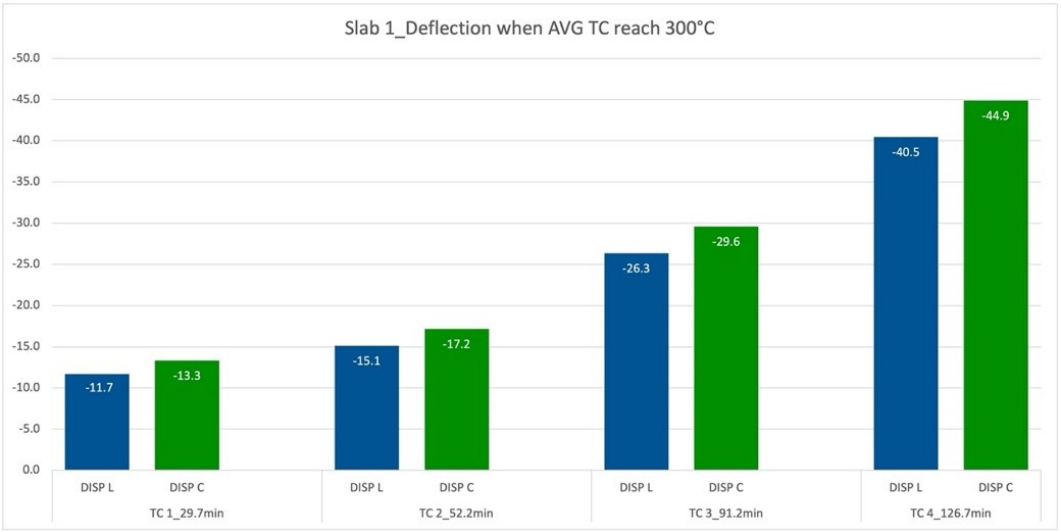

Figure 4.32: Slab 1 deflection when thermocouples reached charring using averaged temperature.

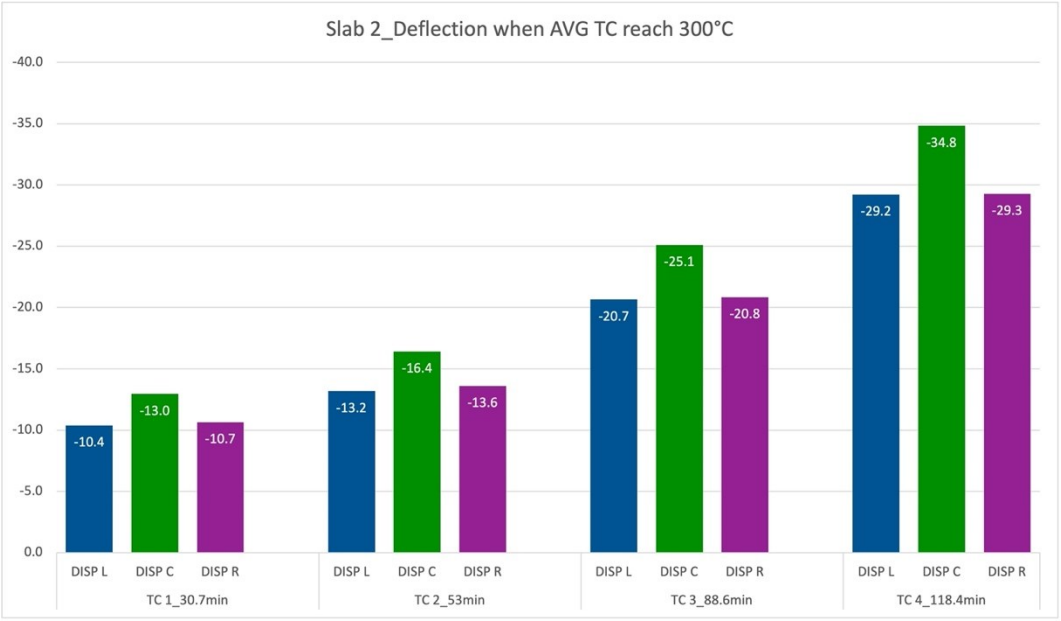

Figure 4.33: Slab 2 deflection when thermocouples reached charring using averaged temperature.

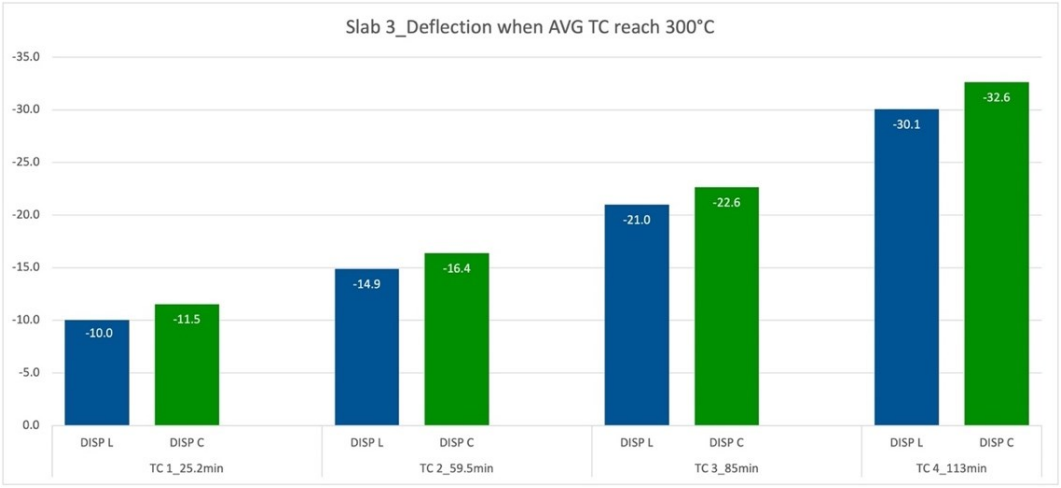

Figure 4.34: Slab 3 deflection when thermocouples reached charring using averaged temperature.

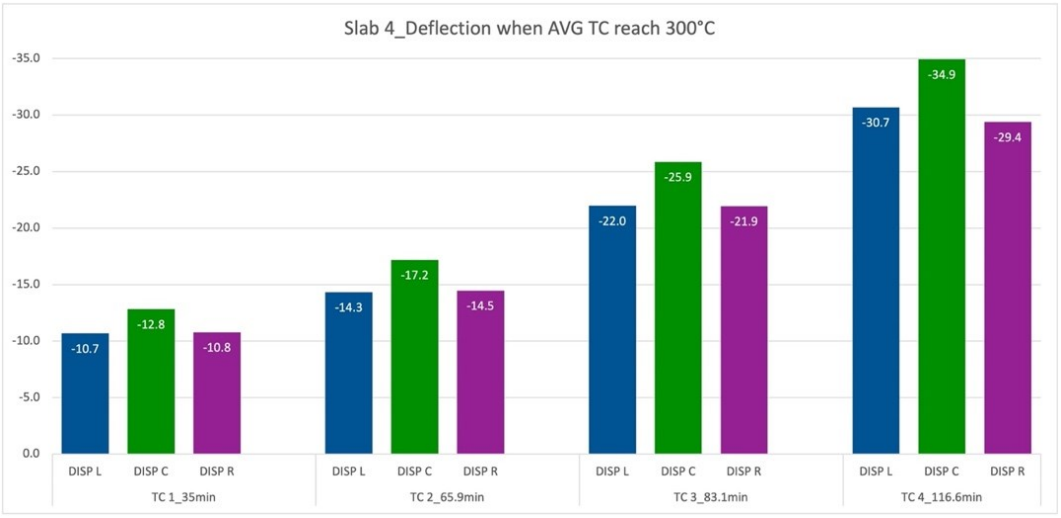

Figure 4.35: Slab 4 deflection when thermocouples reached charring using averaged temperature.

4.4.3 Charring Rate

One of the fundamental principles of designing EWPs for fire resistance is selecting a valid charring rate for the material. As discussed in Chapter 2, the nominal charring value from the European Code is 0.65 mm/min. Additionally, this is the recommendation from the Canadian Wood Council in the Canadian *Engineering design in wood* standards (CSC O86-19) for CLT. The charring rate is 0.65 mm/min when the char depth is within the first ply of a CLT panel and

an increased rate of 0.80 mm/min is considered when the charred front progresses beyond the glue lines. The 0.80 mm/min charring rate is exceedingly higher than expected and previously recorded behaviour; therefore, a value equal to 0.73 mm/min was selected for a charring rate, as discussed in section 3.4.4.1 for the design calculations of the test specimens of this study. This charring rate was chosen by considering the average from previous research studies investigating the behaviour of CLT under fire exposure.

Results from charring rate calculation can be seen in Tables 4.2 through 4.5, showing each thermocouple location as well as the averaged results for the entire test specimen. The typical behaviour can be observed from the results where there is initially a lower charring rate as the fire is just beginning and, therefore, not at the hottest temperatures. Then increases while the fire continues as the CLT is ignited and charring starts to develop upward. However, notice that later locations continue to decrease again as although there is a developed char layer, it works as a layer of insulation to the internal plys.

Comparing the left, right, and middle thermocouple lines, similar relationships can be seen, proving that the slabs are charring at a uniform rate across the fire exposure. There is a slight 0.073 standard deviation in the calculated charring rate values showing no sudden global delamination of the plys regardless of major or minor strength directions. Local delamination is challenging as thermocouples can only measure at a single point, although the total surface area is exposed to fire. No observations were made with ply's falling during testing or sounds that indicated as such. Minimal wood char chucks were on the furnace floor once testing was concluded.

Comparing Slabs 1 and 2 with 45° STS, on average, based on measurements of TC1, the calculated charring rate was 0.58 mm/min, for TC2 was 0.65 mm/min, for TC3 was 0.60 mm/min, and for

TC4 was 0.61 mm/min. While Slabs 3 and 4 with 30° STS, on average, based on measurements of TC1, the calculated charring rate was 0.60 mm/min, for TC2 was 0.55 mm/min, for TC3 was 0.64 mm/min, and for TC4 was 0.61 mm/mins. This shows comparative similarities in the calculated charring rates and that the influence of the screw inclination angle does not affect the burning behaviour nor the thermal profiles within the CLT slabs. This is also consistent with the discussion regarding the measured temperature profiles and charring time of all four specimens. The overall average charring rate for all locations and test specimens is approximately 0.60 mm/min with standard deviation of only 0.073. It also shows the reliability of the European Standard charring rate of 0.65 mm/min and the good agreement with the experimental results of this study.

Table 4.2: Slab 1 calculated charring rates based on thermal measurements

Thermocouple Location		Time when Temp=300°C (min)	Depth in CLT (mm)	Charring Rate (mm/min)
Left	TC 1 L	31.5	17.5	0.56
	TC 2 L	52.8	35	0.66
	TC 3 L	85.5	54	0.63
	TC 4 L	105.8	71.5	0.68
	TC 5 L	125.7	89	0.71
Middle	TC 1 M	26.8	17.5	0.65
	TC 2 M	51.5	35	0.68
	TC 3 M	94.2	54	0.57
Right	TC 1 R	30.8	17.5	0.57
	TC 2 R	68.7	35	0.51
	TC 3 R	90.0	54	0.60
Averaged temperature across the slab	TC 1	29.7	17.5	0.59
	TC 2	52.2	35	0.67
	TC 3	91.2	54	0.59
	TC 4	126.7	71.5	0.56

Table 4.3: Slab 2 calculated charring rates based on thermal measurements

Thermocouple Location		Time when Temp=300°C (min)	Depth in CLT (mm)	Charring Rate (mm/min)
Left	TC 1 L	34.1	17.5	0.51
	TC 2 L	50.8	35	0.69
	TC 3 L	88.2	54	0.61
	TC 4 L	116.6	71.5	0.61
	TC 5 L	142.1	89	0.63
Middle	TC 1 M	25.6	17.5	0.68
	TC 2 M	55.9	35	0.63
	TC 3 M	87.1	54	0.62
	TC 4 M	120.1	71.5	0.60
Right	TC 1 R	36.8	17.5	0.48
	TC 2 R	52.7	35	0.66
	TC 3 R	91.8	54	0.59
	TC 4 R	118.4	71.5	0.60
Averaged temperature across the slab	TC 1	30.7	17.5	0.57
	TC 2	53.0	35	0.66
	TC 3	88.6	54	0.61
	TC 4	118.4	71.5	0.60

Table 4.4: Slab 3 calculated charring rates based on thermal measurements

Thermocouple Location		Time when Temp=300°C (min)	Depth in CLT (mm)	Charring Rate (mm/min)
Left	TC 1 L	25.67	17.5	0.68
	TC 2 L	80.00	35	0.44
	TC 3 L	107.50	54	0.50
	TC 4 L	124.83	71.5	0.57
Middle	TC 1 M	26.67	17.5	0.66
	TC 2 M	59.50	35	0.59
	TC 3 M	79.33	54	0.68
	TC 4 M	108.33	71.5	0.66
	TC 5 M	130.17	89	0.68
Right	TC 1 R	22.33	17.5	0.78
	TC 2 R	49.00	35	0.71
	TC 3 R	83.00	54	0.65
	TC 4 R	113.50	71.5	0.63
Averaged temperature across the slab	TC 1	25.2	17.5	0.70
	TC 2	59.5	35	0.59
	TC 3	85.0	54	0.64
	TC 4	113.0	71.5	0.63

Table 4.5: Slab 4 calculated charring rates based on thermal measurements

Thermocouple Location		Time when Temp=300°C (min)	Depth in CLT (mm)	Charring Rate (mm/min)
Left	TC 1 L	34.45	17.5	0.51
	TC 2 L	70.08	35	0.50
	TC 3 L	85.07	54	0.63
	TC 4 L	111.32	71.5	0.64
	TC 5 L	133.72	89	0.67
Middle	TC 1 M	47.03	17.5	0.37
	TC 2 M	68.73	35	0.51
	TC 3 M	84.85	54	0.64
	TC 4 M	134.53	71.5	0.53
Right	TC 1 R	31.28	17.5	0.56
	TC 2 R	65.38	35	0.54
	TC 3 R	78.75	54	0.69
	TC 4 R	114.18	71.5	0.63
Averaged temperature the across slab	TC 1	35.0	17.5	0.50
	TC 2	65.9	35	0.53
	TC 3	83.1	54	0.65
	TC 4	116.6	71.5	0.61

4.4.4 Residual CLT Thickness

While evaluating the thermal progression throughout the test and comparing temperatures afterward to determine the time each point reached 300°C and calculate charring rates, one more crucial step is required. That is measuring the thickness of the residual section of the CLT panel. As previously mentioned, thermocouples are essential to monitoring temperature, but they are limited by the placement location and can only determine when that spot reaches critical temperatures. By removing the charred thickness and measuring the remaining section, a more holistic view of the slab performance and the differences across the slab can be achieved.

Figure 4.36 shows each test specimen after the fire was in the majority extinguished and before being removing from the furnace. As shown in the photos presented in the said figure, the wood that was charred but remains attached indicates limited locations of either local or global delamination. This is important as when delamination does not occur, this layer of charred timber acts as a layer of insulation to the internal wood section, thereby reducing the charring rate. So, while these plys can no longer resist the applied loads, they can protect the underneath plys that do resist the applied loads. All four test specimens had very similar char layer thickness remaining, with Slabs 1 and 3, and Slabs 2 and 4 are more in line with each other, which relates to the fire exposure of 125 min and 145 min, respectively.

(a) Slab 1

(b) Slab 2

(c) Slab 3

(d) Slab 4

Figure 4.36: All four test assemblies (Slabs 1 through 4) right after fire testing and before the char layer was removed.

Comparing Figure 4.36 (a) and (c) with Figure 4.37 shows the difference when the char layer is removed, thereby exposing the remaining wood to resist the applied loads. The apparent difference in appearance makes it easy to differentiate between charred and robust wood. Only Slabs 1 and 3 had the char removed as they were the tests with a duration of 125 min where fire tests were terminated shortly after passing the two-hour time mark. Therefore, it was essential to know how much wood was remaining. At the same time, it is understood that more fire exposure for the other slabs would simultaneously lead to a more significant reduction in the residual wood section.

(a) Slab 1

(b) Slab 3

Figure 4.37: Slabs with 2-hr fire exposure with char layer removed.

It is easy to distinguish between the major and minor plys from Figure 4.37, with the different ply orientations. However, it is more challenging to know the difference between the middle major ply and the top major ply from the figure alone (Refer to Table 4.6). From the initial examination of the residual CLT panel section of Slabs 1 and 3, similar profiles can be seen. A more significant portion of the middle major ply remains at the bottom of the samples, which correlates to the back

of the furnace. In contrast to the top edge in the photos (furnace front), the transverse ply can be seen. The difference in this behaviour is not representative of the slab performance but rather a testing set-up drawback. The seal between the specimen and the furnace roof panels was not the same when comparing the front and back edges of the test specimens. Therefore, the front edge was not as tight, allowing additional pockets where the heat of the fire could spread, which increased the charring and facilitate two-dimensional charring (from the bottom surface and the edge of the specimen) instead of only one-dimensional charring from the bottom surface. This behaviour is not representative of in situ conditions; therefore, the residual section is more accurate following the centerline of the slab in the longitudinal direction rather than the edges.

The residual depth of the CLT panel was measured at 15 points across Slabs 1 and 3, refer to Table 4.6. The location of each point is as follows, 1.5 m and 0.75 m left of center, center line, and 1.5 m and 0.75 m right of center. Along each line in the transverse direction, checked the depth at points just offset of the STS row locations. One is the row of the STS closest to the front of the furnace, two along the centerline, and three by the row of STS closer to the back of the furnace.

Table 4.6: Residual CLT depths of the slabs with 2-hr fire exposure

Thermocouple Location:		Left 1.5m	Left 0.75m	Centerline	Right 0.75m	Right 1.5m
Slab 1 (mm)	1 - Front	0	51.9	45.6	50.2	64.6
	2 - Center	44.1	54.0	68.9	64.6	42.1
	3 - Back	44.3	62.1	65.6	61.9	25.1
Slab 3 (mm)	1 - Front	0	38.9	41.2	63.0	40.2
	2 - Center	50.2	61.4	58.7	53.6	30.3
	3 - Back	63.1	63.3	61.2	54.9	19.7

Examining all values for the residual depth shows many similarities in Slabs 1 and 3, with difference of 20% on average for each line location and 27% for all values measured for standard deviation. The averaged values for rows one, two, and three are 39.6 mm, 52.8 mm, and 52.1 mm respectively.

It should be noted that residual depth values that are less than 35 mm would mean that the charring progressed to the very top ply (along the major strength direction). While residual depth values that are between 35-54 mm would indicate that the charring progressed into the fourth ply (along the minor strength direction), and values greater than 54 mm would indicate that the charring progressed into the third (or middle) ply (along the major strength direction). The residual section would be in the fourth ply based on the predicted values using an increased charring rate of 0.73 mm/min. While according to this study experimental results with average charring rate calculated based on thermal measurements at 0.60 mm/min, which is very close to the European code nominal charring rate (0.65mm/min), the residual section would be in the third ply.

The overall averaged residual depth is 48.2 mm considering all measured locations. This residual depth correlates to a charring rate of 0.73 mm/min which is the same that used in calculation phase and design of the experimental program. However, if considering only the most representative areas of in situ conditions as previously mentioned, the averaged residual depth is 60.2 mm which correlates to a charring rate of 0.63 mm/min. Giving good agreement with both calculated charring rate in Section 4.4.3 and the European Code Standard.

Therefore, locations did experience increased charring rates corresponding to a reduction in the residual depth of the CLT panel. However, this was not always due to the slab's performance but rather the testing setup. As previously mentioned, the residual depth measurements along the slab

longitudinal centerline at each location is most representative of the slab charring behaviour when exposed to one-dimensional fire exposure as it is not as influenced by the seal between the longitudinal edges of the test specimen and the edges of the front and back furnace roof panels.

As illustrated in Figure 4.38, by comparing (a) and (c) showing the slab ends near the furnace left-side wall and (b) and (d) showing the slab ends near the right-side wall, it can be noticed that in addition to the normal one-dimensional charring from the bottom surface of the test specimen, there was also localized edge charring at the left side of the specimens due to imperfectly even seal between the longitudinal edges of the test specimen and the edges of the front and back furnace roof panels. Further seen in the reduction of residual depth values from Table 4.6, where the left 1.5 m front measured 0 mm and the right 1.5 m back measured 25.1 mm for Slab 1 and 9.7 mm for Slab 3. Therefore, these values and behaviours can be explained by setup and are not accurate representations of the compartment fire scenarios.

Another aspect to understand when examining the ends of the fire-damaged specimens near to the furnace walls is the increased charring and reduced wood section remaining. This is attributed to the change in the flow and dynamics of hot gases when encountering a barrier such as a furnace wall or any insulated surface, causing increased turbulence and fireball. As a result, this led to increased digging into the CLT panel and increased charring rate/depth. This is referred to as a bowling effect, which is discussed further in section 4.5 of this thesis.

Another behaviour of importance is how the charring progressed along the glue lines of the CLT lamellas past the location of the furnace walls. Seen on both sides of each support in Figure 4.38 with the char removed. This behaviour is discussed in greater detail in section 4.5 of this thesis.

(a) Slab 1 - Left Side

(b) Slab 1 - Right Side

(c) Slab 3 - Left Side

(d) Slab 3 - Right Side

Figure 4.38: Close up view of the residual wood depth near the furnace walls.

A clear representation of the difference in the two STS inclination angles studied in this research project can be seen in Figure 4.39. Slab 1 (45° STS) has all STS distinctively shown and extrudes from the residual CLT panel after removing the char layer. In contrast, in Slab 3 (30° STS), the row of STS at the front (top of the figure) can be seen while it is minimal for the center and back rows of STS. Figure 4.39 also illustrates a good comparison of the slabs concerning the charring behaviour, as the remaining CLT is very similar. With the fourth lamella at the front of the slab and the third lamella remaining on the back two-thirds of the slab, minimal depth of the third or

major middle ply remains on the section. As a result, it may not contribute significantly to the structural performance of the section but does act as insulation to the inner and otherwise not yet heated section of the CLT panel.

(a) Slab 1 (b) Slab 3

Figure 4.39: Difference in STS embedment depth.

4.5 Discussions

4.5.1 STS Shear Connection Behaviour

Overall, for designing TCC sections, using a screw connection is a simple and practical solution for the shear connectors. A wide variety of STS can be used, changing in diameter and embedment length to be designed accordingly for each purpose. STS is a standard product in construction and widely available to order, as the TCC section can be designed to what screw dimensions are available. There are ways to optimize the design in terms of length, diameter, and inclination angle, as shown by this study test results and outcomes of previously conducted research that are reported

in the available literature. There are many ways to design TCC sections to match the required performance and product availability.

According to the obtained test results of the thermal and mechanical performance, Slabs 2, 3 and 4 have improved behaviour compared to Slabs 1. Showing a dependable improvement during fire conditions when altering the inclination and embedment depth. Figures 4.40 and 4.41 compare each slab with measured deflections at 30-, 60-, 90-, and 120-min. Results confirm that all slabs deflect symmetrically, as discussed previously, regardless of slight variance in charring rates and times. A comparison of the calculated values for deflections at the same time intervals by using standard equations for simply supported test specimens subjected to two equals line loads and calculating effective bending (Equation 11) with the reduced properties for the CLT and expected loss of cross-section at each time interval using the Eurocode Standard charring of 0.65mm/min. The predicted values calculated were more in line with the results from Slabs 2, 3, and 4 while underestimating the behaviour for Slab 1.

Figure 4.40: Deflection comparison at 30 min intervals for the TCC slabs with STS oriented at 45°.

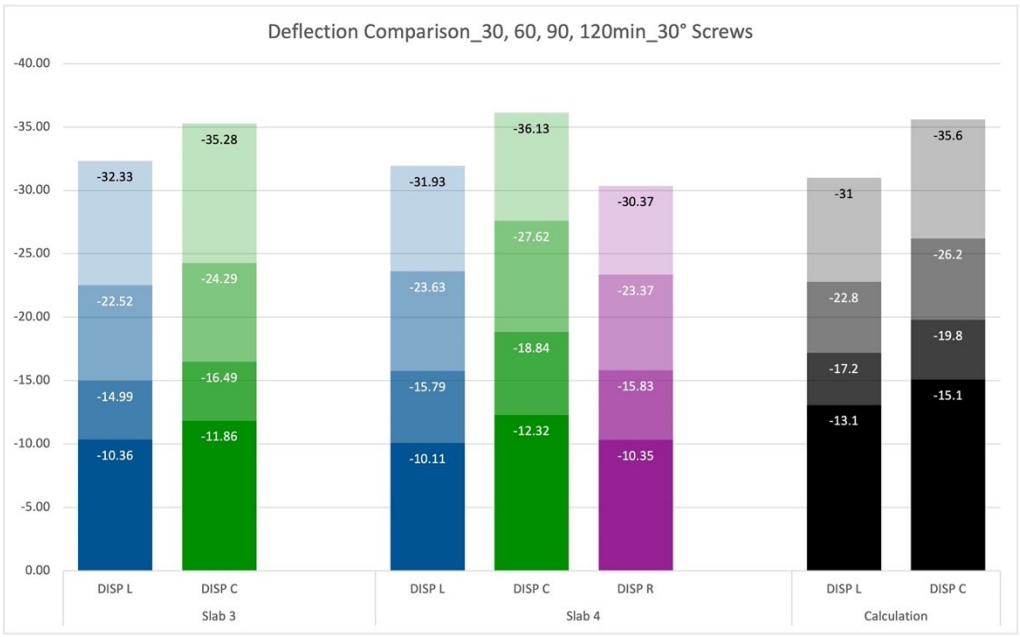

Figure 4.41: Deflection comparison at 30 min intervals for the TCC slabs with STS oriented at 30°.

For the slabs with 45° STS, the deflection at the point loads averaged 32.58 mm and at the midspan 38.99 mm. While for the slabs with 30° STS, the deflection at the point loads averaged 31.54 mm and at the midspan 35.71 mm. Slabs 3 and 4 slightly improved by reducing the STS inclination angle by 15 degrees. However, when comparing Slab 1 with Slabs 2, 3, and 4 shows a much more significant difference in deflection. As for slab 1, the deflection at the point loads is 38.16 mm and at the midspan 42.57 mm. While the other three samples, the deflection at the point loads averaged 30.84 mm and at the midspan 35.61 mm. Verifying that a shallower angle to the horizontal improved the performance repeatedly, a difference is evident for Slabs 1 and 2. Though this relationship is less noticeable at ambient temperature, the shear capacity (Table 3.3) is similar. Still, it changes when considering fire conditions due to the difference in embedment depth of the screws in the CLT.

Figure 4.42: 45° STS oriented at 45° is being exposed during fire testing.

A clear difference can be visually seen in Figure 4.42, where the screws are clearly shown in the fire with the 45° inclination angle near the end of the fire test. Unlike the STS oriented at 30° which were never fully exposed as the char layer remained since there is a difference of about 31mm at the location of the end of the 45° screws and to the end of the 30° screws. Figures 4.40 and 4.41 illustrate that the deflections started at similar values for all slabs but not at later times. For instance, Slabs 1 and 2 deflection values diverge more, corresponding to this same difference. The difference is when the screws are beginning to be exposed to heat more and more for Slabs 1 and 2 but not for Slabs 3 and 4.

Figure 4.43: Interface between the CLT panel and the top concrete layer.

Another observation was made when examining the fire damaged TCC section right after the end of the fire test is the gap at the interface between the CLT panel and the top concrete layer remains

unnoticeably different, as shown in Figure 4.43. The assumption from this observed behaviour is that having the number and frequency of STS helps hold the CLT panel together and not allow for significant slip between the top concrete layer and the CLT panel at the interface. This would be a substantial benefit of using STS as shear connectors in TCC slab-type assembly and an advantage over other types of shear connectors. Additionally, utilizing STS could help prevent delamination that often occurs in CLT panels exposed to fire.

4.5.2 Performance of CLT slabs in Fire

In addition to the results and behaviour analysis of the TCC floor assemblies conducted in the previous section, three critical observations were made during the fire testing. While the CLT panels performed as expected at the location of instrumentation, three behaviours occur at the support that is important to address and consider in designing TCC sections using CLT panels. It should be noted that those behaviours were present in all four specimens tested in this study.

The first is represented in Figure 4.44, with (a) near the beginning of the fire test, and (b) near the conclusion of the test. It can be noticed that there were additional charring and loss of cross-section close to the furnace wall. The first figure has initial uniform ignition and charring, while the bottom figure has a bowling or curve-shaped effect relative to the support. This behaviour results from the additional turbulence and vortex created by the fire flow direction. As it hits the wall, it causes a surplus of heat and makes a location where the fire is felt to a greater extent than the rest of the slab. This follows typical fire dynamic principles that are also expected to occur in situ.

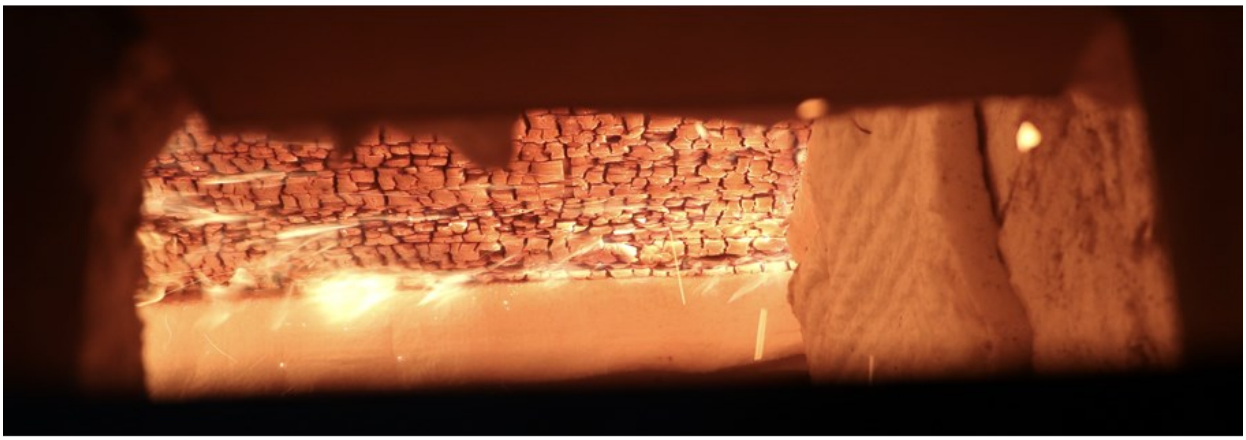

(a) Slab near support at beginning of fire exposure

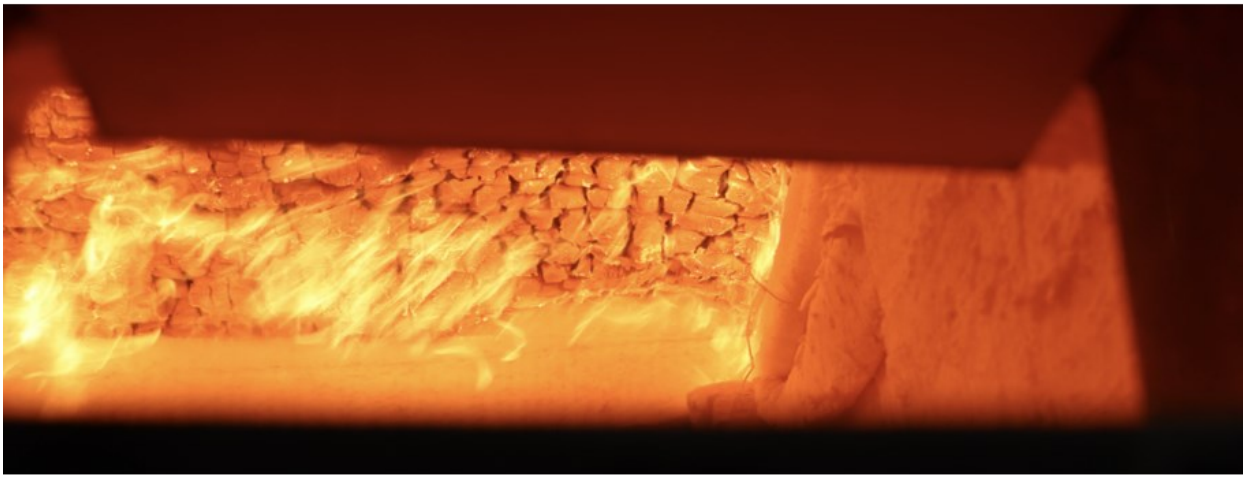

(b) Slab near support at end of fire exposure

Figure 4.44: Support condition through fire exposure.

The second behaviour is the development and progression of horizontal charring, shown in Figure 4.45. This occurs as the fire continues to increase and the char front progresses upward, at the location of the supports where wood was not exposed from underneath. As there is a loss of the cross-section upward creates a path for the fire to spread horizontally. While this behaviour does not occur near the same rate as regular upward charring, it is still an area of interest and is noted when studying the fire performances of these TCC sections with CLT panels. As with the testing setup and the length of the furnace not equal to the clear span of the test assembly, this did not reach the supports but rather at the location of the considerably thick furnace walls and show how

far the fire can spread across and potentially out of the fire compartment if occurred in a realistic setting. A topic not mentioned or discussed previously in literature and one that must be examined more in depth before recommendation can be considered when looking at exposing EWP in construction.

Figure 4.45: Horizontal charring behaviour at the supports.

When exposed to fire conditions, a final observation on the CLT occurred after the fire damaged test specimens were lifted from the furnace and removed. This was the burning and char progression of the test specimens in the horizontal direction outward of the furnace wall but specifically along the glue lines of the bottom ply, as shown in Figure 4.46. The primary reason and cause of this are that the CLT panels used in the test specimens of this study were not edged glued but rather only faced glued. This means that the thin longitudinal voids between the lamellas of the bottom ply create a longitudinal pocket for the fire to spread through more quickly and create a different burning behaviour than the one-dimensional heat transfer and regular upward charring. Accordingly, each lamella was fire exposed on three sides. Whether the CLT ply's edge is glued or not, this does not make a difference in how the panels can sustain the applied loads in fire conditions. However, this creates a significant difference in the manufacturing process with

additional steps and equipment required, which is why many manufacturers choose only face gluing their CLT panels instead of face and edge gluing.

(a) (b)

Figure 4.46: Fire spread and horizontal charring through the glue lines of the bottom ply.

Regardless of these three behaviours, the CLT panels remained structurally sound and sustained the applied loads under prolonged fire exposure for the two-hour duration in all four fire tests conducted in this study due to the activation of the composite action of the TCC sections of those floor assemblies. However, this behaviour represents what can occur and needs to be accounted for in the design process. Therefore, it is essential to consider when designing close to support and when choosing whether the CLT slab should be left exposed or following EMTC procedures close to supports.

4.5.3 Insulation Layer Considerations

A point not previously discussed regarding including layers of insulation at the interface between the top concrete layer and the CLT panel (refer to sections 2.6.1.4 and 3.3.2) is conditions when designing for fire exposure. The benefits and influences are all focused on improvements mainly in ambient condition. Observing Figure 4.47, where a void is visible between the top concrete layer and the charred CLT panel where the insulation layer was once situated. With Figure 4.47 (a)

shows Slab 4 from underneath before lifting it off the furnace, and Figure 4.47 (b) after the slab broke while was placed on the floor and thereby changing its bending profile and cased increased tensile forces in the concrete top layer.

This exaggerated behaviour is not representative of typical or in situ conditions but rather due to testing setup, as the charring rates and cross-section loss were consistent across all four test specimens except at the left support by the furnace wall (Figure 4.36). This occurred in all test assemblies but much more in Slabs 2 and 4 as they were under prolonged fire exposure, allowing additional time for charring. However, as a result, it raised other concerns when choosing to include insulation from a fire safety point of view. As if charring does reach the interface and exposes the insulation layer, this can create a tunnel for the fire to spread along the slab and create a pocket where the CLT slab can experience a fire in multiple directions and on different surfaces. As previously mentioned, the fire spreading through the longitudinal voids between the lamellas that are not edge glued means that the insulation layer could also be compromised in similar way too since the insulation materials are very flammable and fire would spread easily and quickly through them.

(a) Before Breaking (b) After Breaking

Figure 4.47: Loss of the insulation layer due to severe charring near the furnace wall.

Recommendations would be having fire stops in the layer and not having insulation surrounding the shear connectors. If the insulation is ignited, it would create a void and increase fire spread risk. Avoid insulation close to supports, and be mindful of partition walls, as they could cause fire to spread beyond the original fire compartment. Additionally consider have a fire insulating material between the insulation and the surface of the CLT panel. Providing protection to this insulation layer and if exposed not automatically ignited. This would keep the safety factor higher and cognizant of the design of the TCC section and the corresponding fire risk.

It is also very important to realize that this behaviour can occur, but due to the TCC floor assemblies were tested under standard fire exposure that yields extreme temperatures and heat through an ever-increasing time-temperature curve compared to a natural fire where there are both growth and decay stages (Figure 2.3). There would be a valid argument if this could occur in situ as its dependent on the amount of fuel load in the compartment to reach a fire of such magnitude. However, the design needs to consider the most severe case giving a factor of safety for all other cases.

CHAPTER 5: CONCLUSIONS AND RECOMMENDATIONS

5.1 General

The new insurgence of the design involving mass timber elements and increasing the buildings height restrictions under a prescriptive design methodology is tethered to the understanding of the structural fire performance of the main structural systems utilized in such tall timber buildings. Addressing these concerns requires extensive experimental programs to study such mass timber elements and verify their actual fire resistance ratings. Studying TCC sections offers valuable knowledge in expanding their use and design procedures and opening possibilities to progress the mass timber construction further. Both in terms of building taller in timber and having these elements exposed, thereby not limiting design options to EMTC.

While the concept of TCC sections is not new, only limited experimental programs still address their behaviour, especially when considering fire conditions. The extensive options available when designing TCC sections in terms of assembly types, timber materials, strength properties of concrete, and the variety of shear connectors increase the complexity of providing simplified design procedures and recommendations. Therefore, experimental program like the one outlined in this thesis, which is being conducted at LUFTRL, is essential before TCC sections can be validated and implemented into the Canadian *Engineering design in wood* standard (CSA O86). TCC sections are included in other international design standards, although this is primarily limited to ambient condition and does not address the fire exposure considerations.

Although EWP and mass timber generally behave well in fire and have lower heat transfer rates, there is still hesitation in using such elements. The research study completed and presented in this thesis proves that despite the combustible nature of wood, TCC floors systems utilizing CLT

panels can provide solutions to achieve the 2-hour fire resistance rating without any layers of protection on the timber component. This study's unique experimental outcomes offer valuable data regarding the design of TCC sections that utilize CLT panels in slab-type floor assemblies. This is an initial step to expand the framework and design procedures for TCC sections in fire conditions in Canada and North America.

5.2 Conclusions

Based on the results obtained from the experimental program presented in this thesis to investigate the behaviour of TCC floor assemblies and determine the impact of the inclination angle of STS used as shear connectors on their thermal and mechanical performance while exposed to standard fire, the following conclusions can be drawn:

- TCC floor assemblies can successfully be designed to meet the required 2-hour fire resistance. This is an essential requirement to create tall mass timber buildings and limiting factor in the Canadian *Engineering design in wood* standard.

- Accurate design procedures can enhance the fire resistance of CLT panels by converting the floor systems to TCC sections with the addition of shear connectors and top concrete layer. This successfully takes a CLT panel rated for 1-hr fire resistance and achieve 2-hr fire resistance under the same loading. Thereby, doubling the fire resistance time and proving the impact that TCC sections can have on the industry and design recommendations.

- The outcomes of this study show the improvement in the structural fire performance of the TCC floor slabs when reducing the inclination angle of the STS from 45° to 30°, with a

deflection reduction - providing proof of reducing the inclination angle while maintaining the same embedment length when reducing the screw embedment depth. Therefore, the closer the STS to the horizontal, the more enhanced the shear connection of the TCC section with CLT for both ambient and fire conditions.

- The thermal behaviour of the four full-size, one-way TCC floor assemblies experimentally tested in this study was comparable to each other, providing consistency in results and outcomes while studying time-temperature curves and charring behaviour. Furthermore, it agreed with the standardized charring rate of wood under the European Code nominal value of 0.65 mm/min. Also, CLT panels did not globally delaminate.

- Even though the exposed CLT was experiencing elevated temperatures of approximately 1000°C near the end of the 2-hr fire tests, there was still minimal heat transfer at the interface between the top concrete layer and the CLT panel or at any depth in the concrete. This demonstrates the benefits of the TCC slab-type assembly over the beam-type assembly, as it is not needed to consider the thermal effects on the concrete component. Additionally, when the wood charred ply remains intact it acts as an excellent insulator to the inner and yet unexposed plys.

- A benefit of the STS connections used in TCC sections have a seen benefit of holding the CLT panels together and tight them to the top concrete layer. It is shown both by the minimal change in the gap at the interface, even after fire testing and by no significant delamination of the CLT plys. Keeping the CLT panel cohesive is essential for prolonged safety and achieving the required fire resistance rating.

- The unique results of the full-size experimental fire tests conducted and presented in this thesis enhance the current understanding and assist in reducing the knowledge gap on the actual behaviour of TCC floor assemblies utilizing CLT panels when subjected to fire in Canada and globally, especially considering the rarity of large-size fire testing programs. Additionally, providing reliable experimental results for designers to validate the performance-based design and assign appropriate fire resistance times are very beneficial.

5.3 Recommendations for Future Work

While the primary objective of the experimental program presented in this thesis was to determine the effects of the inclination angle of STS in TCC floor systems with CLT panels when exposed to elevated temperatures, other factors require further investigation before knowing the optimum design for the connections in such TCC floor systems. Additionally, other recommendations are about the overall design of TCC sections with slab-type assemblies when accounting for fire exposure. Addressing and evaluating each would help to give a vivid understanding of the connection performance and how to best address the design of such TCC sections for structural engineers.

The following are a few recommendations for future work to be conducted to expand further on the topic and develop a detailed approach when accounting for structural fire design:

- There are many parameters to study when looking at STS connections in TCC sections; to optimize the design process would need to develop analytical and numerical modelling tools to be able to examine the changes in behaviour further and eventually simplify the design process.

- As studying the impact of the screw inclination angle has on the behaviour of the TCC section, there are other possibilities to improve the behaviour of STS connection. First, since screws have such a high tendency to twist and bend, causing a ductile failure, it is recommended to seek a method to prohibit them from turning at the interface between the concrete layer and CLT panel. The second could be using a combination of connectors, such as screws with adhesive strips, as the screws exhibit ductile failure and the adhesive exhibits brittle failure. Such a combination of two different shear connection types can bring the strengths of both connection types, as the screws can act as a backup if the glue suddenly fails in fire conditions.
- To fully understand the behaviour of the TCC floor system in situ and its entirety, it is needed to study the influence of fire exposure at the panel-to-panel longitudinal joints of CLT panels, such as the spline connection.
- From observations made with the additional horizontal charring and charring along the glue lines of the lamellas, it is recommended that designers be mindful of wall locations and the possibility of fire spreading to adjacent compartments. Furthermore, the behaviour along the glue line would recommend studying the difference if the CLT panels are both face and edge-glued, thereby removing the gaps between the lamellas.
- When designing the STS connections for the test specimens of the study presented in this thesis, the spacing transversely and longitudinal were chosen so no screws begin to yield until after the point of 2-hr fire exposure. In addition, to fully understand the anticipated behaviour, it is needed to experimentally test similar TCC floor assemblies with their STS are starting to yield and whether this would influence the fire resistance and resulting deflection rates.

REFERENCES

ANSI/APA PRG 320 (2019). Standard for Performance-Rated Cross Laminated Timber.

ASTM International WC, PA. ASTM E119-16a Standard. Test Methods for Fire Tests of Building Construction and Materials. ASTM International.

Auclair, S. C. (2020). Design Guide for Timber-Concrete Composite Floors In Canada. National Library.

Auclair, S. C., Sorelli, L., & Salenikovich, A. (2016). Simplified nonlinear model for timber-concrete composite beams. International Journal of Mechanical Sciences, 117, 30–42. https://doi.org/10.1016/j.ijmecsci.2016.07.019

Brandner, R., Flatscher, G., Ringhofer, A., Schickhofer, G., & Thiel, A. (2016). Cross laminated timber (CLT): Overview and development. European Journal of Wood and Wood Products, 74(3), 331–351. https://doi.org/10.1007/s00107-015-0999-5

Caldová, E., Vymlátil, P., Wald, F., & Kuklíková, A. (2015). Timber Steel Fiber–Reinforced Concrete Floor Slabs in Fire: Experimental and Numerical Modeling. Journal of Structural Engineering, 141(9), 04014214. https://doi.org/10.1061/(ASCE)ST.1943-541X.0001182

Canadian Wood Council (CWC). (2020). Wood Design Manual, 2020: The complete reference for wood design in Canada. Ottawa, Canada.

CCMC (2019). Evaluation Report: Nordic X-Lam. Canadian Construction Materials Centre Report No. CCMC 13654-L.

CCMC (2020). Evaluation Report: SWG ASSY VG Plus and SWG ASSY 3.0 Self-Tapping Wood Screws. Canadian Construction Materials Centre Report No. CCMC 13677-R.

CEN, Eurocode 5: Design of Timber Structures - Part 1–2: General - Structural Fire Design, British Standards Institute, London, UK, 2009.

Connolly, T., Loss, C., Iqbal, A., & Tannert, T. (2018). Feasibility Study of Mass-Timber Cores for the UBC Tall Wood Building. Buildings, 8(8), Article 8. https://doi.org/10.3390/buildings8080098

COST Action FP1402. (2018). Design of timber-concrete composite structures: A state-of-the-art report by COST Action FP1402/ WG 4 (A. Dias, J. Schänzlin, & P. Dietsch, Eds.; 1. Auflage). Shaker Verlag.

CSA O86. 2019. Engineering design in wood. Canadian Standards Association (CSA), Toronto, Canada.

Dagenais, C., Ranger (Osborne), L., & Cuerrier-Auclair, S. (2016). Understanding Fire Performance of Wood-Concrete Composite Floor Systems. https://research.thinkwood.com/en/permalink/catalogue1777

Du, H., Hu, X., Xie, Z., & Meng, Y. (2021). Experimental and analytical investigation on fire resistance of glulam-concrete composite beams. Journal of Building Engineering, 44(Complete). https://doi.org/10.1016/j.jobe.2021.103244

Frangi, A., Fontana, M., Hugi, E., & Jübstl, R. (2009). Experimental analysis of cross-laminated timber panels in fire. Fire Safety Journal, 44(8), 1078–1087. https://doi.org/10.1016/j.firesaf.2009.07.007

Frangi, A., Knobloch, M., & Fontana, M. (2010). Fire Design of Timber-Concrete Composite Slabs with Screwed Connections. Journal of Structural Engineering, 136(2), 219–228. https://doi.org/10.1061/(ASCE)ST.1943-541X.0000101

Gerber, A. R. (2016). Timber-concrete composite connectors in flat-plate engineered wood products [University of British Columbia]. https://doi.org/10.14288/1.0300229

Higgins, C., Barbosa, A. R., & Blank, C. (2017). Christopher Higgins, Ph.D., P.E. (NY). 76.

Hopkin, D., Enso, S., Krenn, H., & Sleik, T. (2020). Compliance Road-map for the Structural Fire Safety Design of Mass Timber Buildings in England. 8.

Hozjan, T., Bedon, C., Ogrin, A., Cvetkovska, M., & Klippel, M. (2019). Literature Review on Timber–Concrete Composite Structures in Fire. Journal of Structural Engineering, 145(11), 04019142. https://doi.org/10.1061/(ASCE)ST.1943-541X.0002418

Jeleč, M., Rajčić, V., & Varevac, D. (2018). Cross-laminated timber (CLT) – a state of the art report. Journal of the Croatian Association of Civil Engineers, 70(02), 75–95. https://doi.org/10.14256/JCE.2071.2017

Kodur, V. (2014). Properties of Concrete at Elevated Temperatures. ISRN Civil Engineering, 2014, 1–15. https://doi.org/10.1155/2014/468510

Lineham, S. A., Thomson, D., Bartlett, A. I., Bisby, L. A., & Hadden, R. M. (2016). Strucutral repsonse of fire-exposed cross laminated timber beams under sustained loads. Fire Saftey Journal, 85, 23-34. https://doi.org/10.1016/j.firesaf.2016.08.002

Mai, K. Q., Park, A., & Lee, K. (2018). Experimental and numerical performance of shear connections in CLT–concrete composite floor. Materials and Structures, 51(4), 84. https://doi.org/10.1617/s11527-018-1202-3

Mindeguia, J.-C., Mohaine, S., Bisby, L., Robert, F., McNamee, R., & Bartlett, A. (2021). Thermo-mechanical behaviour of cross-laminated timber slabs under standard and natural fires. Fire and Materials, 45(7), 866–884. https://doi.org/10.1002/fam.2938

Mirdad, A. H., & Chui, Y. H. (2019). Load-slip performance of Mass Timber Panel-Concrete (MTPC) composite connection with Self-tapping screws and insulation layer. Construction and Building Materials, 213, 696–709. https://doi.org/10.1016/j.conbuildmat.2019.04.117

Muszyński, L., Gupta, R., Hong, S. hyun, Osborn, N., & Pickett, B. 2019. Fire resistance of unprotected cross-laminated timber (CLT) floor assemblies produced in the USA. Fire Safety Journal, 107, 126–136.

Nguyen, T.-T., Sorelli, L., & Brühwiler, E. (2020). An Analytical Method to Predict the Structural Behavior of Timber-Concrete Structures with Brittle-to-Ductile Shear Connector Laws. Engineering Structures, 221(Complete). https://doi.org/10.1016/j.engstruct.2020.110826

Nordic Structures. (2020). Nordic Structures | nordic.ca | Engineered Wood | Documentation | Technical documents | Nordic X-Lam Technical Guide. https://www.nordic.ca/en/documentation/technical-documents/ns-gt6-ca

Ogrin, A., & Hozjan, T. (2021). Timber-Concrete Composite Structural Elements. IntechOpen. https://doi.org/10.5772/intechopen.99624

Okuni, I. M., & Bradford, T. E. (2020). Modelling of Elevated Temperature Performance of Adhesives Used in Cross Laminated Timber: An Application of ANSYS Mechanical 2020 R1 Structural Analysis Software. Environmental Sciences Proceedings, 3(1), Article 1. https://doi.org/10.3390/IECF2020-07902

Osborne, L. (2015, March). Fire resistance of long span composite wood-concrete floor systems. https://library.fpinnovations.ca/en/permalink/fpipub40130

Owens Corning Canada (OCC). (2013). FOAMULAR C-200 Extruded Polystyrene Rigid Insulation, FOAMULAR CODEBORD Extruded Polystyrene Rigid Insulation. 07 2113.13.OCC

Salem, O. S., & Virdi, V. (2021, May 26-29). Experimental testing of the shear strength of clt-concrete composite sections utilizing screws as shear connectors [Paper Presentation]. CSCE 2021 Annual Conference, Niagara Falls, ON, Canada.

Schmid, J., Klippel, M., Just, A., Frangi, A., & Tiso, M. (2018). Simulation of the Fire Resistance of Cross-laminated Timber (CLT). Fire Technology, 54(5), 1113–1148. http://dx.doi.org/10.1007/s10694-018-0728-9

Shephard, A. B., Fischer, E. C., Barbosa, A. R., & Sinha, A. (2021). Fundamental Behavior of Timber Concrete-Composite Floors in Fire. Journal of Structural Engineering, 147(2), 04020340. https://doi.org/10.1061/(ASCE)ST.1943-541X.0002890

Shi, D., Hu, X., Hong, W., Zhang, J., & Du, H. (2022). Review of connections for timber-concrete composite structures under fire. BioResources, 17(4). https://doi.org/10.15376/biores.17.4.Shi

Su, J. (2018). Fire safety of CLT buildings in Canada. Wood and Fiber Science, 50(Special Issue: CLT/Mass Timber), 102–109.

Su, J., Leroux, P., Lafrance, P.-S., Berzins, R., Gratton, K., Gibbs, E., & Weinfurter, M. (2021). Fire testing of rooms with exposed wood surfaces in encapsulated mass timber construction (2nd edition, p. 75 p.). National Research Council of Canada. Construction. https://doi.org/10.4224/23004642

Wang, Y., Zhang, J., Mei, F., Liao, J., & Li, W. (2020). Experimental and numerical analysis on fire behaviour of loaded cross-laminated timber panels. Advances in Structural Engineering, 23(1), 22–36. https://doi.org/10.1177/1369433219864459

Wiesner, F., Siyimane, M., Robert, F., McNamee, R., Jean-Christophe, M., & Luke, B. (2020). Structural Capacity of One-Way Spanning Large-Scale Cross-Laminated Timber Slabs in Standard and Natural Fires. Fire Technology, 57(1), 291–311. http://dx.doi.org.ezproxy.lakeheadu.ca/10.1007/s10694-020-01003-y

Zhang, C., Li, G.-Q., & Wang, Y.-C. (2012). Sensitivity Study on Using Different Formulae for Calculating the Temperature of Insulated Steel Members in Natural Fires. Fire Technology, 48(2), 343–366. https://doi.org/10.1007/s10694-011-0225-x